U.PORTO

FEUP FACULDADE DE ENGENHARIA
UNIVERSIDADE DO PORTO

# Supercritical Fluid Extraction and Fractionation of Bioactive Natural Products from Cork

A dissertation presented to the
Faculdade de Engenharia da Universidade do Porto
For the degree of PhD in Chemical and Biochemical Engineering

*by*

**Yaidelin Josefina Alves Manrique**

Supervised by Prof. José Miguel Loureiro
Prof. Mª Manuela Vilarinho Ferreira de Oliveira


Laboratory of Separation and Reaction Engineering
Associate Laboratory LSRE-LCM
Department of Chemical Engineering
Faculty of Engineering, University of Porto

**December 2016**

This thesis was financially supported by *Fundação para a Ciência e Tecnologia* (Portugal) through the PhD grant SFRH/BD/71891/2010. The work was also co-financed by: Project POCI-01-0145-FEDER-006984 – Associate Laboratory LSRE-LCM funded by FEDER through COMPETE2020 - Programa Operacional Competitividade e Internacionalização (POCI) – and by national funds through FCT - Fundação para a Ciência e a Tecnologia



## Acknowledgements

Each challenge is a new opportunity to grow up and improve yourself, both professionally and personally, so the responsibility to achieve our goals is plenty ours; however, it is important to highlight that to make this happen, it is essential to have a favourable environment, as well the right people around us to be successful. Therefore, at the end of this journey, there are many people that in one way or another had a contribution, and to whom I would like to express my gratitude.

First, I want to thank to my supervisors Prof. José Miguel Loureiro and Prof. Manuela V. Ferreira de Oliveira, for giving me a vote of confidence to develop this project, for their continuous support and availability and for all ideas and discussions to improve my work; also for the motivation and encouragement when things were not going in the best way.

To the Associate Laboratory LSRE-LCM, represented by Prof. Emeritus A. Rodrigues (ex-coordinator) and Prof. M. Dias (coordinator), for their support whenever I needed. And finally, I have a positive answer to their single question, "*Yes, I have finished this chapter!*"; from now on, new challenges can be taken.

To *Fundação para a Ciência e Tecnologia* (Portugal), for the financial support (research Fellowship: **SFRH/BD/71891/2010**).

To António Almeida, Cortiças, S.A., for supplying all cork samples and for their explanations of cork industrial processing; this work was all about cork...

To all my colleagues of LSRE; I know that mentioning only a few of you is very unfair; for that reason, I would like to express my gratitude to all of you without forgetting anyone. Since the beginning of this special journey, many of you still remain at my side, others had to go far away to embrace new professional challenges, some were here for a specific period and others are still here; working with each of you was exciting; we always gave our best to be better (professionally and personally). I really want to thank all of you for all our discussions and great ideas, the support and the continuous motivation, and specially all the great moments spent together (in and out of work), with all of you this journey was enriching; regardless of the new ways for our future, I know that I won friends for my life.

To my friends, in particular those who I won in this journey, you became my family. Undoubtedly, *friends are the family you choose*, thank you for being always present and making possible what seems impossible. With all of you *to infinity and beyond*!

To those who made all this possible since the first day of my life, **my family** that always supports all my decisions and gives me the freedom to follow my path to achieve my goals, even when it takes me far away from the comfort zone. You always believed, even when I could not. **I am grateful for all**, especially because whenever things got more difficult, you always encouraged me to not give up

and to go even further, and you taught me that the difficulties are not what make us stronger but instead our attitude and faith to keep on. Today, I am here only because of you. **Thank you for everything**!

To each one of you, thank you very much!
With all of you ***everything is possible!***

To my family

*"The greatest gift you can give someone is your time.*
*Because when you give your time,*
*you are giving a portion of your life*
*that you will never get back"*
**Anonymous**

## Abstract

Cork is the bark of the cork oak (*Quercus Suber L.*), a hundred percent natural plant tissue, that is composed, in average, by 14% extractives; these extractives are mainly constituted by triterpenic compounds (e.g., cerin, betulin – B, friedelin, betulinic acid – BA) that have promising applications as bioactive compounds or precursors to drug ingredients. Therefore, these compounds can have a very high-value.

Portugal is the world leader in the production, processing and marketing of cork. In 2014, the total sales of Portuguese cork industry represented 1 288 million euros; that represents ca. 182 thousand tons of cork by year (2014). The most important sector to the cork industry is the production of cork stoppers; in the process of natural cork stoppers production, ca. 60% of initial raw material is rejected; this rejected material is milled to be used in other applications, e.g. technical cork stoppers, agglomerated, etc.

This work aims to "*Add a New Value to Cork*", i.e., it intends to use the cork as a "possible" source of high-added value chemicals, by introducing in the cork mill process a valorisation step, but without compromising the traditional uses of this granulated material.

To evaluate the potential of this material as a source of bioactive compounds, several samples (A1 to A9) of granulated industrial cork and cork powder were extracted by soxhlet and supercritical fluid extraction (SFE) with and without co-solvent. In the soxhlet extractions were used solvents with different polarities; for all samples, the yield increases with the polarity of the solvent, regardless of the average particle size (or cork density). E.g., for sample A1 (0.75 mm), the yield was 94.7, 84.3, 70.4 and 48.5 $g_{extract} \cdot kg_{DryCork}^{-1}$ for ethanol, acetone, dichloromethane and hexane, respectively. These results represented a benchmark to the supercritical fluid extraction (SFE) with and without co-solvent.

The results obtained are compatible with the hypothesis that the particles bigger than cork powder are not totally extracted, i.e., only an outer layer was extracted; also, it seems that this layer is nearly constant, for particles bigger than 1 mm, for each solvent.

To perform the SFE, an experimental setup at bench scale was designed (up to 80°C and 300 bar), assembled and tested; this setup can be operated with and without co-solvent. The best performance of SFE without co-solvent was 19.7 $g_{extract} \cdot kg_{DryCork}^{-1}$ obtained at 210 bar and 41°C; when 10% of ethanol was added, the yield increases almost 86% (to 36.6 $g_{extract} \cdot kg_{DryCork}^{-1}$).

To describe the experimental results for both soxhlet and SFE, two phenomenological models are developed, a diffusional and a shrinking core models. For the two models, negligible film resistance and that only an outer

layer of particles is extracted were considered. The diffusional model described reasonably well the experimental results, for soxhlet, when ethanol was used as solvent; it was calculated the effective diffusivity as $1.7\ x10^{-8}\ cm^{2} \cdot s^{-1}$, while for the SFE with 5% and 10% of ethanol with the $CO_2$ at supercritical conditions (~210 bar and 41°C), the effective diffusivity was estimated as $1.4\ x10^{-8}\ cm^{2} \cdot s^{-1}$ and $0.9\ x10^{-8}\ cm^{2} \cdot s^{-1}$, respectively.

For the identification and quantification of target compounds (B and BA) in the cork extracts, an analytical method was developed. Although the yields obtained with hexane were the lowest (soxhlet), the cork extracts had the highest content of B and BA. For all cork extracts, the BA content is 2.5 to 4.6 times higher than the content of B. When a mixture of 10% of ethanol with $CO_2$ at supercritical conditions was used, the composition of the cork extract (sample A1) was $11\ mg_{Betulin} \cdot g_{extract}^{-1}$ and $39\ mg_{Betulinic\ Acid} \cdot g_{extract}^{-1}$, that is comparable with the results obtained for the hexane (soxhlet). However, for SFE without co-solvent, the BA and B contents were 12.3 and 3.4 times lower than the ones obtained with hexane (soxhlet).

Fractional collections of the extract during the SFE extraction enable to duplicate the contents of the target compounds in some fractions of the cork extract.

## Resumo

A cortiça é a casca do sobreiro (*Quercus Suber L.*), sendo cem por cento tecido vegetal natural, constituída em média por 14% de extrativos; estes extrativos são principalmente compostos triterpénicos (por exemplo, cerina, betulina - B, friedelina, ácido betulínico - BA) que têm aplicações promissoras como compostos bioativos ou precursores de ingredientes de fármacos. Por isso, estes compostos podem ter um valor muito elevado.

Portugal é o líder mundial na produção, transformação e comercialização da cortiça. Em 2014, o total das vendas da indústria portuguesa de cortiça representaram 1 288 milhões de euros; em termos de massa, isto representa ca. 182 mil toneladas de cortiça por ano. O sector mais importante para a indústria da cortiça é a produção de rolhas de cortiça; no processo de produção de rolhas de cortiça naturais, ca. 60% da matéria-prima inicial é rejeitada; contudo este material não é considerado como desperdício, uma vez que é moído para ser utilizado noutras aplicações, e.g. rolhas técnicas de cortiça, aglomerados, etc.

Este trabalho pretende "*acrescentar um novo valor à cortiça*", ou seja, pretende utilizar a cortiça como uma "possível" fonte de produtos químicos com elevado valor acrescentado, através da introdução no processo de produção de rolhas de cortiça naturais de um novo passo de valorização, mas sem comprometer o uso habitual do granulado de cortiça.

Para avaliar o potencial deste material como fonte de compostos bioativos, foram extraídas várias amostras (A1 a A9) do granulado industrial de cortiça e pó de cortiça por extração com soxhlet e também usando dióxido de carbono em condições supercríticas (SFE) com e sem co-solvente. Na extração soxhlet foram utilizados solventes com diferentes polaridades; verificou-se que para todas as amostras, o rendimento aumenta com a polaridade do solvente, independentemente do tamanho médio das partículas (ou da densidade da cortiça). Por exemplo, para a amostra A1 (0,75 mm), obteve-se um rendimento de 94,7, 84,3, 70,4 e 48,5 $g_{extrato} \cdot kg^{-1}_{CortiçaSeca}$ para o etanol, a acetona, o diclorometano e o hexano, respetivamente. Estes resultados constituem uma referência para a extração supercrítica (SFE) com e sem co-solvente.

Os resultados obtidos são compatíveis com a hipótese de que só o pó de cortiça é totalmente extraído, sendo que apenas uma camada externa é extraída para todas as outras partículas de maior tamanho; também, de acordo com os resultados obtidos, esta camada é praticamente constante, para partículas maiores que 1 mm, e para cada solvente.

Para efetuar as extrações supercríticas (SFE), foi projetada, construída e testada uma instalação experimental à escala de bancada (até 80°C e 300 bar). Esta instalação pode ser operada com e sem co-solvente. O maior rendimento obtido usando $CO_2$ supercrítico e sem adicionar co-solvente foi de

19,7 $g_{extrato} \cdot kg^{-1}_{Cortiça\ Seca}$ a 210 bar e 41°C; quando se adicionou 10% de etanol, o rendimento aumentou ca. 86% (até 36,6 $g_{extrato} \cdot kg^{-1}_{Cortiça\ Seca}$).

Para descrever os resultados experimentais obtidos nas extrações soxhlet e SFE, foram desenvolvidos dois modelos fenomenológicos, um modelo difusional e um modelo de núcleo a contrair ("shrinking core"). Para os dois modelos, considerou-se desprezável a resistência do filme à volta das partículas e que apenas uma camada externa das partículas era extraída. O modelo difusional descreveu razoavelmente bem os resultados experimentais, no caso da extração soxhlet, usando como solvente o etanol; a difusividade efetiva foi estimada como sendo $1,7 \times 10^{-8}\ cm^2 \cdot s^{-1}$, enquanto que para a SFE com 5% e 10% de etanol na mistura com $CO_2$ em condições sobrecríticas (~210 bar e 41°C), a difusividade efetiva estimada foi de $1,4 \times 10^{-8}$ e $0,9 \times 10^{-8}\ cm^2 \cdot s^{-1}$, respetivamente.

Para a identificação e quantificação dos compostos alvo (B e BA) nos extratos de cortiça, foi desenvolvido um método analítico. Embora os rendimentos obtidos com hexano, em termos de massa de extrato por massa de cortiça, tenham sido os mais baixos (soxhlet), os extratos de cortiça têm o maior teor de B e BA $\left(mg_{B\ or\ BA} \cdot g^{-1}_{extrato}\right)$. Para todos os extratos de cortiça, o teor de BA é 2,5 a 4,6 vezes superior ao conteúdo de B. Quando 10% de etanol foi acrescentado ao $CO_2$ em condições sobrecríticas, a composição do extrato de cortiça (amostra A1) foi de $11\ mg_B \cdot g^{-1}_{extrato}$ e $39\ mg_{BA} \cdot g^{-1}_{extrato}$, o que é comparável com os resultados obtidos para o hexano (soxhlet). No entanto, para SFE sem co-solvente, os conteúdos em BA e B foram 12,3 e 3,4 vezes inferiores aos conseguidos com hexano (soxhlet).

A recolha fracionada do extrato durante a extração supercrítica com co-solvente, permitiu duplicar o conteúdo dos compostos alvos em algumas frações do extrato de cortiça.

## Résumé

Le liège est l'écorce du chêne-liège (*Quercus Suber L.*), étant cent pour cent du tissu végétal naturel, il se compose en moyenne de 14% extractibles ; ces extractibles sont principalement composés triterpéniques (par exemple, cérine, bétuline – B, friedeline, acide bétulinique – BA) qui ont des applications prometteuses telles que des agents bioactifs ou des précurseurs d'ingrédients pharmaceutiques. Par conséquent, ces composés peuvent avoir une valeur très élevée.

Le Portugal est le leader mondial dans la production, la transformation et la commercialisation du liège. En 2014, le total des ventes de l'industrie portugaise du liège ont représenté € 1.288 millions ; ce qui représente, en termes de masse, environ 182.000 tonnes de liège par an. Le secteur le plus important pour l'industrie du liège est la production de bouchons de liège ; dans le processus de production de bouchons en liège naturel, ca. 60% de la charge initiale est rejetée ; toutefois, ce matériau n'est pas considéré comme un déchet, une fois qu'il est broyé pour être utilisé dans d'autres applications, par exemple bouchons techniques de liège, agglomérés, etc.

Ce travail vise à "*ajouter une nouvelle valeur au liège*", c'est-à-dire, il veut utiliser le liège comme une source "possible" de produits chimiques à haute valeur ajoutée grâce à l'introduction, au processus de production de bouchons en liège naturel, d'une nouvelle étape de valorisation, mais sans compromettre l'utilisation habituelle de granulés de liège.

Pour évaluer le potentiel de ce matériau en tant que source de composés bioactifs, plusieurs échantillons ont été extraits (A1 à A9) du granulé industriel de liège et de la poussière de liège en utilisant le procédé soxhlet et aussi le dioxyde de carbone en conditions supercritiques (SFE) avec et sans co-solvant. Concernant l'extraction soxhlet, plusieurs solvants avec des polarités différentes ont été utilisés ; il a été constaté que, pour tous les échantillons, le rendement augmente avec la polarité du solvant, quelle que soit la taille moyenne des particules (ou la densité du liège). Par exemple, l'échantillon A1 (de 0,75 mm) a donné un rendement de 94,7, 84,3, 70,4 et 48,5 $g_{extrait} \cdot kg_{LiègeSec}^{-1}$ quand on utilise l'éthanol, l'acétone, le dichlorométhane et l'hexane, respectivement. Ces résultats fournissent une référence pour l'extraction supercritique (SFE) avec et sans co-solvant.

Les résultats sont cohérents avec l'hypothèse selon laquelle seul le liège en poudre est complètement extrait, et une seule couche externe est extraite pour toutes les autres particules plus grandes ; en outre, d'après les résultats, cette couche est sensiblement constante pour les particules supérieures à 1 mm, et pour chaque solvant.

Une installation expérimentale à l'échelle de laboratoire (jusqu'à 80°C et 300 bar) a été conçue, construite et testée pour effectuer l'extraction supercritique (SFE). Cette installation peut fonctionner avec ou sans co-solvant.

Le rendement le plus élevé obtenu en utilisant le $CO_2$ supercritique et sans ajouter de co-solvant était de 19,7 $g_{extrait} \cdot kg^{-1}_{LiègeSec}$ à 210 bar et 41°C; lors de l'ajout de 10% d'éthanol, le rendement a augmenté ca. 86% (jusqu'à 36,6 $g_{extrait} \cdot kg^{-1}_{LiègeSec}$ ).

Pour décrire les résultats expérimentaux obtenus dans les extractions soxhlet et SFE on a développé deux modèles phénoménologiques, un modèle de diffusion et un modèle de rétrécissement de nucléo («shrinking core»). Pour les deux modèles, il a été considéré comme négligeable la résistance du film autour des particules et que seulement une couche extérieure des particules était extraite. Le modèle de diffusion décrit assez bien les résultats expérimentaux dans le cas d'une extraction soxhlet, en utilisant de l'éthanol comme solvant ; la diffusivité effective a été estimée à $1,7 \times 10^{-8} cm^2 \cdot s^{-1}$, tandis que pour la SFE avec 5% et 10% d'éthanol en mélange avec le $CO_2$ en conditions surcritiques (~ 210 bar et 41°C), la diffusivité effective estimée était $1,4 \times 10^{-8}$ e $0,9 \times 10^{-8} cm^2 \cdot s^{-1}$, respectivement.

Pour l'identification et la quantification des composés désirés (B et BA) dans les extraits de liège, une méthode d'analyse a été développée. Bien que les rendements obtenus avec l'hexane, en termes de masse extraite par masse de liège, ont été les plus faibles (soxhlet), les extraits de liège ont la plus haute teneur en B et BA $\left(mg_{B \text{ ou } BA} \cdot g^{-1}_{extrait}\right)$. Pour tous les extraits de liège, le contenu de BA est de 2,5 à 4,6 fois supérieure à la teneur en B. Lorsque 10% d'éthanol est ajouté au $CO_2$ en conditions supercritiques, la composition de l'extrait de liège (échantillon A1) était de 11 $mg_B \cdot g^{-1}_{extrait}$ et 39 $mg_{BA} \cdot g^{-1}_{extrait}$ , ce qui est comparable aux résultats obtenus avec l'hexane (soxhlet). Cependant, pour la SFE sans co-solvant, les contenus en BA et B étaient 12,3 et 3,4 fois inférieurs à ceux obtenus avec de l'hexane (soxhlet).

La collecte fractionnée de l'extrait pendant l'extraction supercritique avec le co-solvant, a permis de doubler le contenu des composés désirés dans quelques fractions de l'extrait de liège.

# Table of Contents

List of Tables ..... xxiii

List of Figures ..... xxv

1 Introduction ..... 1

1.1 Motivation ..... 3

1.2 Main Goals and tasks ..... 6

1.3 Organization ..... 7

References ..... 10

2 Cork ..... 13

2.1 Cork, its history and Portugal ..... 15

2.2 Cork, its main properties & applications ..... 21

2.2.1 Chemical composition of cork ..... 22

2.2.2 Applications of cork extractives ..... 24

2.3 Manufacturing of cork – The granulated industrial cork ..... 28

References ..... 31

3 Soxhlet Extraction ..... 35

3.1 Characterization of samples ..... 35

3.1.1 Cork density, bulk density and particle size ..... 37

3.2 Soxhlet extraction ..... 39

3.2.1 Yields ..... 45

3.3 Layer thickness of cork accessible to extraction ..... 47

3.4 Quantification of betulin and betulinic acid ..... 50

Notation ..... 56

List of Acronyms ..... 56

References ..... 57

4 Supercritical Fluid Extraction & Experimental Setup ..... 59

4.1 Supercritical Fluid Extraction (SFE) ..... 60

4.2 Design and construction of a bench-scale supercritical fluid extraction (SFE) setup ..... 66

4.2.1 Feed section ..... 67

4.2.2 Extraction section ..... 68

4.2.3 Separation section ..... 72

4.2.4 Purge ..... 73

4.2.5 Program – SFE ..... 78

4.3 Startup, operation and shutdown of the SFE bench scale setup ..... 81

4.3.1 Start-up of SFE setup ..... 81

4.3.2 Operation of the SFE setup ..... 82

4.3.3 Shutdown of the SFE ..... 83

4.4 Experimental Results ..... 84

4.5 Conventional extraction *vs*. SFE ..... 85

4.6 SFE setup improvement to add co-solvent ..... 87

4.7 Experimental results, $scCO_2$ and Ethanol ..... 89

Notation ..... 92

List of Acronyms ..... 92

References ..... 93

5 Modelling Extraction Process ..... 95

5.1 Desorption Model ..... 97

5.1.1 Diffusional model ..... 99

5.1.2 Shrinking core model ..... 105

5.2 Validation of models ..... 111

Notation ..... 120

Greek letters ..... 121

List of Acronyms ..... 121

References ..... 122

6 Fractionation of the cork extracts ..... 123

6.1 Soxhlet extraction ..... 125

6.2 Supercritical Fluid Extraction (SFE) ..... 126

Conclusions ..... 129

Future Work ..... 133

Appendix 1 - Analytical Methods ..... 1

Gas Chromatography / Flame Ionization Detector (GC-FID) ..... 1

Gas Chromatography / Mass Spectrometry (GC-MS) ..... 2

References ..... 4

Appendix 2 - Response Surface Methodology (RSM) ..... 1

Design of experiments using response surface methodology ..... 1

References ..... 4

## List of Tables

Table 2.1 – Properties and structures for the main triterpenes of cork extractives.....26

Table 3.1 – Particle size, bulk density, apparent density and moisture content of industrial granulated cork samples. .....37

Table 3.2 – Yields obtained in the cork extract from several cork samples.....42

Table 3.3 – Parameters for the Soxhlet extraction.....43

Table 3.4 – Yields for sequential extractions of several cork samples. .....48

Table 4.1 – Critical constants of the main solvents considered in supercritical extraction. Data from Perry (2008) .....61

Table 4.2 – Constants for the equations of melting (Eq. 4.1) sublimation (Eq. 4.2) and vapour pressures (Eq. 4.3).....63

Table 4.3. – Density of $CO_2$ $\left(kg \cdot m^{-3}\right)$ for the critical point and above it.....64

Table 4.4 – Commercial-scale supercritical $CO_2$ extraction plants and processes. .....64

Table 4.5 – List of material in the supercritical fluid extraction setup .....75

Table 5.1 – Dimensionless numbers.....101

## List of Figures

Figure 1.1 – Annual Portuguese sales of cork industry ..... 4

Figure 1.2 – a) Distribution of sales of Portuguese cork industry in 2013, b) Cork sales structure by Product Type in percentage in 2013 ..... 4

Figure 1.3 – Scheme of the main sections of this thesis. ..... 9

Figure 2.1 – Harvesting cork (http://www.casarosdenportugal.com/portugal-cork/) ..... 13

Figure 2.2 – Geographical distribution of cork oak ..... 15

Figure 2.3 – First draw of cork cellular structure made by Robert Hooke after his microscope observation ("Robert Hooke," 2015) ..... 17

Figure 2.4 – The first industrial machine to produce cork stopper, the "*Garlopa*" (Corticeira_Amorim, 2005) ..... 18

Figure 2.5 – Percentage of Portuguese corks exports by type of products (1851 – 2000). Data from: Carvalho, A. (2002) ..... 19

Figure 2.6 – a) Value of world's cork exports. b) Percentage of cork exports according to HS Code Chapter 45: Cork and articles of cork ..... 20

Figure 2.7 – Schematic representation of the axial section of a cork oak stem, showing the different layers ..... 21

Figure 2.8 – Diagram of the cellular structure of cork (Gil *et al.*, 2000) ..... 22

Figure 2.9 – Average chemical composition of cork. ..... 23

Figure 2.10 – New process step to add a new value to cork ..... 30

Figure 3.1 – Punched cork planks. ..... 36

Figure 3.2 – SEM for samples A1 to A6 that correspond to inner section of plank. ..... 36

Figure 3.3 – Granulated industrial cork from two sections of cork planks: inner (A1 to A6) and outer (A7 and A9). ..... 38

Figure 3.4 – Total void space ( $\varepsilon_t$ ) for each sample *vs*. average particle size..... 39

Figure 3.5 – Internal porosity ( $\varepsilon_p$ ) *vs*. average particle size. ..... 39

Figure 3.6 – Schematic representation of a soxhlet extractor. ..... 40

Figure 3.7 – Conventional method for soxhlet extraction. ..... 44

Figure 3.8 – Yields of conventional soxhlet extraction of industrial granulated cork as a function of particle size, for the three solvents tested: (black) acetone, (gray) dichloromethane, (light gray) hexane. (A8) cork powder, (A1 to A6) inner bark and (A7 and A9) outer bark samples. The diamonds represent the average particle size and the circles the cork density. ..... 45

Figure 3.9 – Dimensionless thickness of the extractable outer cork layer *vs*. average particle size. ..... 50

Figure 3.10 – Procedure for derivatization of cork extracts before GC Analysis. 51

Figure 3.11 – Betulin (a) and betulinic acid (b) content in each extract sample *vs*. particle size, for the three solvents tested. (A8) cork powder, (A1 to A6) inner bark and (A7 and A9) outer bark samples. Solvents: (black) acetone, (gray) dichloromethane, (light gray) hexane. The diamonds represent the average particle size and the circles the cork density. ..... 52

Figure 3.12 – Betulin (a) and betulinic acid (b) contents in each sample *vs*. particle size, for the three solvents tested. (A8) cork powder, (A1 to A6) inner bark and (A7 and A9) outer bark samples. Solvents: (black) acetone, (gray) dichloromethane, (light gray) hexane. The diamonds represent the average particle size and the circles the cork density. ..... 54

Figure 4.1 – Physical properties of different phases; adapted fromFrancis *et al.* (1999). ..... 60

Figure 4.2 – $CO_2$ Phase Diagram....62

Figure 4.3 – PVT diagram of $CO_2$. ....63

Figure 4.4 – Schematic representation of SFE setup ....66

Figure 4.5 – Schematic representation of the feed section. ....68

Figure 4.6 – Schematic 3D drawing of feed section of the experimental SFE setup. ....68

Figure 4.7 – Schematic representation of the extraction section of the SFE setup ....69

Figure 4.8 - 3D drawing of a) the extractor, b) its cover and c) the raw material basket. ....70

Figure 4.9 – Schematic 3D drawing of the extraction section of the experimental SFE setup. ....71

Figure 4.10 – Schematic representation of the separation section of the SFE setup. ....72

Figure 4.11 – 3D drawing of a) the separator and b) its cover. ....72

Figure 4.12 – Schematic 3D drawing of the separation section of the experimental SFE setup. ....73

Figure 4.13 – Schematic 3D drawing and photo of the SFE setup after assembling. ....74

Figure 4.14 – Principal windows of the SFE Program. ....79

Figure 4.15 – Process windows of the SFE Program ....80

Figure 4.16 – Yields obtained with sample A1 (granulated industrial cork – particle size 0.75 mm) for the SFE at 41°C in a range of pressures from 170 up to 243 bar. ....84

Figure 4.17 – Yields obtained with sample A1 (granulated industrial cork – particle size 0.75 mm) for the SFE at 41, 59 and 78°C and ca. 210 bar. ..... 85

Figure 4.18 – Yields of the conventional solvent extraction *vs.* SFE (41, 59 and 78°C at ~210 bar). For granulated industrial cork with particle size 0.75 mm (sample A1) ..... 86

Figure 4.19 – Betulin and betulinic acid (BA) contents in the different extracts, soxhlet extraction (acetone, dichloromethane and hexane) and SFE. ..... 87

Figure 4.20 – Flowsheet of SFE setup with co-solvent. ..... 87

Figure 4.21 – Schematic 3D drawing of the SFE setup using co-solvent. ..... 88

Figure 4.22 – Yields of the conventional solvent extraction *vs.* SFE at 41°C and ~185 bar and ~210 bar with different concentrations of ethanol (10%, 5% and 0%). For granulated industrial cork with particle size 0.75 mm (sample A1). ... 90

Figure 4.23 – Contents of betulin and betulinic acid (BA): a) in the extracts and b) in the cork. For granulated industrial cork with particle size 0.75 mm (sample A1). For the conventional solvent extraction and SFE at 41°C and ~210 bar with different concentrations of ethanol (0, 5 and 10%). ..... 91

Figure 5.1 – Considerations to describe a model for extraction processes (e.g., supercritical fluid extraction) ..... 96

Figure 5.2 – Histories of amount of solute in the fluid phase at the outlet of the packed-bed for different Péclet number values (0.01 to 1000) and $Bi_m = 1$. (a) $N_f = N_d = 0.1$; (b) $N_f = N_d = 1$; (c) $N_f = N_d = 10$ ..... 102

Figure 5.3 – Histories of amount of solute in the fluid phase at the outlet of the packed-bed. $N_f$ = 0.01 to 10; $N_d$ = 10 and Péclet number is 100. ..... 103

Figure 5.4 – Histories of amount of solute in the fluid phase at the outlet of the packed-bed. $N_d$ = 0.01 to 10; $N_f$ = 10 and Péclet number is 100 ..... 104

Figure 5.5 – Volume used according to internal radius $\left(\xi_c = r_c / R_p\right)$ ..... 105

Figure 5.6 – Histories of the amount of solute in the fluid phase at outlet of the packed-bed for several Péclet number values (0.01, 1 and 1000) and $Bi_m = 1$. (a) $N_f = N_d = 0.1$; (b) $N_f = N_d = 1$; (c) $N_f = N_d = 10$ ..... 108

Figure 5.7 – Histories of amount of solute in fluid phase at the outlet of the packed-bed. $N_f$ = 0.01 to 10; $N_d$ = 10 and Péclet number is 100. ..... 109

Figure 5.8 – Histories of amount of solute in fluid phase at the outlet of the packed-bed. $N_d$ = 0.01 to 10; $N_f$ = 10 and Péclet number is 100. ..... 110

Figure 5.9 – Histories of amount of solute in fluid phase at the outlet of the packed-bed. $N_d$ = 0.01; 0.1 and 10; $N_f$ = 10 and Péclet number is 100. Diffusional model is represented by solid lines and shrinking core model by dashes lines ..... 110

Figure 5.10 – Histories of amount of solute in fluid phase at the outlet of the packed-bed. $N_f$ = 0.01; 0.1 and 10; $N_d$ = 10 and Péclet number is 100. Diffusional model is represented by solid lines and shrinking core model by dashed lines ..... 111

Figure 5.11 – Yields of conventional soxhlet extraction of industrial granulated cork as a function of particle size, for the different solvents tested: (hexagon-open) ethanol, (hexagon-half up) acetone, (diamond-half right) dichloromethane, (diamond-half down) hexane. ..... 112

Figure 5.12 – Dimensionless core radius *vs*. particle size, for the different solvents tested: (hexagon-open) ethanol, (hexagon-half up) acetone, (diamond-half right) dichloromethane, (diamond-half down) hexane..... 113

Figure 5.13 – Histories of amount of solute in fluid phase at the outlet of the packed-bed. For three particle size of granulated industrial cork: (triangle) 5 mm, (diamond) 0.75 mm and (circle) <0.20 mm – cork powder. Solvent: Ethanol. Solid lines represent the diffusional model and dash lines represent the shrinking core model while the red lines show the results for variable $N_d$. ..... 114

Figure 5.14 – Histories of $N_d$ value used in diffusional and shrinking core model for each particle size: (triangle) 5 mm, (diamond) 0.75 mm and (circle) <0.20 mm – cork powder; the dashed line represents the value of $N_d$ over the time when was assumed the possible formation of agglomerates (A8*). ..... 114

Figure 5.15 – $N_d$* (the outer layer extracted) *vs*. $N_d$ (whole particle). ..... 115

Figure 5.16 – Histories of amount of solute in fluid phase at the outlet of the packed-bed; for sample A1 (0.75 mm). a) $CO_2$ and 5% ethanol and b) $CO_2$ and 10% ethanol. Pressure ~210 bar and 40°C. Continuous lines represent the diffusional model and dashed dot lines represent the shrinking core model... 117

Figure 5.17 – Histories of amount of solute in fluid phase at the outlet of the packed-bed; for sample A1 (0.75 mm) and $CO_2$ and 10% ethanol at ~210 bar and 40°C. Continuous lines represent the diffusional model and dashed dot lines represent the shrinking core model considering a variable $N_d$ ..... 118

Figure 5.18 – Histories of amount of solute in fluid phase at the outlet of the packed-bed. For sample A5 (5 mm) using 10% ethanol and pressure ~210 bar and 40°C. Continuous line represents the diffusional model and dashed dot line represents the shrinking core model. ..... 119

Figure 6.1 – Yields obtained for Soxhlet (ethanol, acetone, dichloromethane and hexane) and $scCO_2$ without co-solvent (at ~210bar and 41°C) for granulated industrial cork; samples A8 (powder), A1 (0.75 mm) and A5 (5 mm) ..... 123

Figure 6.2 – Betulinic acid and betulin content a) in the cork extract and b) in the cork; for Soxhlet (ethanol, acetone, dichloromethane and hexane) and $scCO_2$ without co-solvent (at ~210bar and 41°C) for granulated industrial cork, samples A8 (powder), A1 (0.75 mm) and A5 (5 mm). ..... 124

Figure 6.3 – Betulinic acid and betulin contents in the cork extracts for Soxhlet extraction at different times. Solvent: Ethanol. Samples: A8 (cork powder), A1 (0.75 mm) and A5 (5 mm). ..... 126

Figure 6.4 – Betulinic acid and betulin contents in the cork extracts for SFE with 10% ethanol at different times, (0-1h; 1-2h and 2-3h). Operating conditions: ~210 bar and 41°C. ..... 127

Figure 6.5 – Betulinic acid and betulin contents in the cork extracts for SFE at different times. Co-solvent: Ethanol. Operating conditions: ~210 bar and 41°C. For granulated industrial cork (0.75 mm – sample A1)..... 128

*"Cork is 100% natural,*
*100% recyclable and…*
*'essentially' Portuguese."*

# 1 Introduction

Natural products are chemical compounds produced by a biological source (Bart, 2011) and they commonly have biological activity that may have therapeutic benefits in treating some diseases, wherein these products generally represent, in traditional medicines, the active components (Brahmachari, 2010). Then, it is possible that the extraction of those natural products has aroused a huge interest, probably since the discovery of fire (Chemat *et al.*, 2012).

Nowadays, several studies are being done to evaluate the potential to obtain bioactive compounds from natural products; wherein bark, branches, roots, rhizomes, seeds, fruits, leaves and also flowers can be sources of those products (Azmir *et al.*, 2013; Bart, 2011; Gan *et al.*, 2011; Martins *et al.*, 2011; Wijngaard *et al.*, 2012). And the extraction techniques have been focused on finding a clean, sustainable and efficient process (Azmir *et al.*, 2013; Ghafoor *et al.*, 2010; Martinez *et al.*, 2011; Mendiola *et al.*, 2013; Pereira, C. G. *et al.*, 2009; Shi *et al.*, 2007; Wijngaard *et al.*, 2012). In this way, de Melo, M., *et al.* (2014) published a work that summarizes a wide-range of extracts from vegetable matrices using supercritical fluid in a period larger than a decade, being the work of Castola *et al.* (2005) the unique reported as using carbon dioxide at supercritical condition to powdered cork extraction.

Cork is the bark of the cork oak (*Quercus Suber L.*); it is a hundred percent natural plant tissue that consists of a honeycomb of microscopic cells. This natural product conceals a fraction of non-structural compounds, the extractives, which can be easily extracted.

According to the literature, the cork extractives are mainly constituted by polyphenols, long chain alkanols, triterpenes and, in minor quantities, long chain fatty acids (Castola *et al.*, 2002, 2005, Conde *et al.*, 1998, 1999a, 1999b; Cordeiro *et al.*, 1998; Pereira, H., 1988, 2013; Sousa *et al.*, 2006). The main triterpenes identified were friedelin, cerin, betulin and betulinic acid that have promising applications as bioactive compounds or as precursors to drug ingredients (Alakurtti *et al.*, 2006; Cichewicz *et al.*, 2004; Sousa *et al.*, 2006). They also have some cosmetics applications (Betulin, 2009b; "Skin Actives Scientific," 2015); e.g. Birken AG[1], produces a series of lotions and creams to skin care that use betulin as active ingredient in their formulations; likewise the pantent US5529769A (Cho *et al.*, 1996) shows the betulinic acid as main content in some cosmetic applications.

It is to remark that friedelin has been studied and described as antioxidant, anti-inflammatory or even as an anti-cancer agent (Antonisamy *et al.*, 2011; Silva *et al.*, 2005); betulin possesses a wide range of biological capabilities including anti-viral, anti-inflammatory, and anti-cancer properties (Wu *et al.*, 2014); and betulinic acid has a moderate anti-inflammatory activity (Costa *et al.*, 2014) and it has also been tested in the treatment of melanoma and other serious diseases (Betulin, 2009a).

The world's area of cork oak forests is ca. 2,139,942 hectares, and the Portuguese forest has the first place, with ca. 34% of this area; however, with refers to the national forest inventory, the cork oak represents only a 23% of the Portuguese forest area by species, the second place, after the Eucalyptus (APCOR, 2013, 2014).

[1] Birken AG was founded in 2000 in Niefern-Öschelbronn, Germany; this is a biopharmaceutical and dermo-cosmetic company.

The development of efficient and sustainable processes for the extraction of those high added-value products from cork have an enormous positive impact. Since the cork may be used in its common applications after being subjected to the extraction process, which means a new value added to cork, as a result of introducing new markets and products. Removal of cork extractives may not modify the internal structure of cork (Pereira, H., 2007).

## 1.1 Motivation

Cork has an enormous relevance to Portugal, both culturally and economically. The cork oak is considered a national heritage, being established as the Portugal's national tree since December 22, 2011 (*Resolução da Assembleia da República nº 15/2012*). Its forest has been legally protected for centuries, the only way to cut them down being their recognition as unproductive by the forestry department; the Portuguese law also protects its harvest to ensure the quality of this resource ("Cork Institute of America," 2008). Portugal is the world leader in the production, processing and marketing of cork, making the cork industry sector very relevant to the Portuguese economy.

More than 50% of the worldwide sales of cork products are assumed by the Portuguese cork industry; Figure 1.1 shows the total sales value for the Portuguese cork industry in the period from 2000 to 2014; in average, this industry represents to Portuguese economy 1 142 million euros in sales by year.

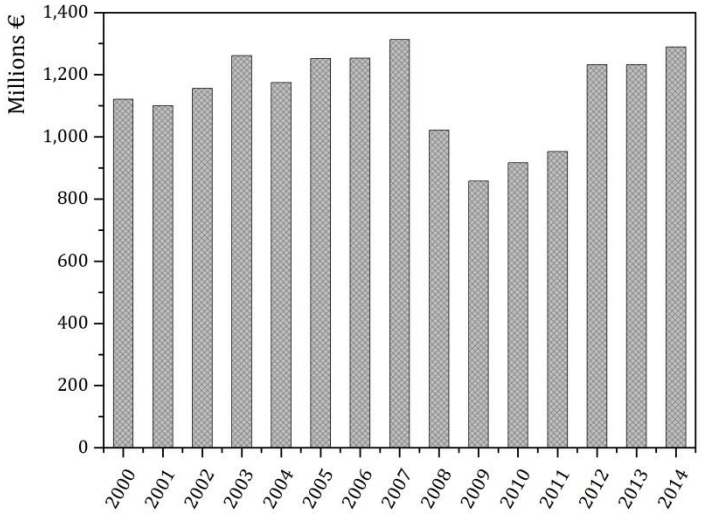


Figure 1.1 – Annual Portuguese sales of cork industry[2]

In 2014, the total sales of Portuguese cork industry was 1 288 million euros, where ca. 37% corresponds to the national market (Figure 1.2a). Likewise, the total sales associated to cork stoppers (both natural and agglomerated) are 71% (Figure 1.2b). The most important sector to the cork industry is still, without doubt, the production of cork stoppers, being the wine industry the main focus.

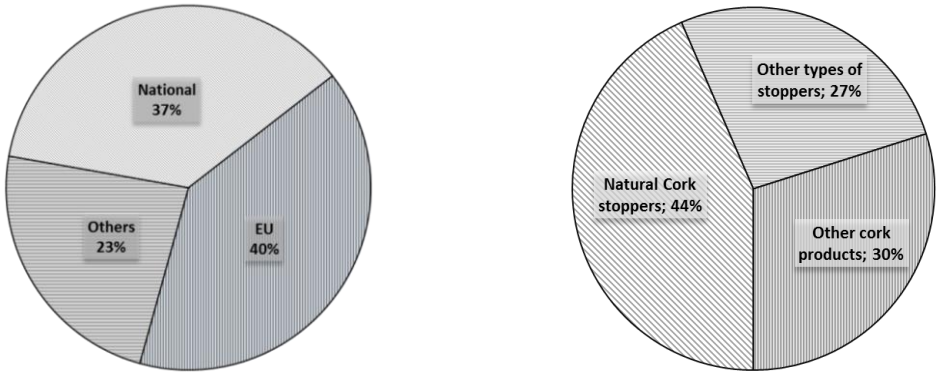


a) b)

Figure 1.2 – a) Distribution of sales of Portuguese cork industry in 2013, b) Cork sales structure by Product Type in percentage in 2013[3]

In the process of natural cork stoppers production ca. 60% of initial raw material is rejected, but it is not waste, since it can be used in other applications, e.g. cork powder can be used as a source of energy (Gil, 1997). Then, in the way

[2] Corresponding to code 16290 (Cork Industry), according to CAE-Rev.3 (Portuguese Classification of Economic Activities – Revision 3).
[3] Value corresponding to code 16290 (Cork Industry), according to code CAE-Rev.3 (Portuguese Classification of Economic Activities – Revision 3).

to produce a natural cork stopper the selected planks are punched, these planks after punching, as well as the material without the specifications to be a natural cork stopper, are granulated and automatically separated into different sizes and densities according to their subsequent application, from technical to agglomerated stoppers, agglomerates for floor and wall coverings, flooring panels, decorative home and office items, works of art and design, shoe soles, applications for the automobile industry, among many others (APCOR, 2009). Even the cork powder can be burned to generate energy (Gil, 1997); in the cork industry it is possible to take advantage of all the material, i.e., "*nothing is waste*".

A few studies define cork as a "possible" source of high-added value chemicals (Cordeiro *et al.*, 1998; Pereira, H., 2007; Silvestre *et al.*, 2008), as a consequence of its chemical composition; however, until now, to the author best knowledge, there is no evaluation of the particular use proposed in this work.

Nowadays, supercritical fluid extraction (SFE) has been widely used to successfully extract some compounds from natural matter (de Melo *et al.*, 2014; Reverchon *et al.*, 2006). SFE is a flexible process since a continuous modulation of the solvent-power/selectivity is possible; also, SFE avoids the expensive post-processing of the extracts for the solvent elimination, once it avoids the use of polluting organic solvents. Moreover, the use of the carbon dioxide presents several advantages as supercritical fluid; it is cheap, readily available, safe, and allows operating at relatively low pressures and near-room temperatures.

In the cork industry, SFE has been applied to extract the 2,4,6-Trichloroanisole (TCA) and other contaminants from granulated cork, being the TCA (so-called *cork taste*) one of the most sensitive points in the worldwide cork and wine industries (Silva *et al.*, 2005); through the DIAMANT® process the granulated industrial cork is pretreated with supercritical $CO_2$ to remove all contaminants, and ensuring lower level of TCA in cork, with the aim to produce a clean cork stopper (Iversen *et al.*, 2012; NATEX, 2011; Sanjuan, 2010; "Tecnología Diamant," 2011). In the same way, there is a patent with a "*method to direct treatment of natural cork stoppers, using supercritical fluid*" (Da Ponte *et al.*,

2010; Lumia *et al.*, 2001, 2007) the properties and shape of the cork stoppers, after the treatment, are unchanged.

It is to highlight that, until now, all processes are focused in solving the problem of contaminants to preserve the market of cork stoppers; they do not introduce a new value for the cork industry, i.e., cork was not explored as a potential source of high added-value chemicals, keeping its traditional uses.

If one considers that over 15,000 million cork stoppers are produced each year, even if only a small percentage leads to cork taste, serious economic implications arise, especially in wines and champagnes of high commercial value (Silva *et al.*, 2005). In fact, as consequence of cork taste problems, some alternative products to cork stoppers are emerging over the years; however, the "unique" cork's properties still associate the best wines with natural cork stoppers.

The main purpose of this work is the development of a sustainable, clean and efficient process for the extraction of triterpenic compounds from cork that would add value to granulated industrial cork and cork powder. The key idea is to extract from cork very high added-value compounds, maintaining the traditional applications for the cork, after extraction; e.g., it is known that cork powder is burned to produce energy; this material may be an abundant source of valuable triterpenic compounds, that can be extracted prior to combustion.

## 1.2 Main Goals and tasks

The main objective of this work is to "*Add a New Value to Cork*". Since, it does not intend to replace traditional cork applications but to introduce in the cork mill process a valorisation step as a means of getting additional value to cork and enlarging its markets.

Several samples of granulated industrial cork with different particle sizes (0.5 to 6 mm) and also of cork powder were studied.

A conventional extraction (soxhlet) was performed to be a reference for the supercritical fluid extraction (SFE). In the soxhlet extraction, several solvents with different polarities were used.

An experimental setup for supercritical fluid extraction at bench scale (ca. 200 mL extraction vessel) using carbon dioxide up to 80 °C and 300 bar, was designed, assembled and tested. In a second stage, this experimental setup was adapted to use mixtures of $CO_2$ and co-solvent, for the same range of temperature and pressure.

It was necessary to analyse cork extracts both from conventional (soxhlet) and supercritical fluid extraction (SFE). An analytical method had to be implemented with the purpose to identify and quantify the compounds extracted, for example, by GC-FID and GC-MS.

The SFE was performed at bench scale in order to optimize the extraction yield and the extract composition by changing parameters as pressure, temperature, extraction time. Preliminary tests of SFE provided information on the effect of all those parameters individually. Due to the particular and increasing interest in friedelin, betulin (B), betulinic acid (BA) and their derivatives, special attention was paid to obtain a rich fraction of these compounds.

## 1.3 Organization

In this first chapter, it was described the relevance and motivation of this work that pretend to add a new value to cork, enlarging its markets; the main goals were listed.

The 2nd chapter was focused on cork, its properties, uses and main applications through time; in last years the production of natural cork stoppers represents more than a half of billed of cork industry, the granulated industrial cork used in this work generated as a by-product of that process.

A conventional solvent extraction (soxhlet) was studied, in the third chapter, as a reference to the supercritical extraction; all cork samples were extracted with

solvents with different polarity, hexane, dichloromethane and acetone; also, ethanol was used for smaller and larger particle sizes. To follow, the supercritical fluid extraction (SFE) setup was design and assembly, to performed extraction using $CO_2$ at supercritical conditions with and without co-solvent (ethanol). The yields obtained with soxhlet and SFE were compared (Chapter 4).

The fifth chapter summarized a phenomenological model of the supercritical fluid extraction of bioactive compounds from cork in order to optimize the process. To follow (Chapter 6), the histories for the composition of the cork extracts were analysed for both extractions, soxhlet and SFE. And last chapter reported the principal conclusions to this research and also several tasks were proposed as future work. Figure 1.3 depicts the global organization of the thesis.

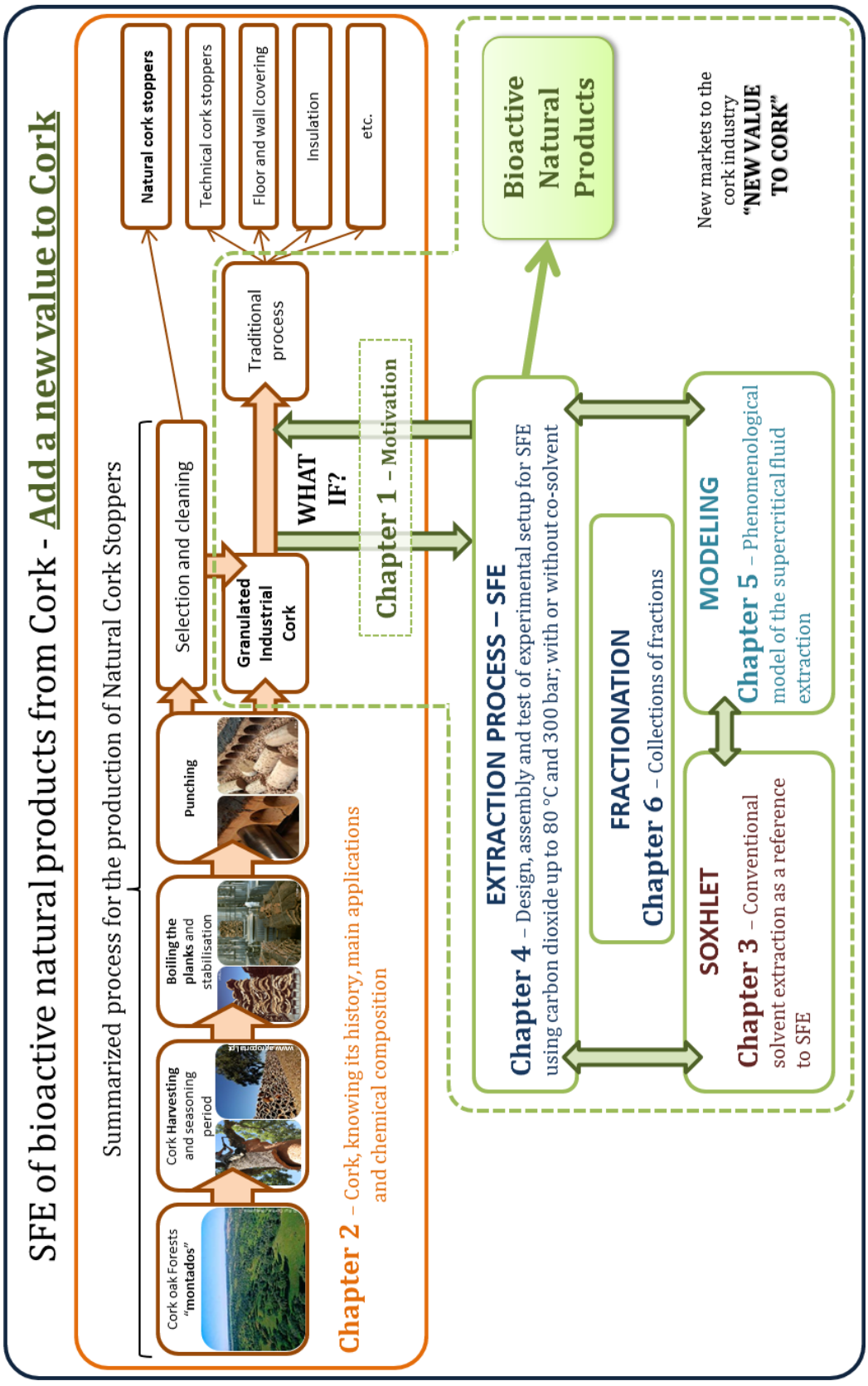


Figure 1.3 – Scheme of the main sections of this thesis.

# References


Alakurtti, S., Mäkelä, T., Koskimies, S., and Yli-Kauhaluoma, J. (**2006**). "Pharmacological properties of the ubiquitous natural product betulin." *European Journal of Pharmaceutical Sciences*, *29*(1), 1–13. doi:10.1016/j.ejps.2006.04.006

Antonisamy, P., Duraipandiyan, V., and Ignacimuthu, S. (**2011**). "Anti-inflammatory, analgesic and antipyretic effects of friedelin isolated from Azima tetracantha Lam. in mouse and rat models." *The Journal of Pharmacy and Pharmacology*, *63*(8), 1070–1077. doi:10.1111/j.2042-7158.2011.01300.x

APCOR. (**2009**). "Yearbook 2009." Associação Portuguesa da Cortiça.

APCOR. (**2013**). "Yearbook 2013." Associação Portuguesa da Cortiça.

APCOR. (**2014**). "Yearbook 2014." Associação Portuguesa da Cortiça.

Azmir, J., Zaidul, I. S. M., Rahman, M. M., Sharif, K. M., Mohamed, a., Sahena, F., … Omar, a. K. M. (**2013**). "Techniques for extraction of bioactive compounds from plant materials: A review." *Journal of Food Engineering*, *117*(4), 426–436. doi:10.1016/j.jfoodeng.2013.01.014

Bart, H.-J. (**2011**). "Extraction of Natural Products from Plants–An Introduction." In H.-J. Bart & S. Pilz (Eds.), *Industrial Scale Natural Products Extraction* (First Edit, pp. 1–26). WILEY-VCH Verlag GmbH. doi:10.1002/9783527635122

Betulin. (**2009a**). "Betulin." Retrieved March 1, 2015, from http://www.betulin.ca/

Betulin. (**2009b**). "Betulin and Birch Bark Extract." Retrieved March 1, 2015, from http://betulin.ca/betulin-for-cosmetics.html

Brahmachari, G. (**2010**). "Handbook of Pharmaceutical Natural Products." (Wiley-VCH, Ed.). Weinheim.

Castola, V., Bighelli, A., Rezzi, S., Melloni, G., Gladiali, S., Desjobert, J.-M., and Casanova, J. (**2002**). "Composition and chemical variability of the triterpene fraction of dichloromethane extracts of cork (Quercus suber L.)." *Industrial Crops and Products*, *15*(1), 15–22. doi:10.1016/S0926-6690(01)00091-7

Castola, V., Marongiu, B., Bighelli, A., Floris, C., Laï, A., and Casanova, J. (**2005**). "Extractives of cork (Quercus suber L.): chemical composition of dichloromethane and supercritical CO2 extracts." *Industrial Crops and Products*, *21*(1), 65–69. doi:10.1016/j.indcrop.2003.12.007

Chemat, F., Vian, M. A., and Cravotto, G. (**2012**). "Green extraction of natural products: concept and principles." *International Journal of Molecular Sciences*, *13*(7), 8615–27. doi:10.3390/ijms13078615

Cho, S. H., Gottlieb, H., and Santhanam, U. (**1996**). "Cosmetic Compositions Containing Betulinic Acid." United States Patent: US005529769A.

Cichewicz, R. H., and Kouzi, S. A. (**2004**). "Chemistry, biological activity, and chemotherapeutic potential of betulinic acid for the prevention and treatment of cancer and HIV infection." *Medicinal Research Reviews*, *24*(1), 90–114. doi:10.1002/med.10053

Conde, E., Cadahía, E., Garcia-Vallejo, M. C., and Gonźalez-Adrados, J. R. (**1998**). "Chemical Characterization of Reproduction Cork from Spanish Quercus Suber." *Journal of Wood Chemistry and Technology*, *18*(4), 447–469. doi:10.1080/02773819809349592

Conde, E., Garcia-Vallejo, M. C., and Cadahía, E. (**1999a**). "Waxes composition of Quercus

suber reproduction cork from different Spanish provenances." *Wood Science and Technology*, *33*(4), 271–283. doi:10.1007/s002260050115

Conde, E., Garcia-Vallejo, M. C., and Cadahía, E. (**1999b**). "Waxes composition of reproduction cork from Quercus suber and its variability throughout the industrial processing." *Wood Science and Technology*, *33*(3), 229–244. doi:10.1007/s002260050112

Cordeiro, N., Belgacem, M. N., Silvestre, A. J. D., Neto, C. P., and Gandini, A. (**1998**). "Cork suberin as a new source of chemicals. 1. Isolation and chemical characterization of its composition." *International Journal of Biological Macromolecules*, *22*(2), 71–80. doi:10.1016/S0141-8130(97)00090-1

"Cork Institute of America." (**2008**). Retrieved December 1, 2014, from http://www.corkinstitute.com/

Costa, J. F. O., Barbosa-Filho, J. M., de Azevedo Maia, G. L., Guimarães, E. T., Meira, C. S., Ribeiro-dos-Santos, R., … Soares, M. B. P. (**2014**). "Potent anti-inflammatory activity of betulinic acid treatment in a model of lethal endotoxemia." *International Immunopharmacology*, *23*(2), 469–474. doi:10.1016/j.intimp.2014.09.021

Da Ponte, M. L., Lopes, J. A., Vesna, N.-V., Manic, M., Mesquita, A. C., Da Silva, R. P., and Allegro, I. M. (**2010**). "Method for direct treatment of cork stoppers, using supercritical fluids." WO 2010093273 A1.

de Melo, M. M. R., Silvestre, A. J. D., and Silva, C. M. (**2014**). "Supercritical fluid extraction of vegetable matrices: Applications, trends and future perspectives of a convincing green technology." *The Journal of Supercritical Fluids*. doi:10.1016/j.supflu.2014.04.007

Gan, C.-Y., and Latiff, A. A. (**2011**). "Optimisation of the solvent extraction of bioactive compounds from Parkia speciosa pod using response surface methodology." *Food Chemistry*, *124*(3), 1277–1283. doi:10.1016/j.foodchem.2010.07.074

Ghafoor, K., Park, J., and Choi, Y.-H. (**2010**). "Optimization of supercritical fluid extraction of bioactive compounds from grape (Vitis labrusca B.) peel by using response surface methodology." *Innovative Food Science & Emerging Technologies*, *11*(3), 485–490. doi:10.1016/j.ifset.2010.01.013

Gil, L. (**1997**). "Cork powder waste: An overview." *Biomass & Bioenergy*, *13*(1–2), 59–61.

Iversen, S., Felsvang, K., Larsen, T., Luthje, V., and Henriksen, O. (**2012**). "A method and process for controlling the temperature, pressure and density profiles in dense fluid processes and associated apparatus." WO 2005/049170.

Lumia, G., Perre, C., and Aracil, J.-M. (**2001**). "Methods for treating and extracting cork organic compounds, with a dense fluid under pressure." France: AU 200075317.

Lumia, G., Perre, C., and Aracil, J.-M. (**2007**). "Method for treating and extracting cork organic compunds, with a dense fluid under pressure." France: US 007192490B1.

Martinez, J. L., and Tapriyal, D. (**2011**). "Supercritical Fluid Extraction of Bioactive Compounds from Cereals." In *Fruit and Cereal Bioactives*. doi:10.1201/b10786-24

Martins, S., Mussatto, S. I., Martínez-Avila, G., Montañez-Saenz, J., Aguilar, C. N., and Teixeira, J. a. (**2011**). "Bioactive phenolic compounds: production and extraction by solid-state fermentation. A review." *Biotechnology Advances*, *29*(3), 365–73. doi:10.1016/j.biotechadv.2011.01.008

Mendiola, J. A., Ibáñez, E., and Herrero, M. (**2013**). "Compressed fluids for the extraction of bioactive compounds." *Trends in Analytical Chemistry*, *43*, 67–83. doi:10.1016/j.trac.2012.12.008

NATEX. (**2011**). “New Application.”

Pereira, C. G., and Meireles, M. A. a. (**2009**). “Supercritical Fluid Extraction of Bioactive Compounds: Fundamentals, Applications and Economic Perspectives.” *Food and Bioprocess Technology*, *3*(3), 340–372. doi:10.1007/s11947-009-0263-2

Pereira, H. (**1988**). “Chemical composition and variability of cork from Quercus suber L.” *Wood Science and Technology*, *22*(3), 211–218. doi:10.1007/bf00386015

Pereira, H. (**2007**). “Cork: biology production and uses” (1st ed.). Lisbon: Elsevier.

Pereira, H. (**2013**). “Variability of the Chemical Composition of Cork.” *BioResources*, *8*(2), 2246–2256.

Reverchon, E., and de Marco, I. (**2006**). “Supercritical fluid extraction and fractionation of natural matter.” *The Journal of Supercritical Fluids*, *38*(2), 146–166. doi:DOI 10.1016/j.supflu.2006.03.020

Sanjuan, B. (**2010**). “Method for extractiong organic compounds from granulated cork.” Spain: EP 2404647 A1.

Shi, J., Kassama, L. S., and Kakuda, Y. (**2007**). “Supercritical Fluid Technology for Extraction of Bioactive Components.” In *Functional Food Ingredients and Nutraceuticals*. Taylor & Francis Group.

Silva, S. P., Sabino, M. A., Fernandes, E. M., Correlo, V. M., Boesel, L. F., and Reis, R. L. (**2005**). “Cork: properties, capabilities and applications.” *International Materials Reviews*, *50*(4), 345–365. doi:10.1179/174328005X41168

Silvestre, A. J. D., Neto, C. P., and Gandini, A. (**2008**). “Cork and Suberins: Major Sources, Properties and Applications.” In *Monomers, Polymers and Composites from Renewable Resources* (p. 549). Elsevier.

“Skin Actives Scientific.” (**2015**). Retrieved March 1, 2015, from http://www.skinactives.com/betullinic-acid.html

Sousa, A. F., Pinto, P. C. R. O., Silvestre, A. J. D., and Neto, C. P. (**2006**). “Triterpenic and other lipophilic components from industrial cork byproducts.” *Journal of Agricultural and Food Chemistry*, *54*(18), 6888–6893. doi:10.1021/Jf060987+

“Tecnología Diamant.” (**2011**). *Europacork*, 37.

Wijngaard, H., Hossain, M. B., Rai, D. K., and Brunton, N. (**2012**). “Techniques to extract bioactive compounds from food by-products of plant origin.” *Food Research International*, *46*(2), 505–513. doi:10.1016/j.foodres.2011.09.027

Wu, Q., Li, H., Qiu, J., and Feng, H. (**2014**). “Betulin protects mice from bacterial pneumonia and acute lung injury.” *Microbial Pathogenesis*, *75*, 21–28. doi:10.1016/j.micpath.2014.08.005

*"Cork is an unique natural material from past to present, ensuring the future"*

# 2 Cork

Cork corresponds to the thick bark of *Quercus Suber L.* (commonly known as cork oak) that can be harvested (Figure 2.1), almost completely, without killing or endangering the tree, which is a rare characteristic, since most plant species die when a ring of bark is harvested (APCOR, 2009; Silva *et al.*, 2005). Besides, after harvested, the cork oak can produce even more cork than one that never was harvested. This species is native of the western Mediterranean region, and lives about 150 – 200 years and it usually grows to a height of 15 to 20 meters.

Figure 2.1 – Harvesting cork (http://www.casarosdenportugal.com/portugal-cork/)

The cork may be easily stripped off from the tree in late spring and early summer when the phellogen is in full activity (cell generation), allowing an easy separation of the cork layers (Silva *et al.*, 2005). In Portugal, this process is made between May and July.

The first harvest occurs when the tree has about 20 – 30 years of age and its diameter reaches 25 cm; this extracted material is known as "*virgin cork*", it has an irregular structure, thickness and density, and it also is hard-rough (Silva *et al.*, 2005). "*Virgin cork*" is only used for insulation, cork board, gaskets, shoe soles, etc. The following stripping off usually occurs 9 – 12 years later, depending on the culture region; in Portugal, harvesting takes place each 9 years.

The second harvest, "*reproduction cork*", has a more regular structure, being less hard; however, it is still not suitable for cork stoppers. The next harvest, i.e., the second cycle of 9 – 12 years, results in a material with a better quality, called "*amadia*"; this cork is mainly used to cork stoppers production, essentially to the wine sector. Until then, the farmers invested over 40 years; the wise country folks say "*plant a cork oak forest for your grandchildren*".

Even today, cork stripping continues to be a delicate process, because it is achieved with traditional tools and methods using an axe; being one of the better paid in seasonal agriculture works, since it requires qualified staff, i.e., with experience. The regular harvesting improves the health and vigour of the tree. When cork is removed from the tree a new layer begins to grow again, and this resource is constantly replaced. In average, each cork oak tree provides an average of 16 harvests over its lifespan.

The yield of stripping cork depends upon the size and age of the tree; it has enormous variation and can reach from twenty to seventy-five kg per tree; regarding the thickness of planks, they may have from about 1.27 up to 6.85 cm (Stecher, 1914, p. 17).

Cork is 100% natural, renewable and biodegradable (WWF, 2006). The human being took advantage of this noble material, even before knowing about its structure or its chemical composition, and its value continues to grow over the years; the section "*2.1 Cork, its history and Portugal*" describe a brief history of cork and how Portugal became the world leader in its production, processing and marketing. Likewise, in section "*2.2 Cork, its main properties & applications*", some of its applications that result from its distinctive cellular structure as well

as its chemical composition (Pereira, 2007; Pereira *et al.*, 1987) will be described. In the last section, of this chapter, it is summarized the manufacturing process for the production of natural cork stoppers, i.e., it shows the origin of the granulated used in this work.

## 2.1 Cork, its history and Portugal

The cork oak was established in the Mediterranean region around ten thousand years ago, and it is distributed today as shown in Figure 2.2; however, the first tree identified as a cork oak dates back from millions of years (Cork_Information_Bureau, 2010). This species is typical of the Mediterranean region, its first known application was as fishing tackle, and it was found in China, Egypt, Babylon and Persia nearly 3000 B.C. (Cork_Information_Bureau, 2010).


Figure 2.2 – Geographical distribution of cork oak.

In some Egyptian sarcophagus from the 5$^{th}$ century B.C., amphorae with cork lids for foodstuffs storage were found (Cork_Information_Bureau, 2010). While, several objects made of cork from the 4$^{th}$ century B.C. were found in Italy, such as floats, sandals (footwear), stoppers for casks and roofing materials (APCOR, 2015a). Theophrastus, an ancient Greek philosopher (4$^{th}$-3$^{th}$ century B.C.), refers in his botanical treatise "*Historia Plantarum*", that cork oak has the ability to renew its bark after removing it, and the new bark had a better quality than the previous one (Carvalho M., 2002; Cooke, 1931; Cork_Information_Bureau, 2010).

The cork uses were continuously increasing; Virgil (70 - 19 B.C.) referred that cork slabs were used for houses roofs, and Roman soldiers also used cork in their helmets against the sun heat, taking advantage of its properties as a thermal insulator (Cooke, 1931; Cork_Information_Bureau, 2010).

For centuries, this novel material was applied as one of the most versatile and broadly accepted raw materials found in nature. In the 1st century, Gaius Plinius Secundus, a Roman naturalist, known as *Pliny the Elder*, made an extensive reference to cork oaks in his "*Naturalis Historia*" (1669); he described that this particular tree, in Greece, had a high value, considering it as a symbol of honour, being the priests the only ones that were allowed to cut them down (Cork_Forest_Conservation_Alliance, 2015). Moreover, in the 2nd century A.D., Dioscorides, a Greek physician, pharmacologist and botanist, remarks some of its medicinal applications, specifically against baldness (Carvalho M., 2002; Pereira, 2007).

With regards to environmental protection legislation, Portugal was the pioneer. In 1292, Dinis, king of Portugal, banned the cutting down of cork oaks in "*Alcáçovas*"; being the first explicit reference to cork extraction activity (Carvalho M., 2002).

In medieval Europe, the main use of cork was as soles for footwear that provide isolation against the cold castles floor, particularly in winter. The use of cork as nowadays is known, i.e., as stopper for bottles holding liquids, took place only after the late 1500s (Taber, 2007).

On the other hand, in the early 1660s, Robert Hooke, an English physicist, was the first to observe cork through a microscope that he developed with fifty-times magnification, more than others at that time (Taber, 2007, p. 6); Hooke through its lens plainly perceived the structure of this material, all perforated and porous, comparable with a honey-comb, and also made rigorous drawings of its cellular structure; a reproduction of Hooke's drawings about cork cell structure is shown in Figure 2.3; he also calculated that in a cubic inch of cork must be approximately twelve hundred million cells (Taber, 2007, p. 6).

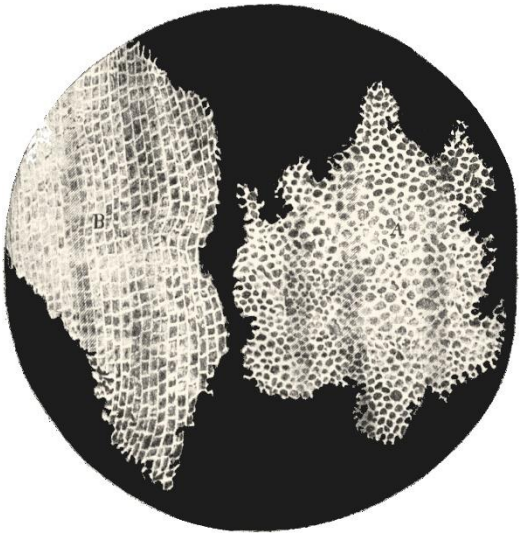

Figure 2.3 – First draw of cork cellular structure made by Robert Hooke after his microscope observation ("Robert Hooke," 2015)

Nowadays, no one knows for sure when it was the first time that cork were used as known at present time as cork stoppers. However, some stories refer that in the last quarter of the 17th century A.D., the French Benedictine monk Dom Pierre Pérignon was the first to seal its Champagne bottles with cork. Apparently, two Spanish monks on their way to Sweden visited the Abbey of Hautvillers, and they were using cork stoppers in their water gourds; then, Dom Pérignon inquired his visitors about those stoppers, and they described that they came from the bark of a tree that grew in Catalonia and provided a great way to seal a container. Afterwards, Dom Pérignon started to use cork to seal its famous champagne (1680). Despite this history be widely accepted, the true is that he was not the first to use cylindrical cork; sparkling wine was already marketed during the 60s and 70s of the 17th century, before Pérignon monks started to use it (Taber, 2007). Nonetheless, in this period the use of cork stopper bloomed, being known that the choice was also assumed by Ruinart Reims (1729) and by Moët et Chandon (1743), which is similar to today's practice (Carvalho M., 2002; Cork_Information_Bureau, 2010).

Initially, the manufacturing process to produce natural cork stoppers was completely manual; experienced workers cut the stoppers by hand, producing about three stoppers per minute (*Peres, 1988 Reminiscências de há 50 anos. Suplemento do Boletim da Junta Nacional da Cortiça Nº 600, pp. 71-75*). The 19th

century was characterized by the development of the cork industry, highlighting that the production process was systematized. In 1820, the "*garlopa"*, that was the first machine to manufacture stoppers, appeared (Figure 2.4), which allowed the systematic production of cylindrical corks, increasing their production, and it was possible to achieve values three times larger than that of an experienced worker (Pestana *et al.*, 2009); over time, auxiliary equipment arose, such as machines for stopper counting and calibration (APCOR, 2015b).

Figure 2.4 – The first industrial machine to produce cork stopper, the "*Garlopa*" (Corticeira_Amorim, 2005)

The systematization of the production process brought an increase of the market, and the waste generated by the natural cork stoppers production started to be used in new applications; then agglomerated cork was developed. In 1891, John Smith verified that when granulated cork is overheated, it is possible to obtain agglomerated cork (expanded pure agglomerate); moreover, in 1909, Charles McManus found that if those cork wastes (granulated cork) were combined with a binder they could also produce a functional product as composed agglomerated (Pestana *et al.*, 2009). With this development the applications for cork were expanded and agglomerate uses blossomed (Cork_Institute_of_America, 2008a). And the cork stoppers with a body of agglomerate and natural cork discs turned up (Cork_Forest_Conservation_Alliance, 2015).

In the last quarter of the 19$^{th}$ century, Portugal was the leader with regards to cork production, and in the beginning of the 20$^{th}$ century it held around 50% of the world production. Nevertheless, in terms of the industrial production and

exportation, Portugal assumed a leadership after the Spanish Civil War (1936-1939), because the Catalan industry, which was the largest in that period, was seriously damaged (Carvalho M., 2002).

In this sense, Figure 2.5 shows the evolution of the Portuguese cork exportation through the last century, and it is possible to remark that since the mid-20th century the value of the exportations of manufactured cork products, i.e., natural and disc cork stoppers, agglomerated and disc cork stoppers, agglomerated insulation or coating, have been increasing when comparing with non-manufactured cork products, i.e., virgin and reproduction plank cork; the same happened with semi-manufactured cork products, i.e., granulated.

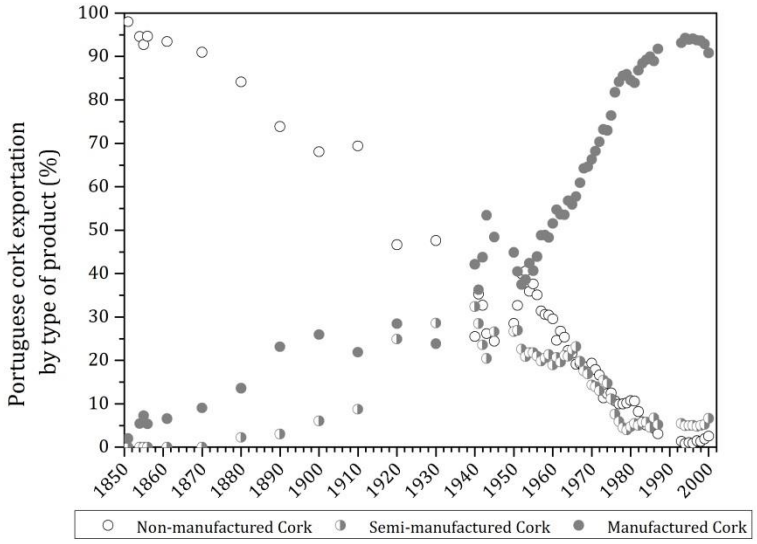


Figure 2.5 – Percentage of Portuguese corks exports by type of products (1851 – 2000). Data from: Carvalho, A. (2002)

Nowadays, Portugal keeps the leadership in the cork world market. In the last fourteen years, as shown in Figure 2.6, Portugal holds more than 60% of the value of the world's cork exports, according to the "Harmonized System Code of Chapter 45: Cork and articles of cork"; and Portugal also represents more than 67% regarding to EU28 which has about 90% of the total value.

Cork stoppers, both natural and agglomerated, represent more than half of the amount billed by the cork industry, followed by the construction industry with insulation and interior decoration and coatings (*Definição de uma estratégia de marketing para o sector da cortiça*, 1992). As a consequence, the cork industry

developed an exceptional synergy with the wine sector, since its main focus is to produce stoppers essentially for the wine sector, but not only, since some of the most expensive beers in the world (e.g. "*Jacobsen Vintage by Carlsberg"*) also use cork stoppers.

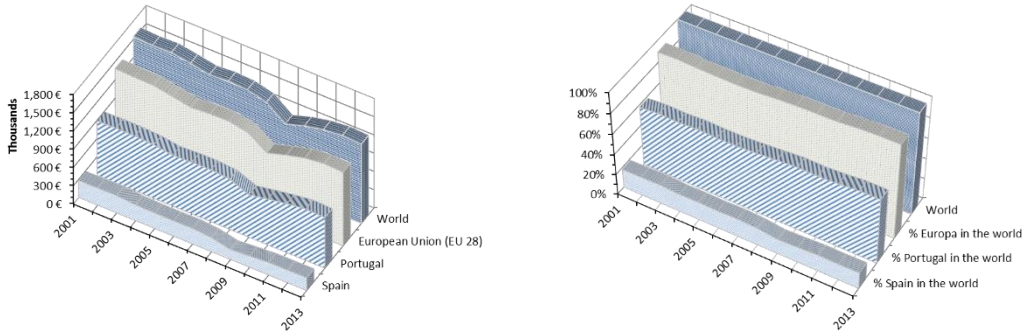


a) b)

Figure 2.6 – a) Value of world's cork exports. b) Percentage of cork exports according to HS Code Chapter 45: Cork and articles of cork

As mentioned in the previous chapter, in the last decades some problems arose; cork was identified as responsible of the so-called "*cork taste"* in wine and moreover alternatives to cork, e.g. the screwcap and plastic stoppers, appeared. Notwithstanding, the cork industry made a big effort to hold its market positions; the research being focused in way to reduce (nearly eradicate) the TCA problem and several studies and patents have been published. In spite of those challenges, the cork industry has assured its market place in world; the cork products remain to be synonymous of high quality. It is to remark that a study on the life cycle of cork stoppers shows that the natural cork stoppers are the best sealing option for wine producers, distributors and retailers who want to minimize their carbon footprint and adopt best practices in relation to environmental performance (Moreira da Silva, 2009).

Even with the cork industry focused to produce stoppers, cork continues to have endless applications, both in its natural condition and also when it is compounded with other materials. It is a material with a unique quality; in 2013, expanded cork agglomerate was recognized as one of the most innovative products for sustainable construction, integrating the "Top-10 Green Building Products" by BuildingGreen, publisher of the GreenSpec directory and Environmental Building News (EBN) (Amorim, 2012; BuildingGreens, 2013).

## 2.2 Cork, its main properties & applications

As was previously mentioned, cork can be used in wide range of applications as stoppers, isolation and flooring panels, footwear, textile material, toys and decorative items and even more, until materials to send to the space; this can be one material for the future; cork has also been incorporated into heat shields and plates lining of NASA spacecraft (Amorim, 2015).

Cork is chemically stable and mostly unaffected by microbial activity. This material is elastic and flexible with a low permeability to both liquids and gases, giving it superior sealing capabilities and avoiding, e.g. wine oxidation. It has also a very light weight and does not absorb water, being used as material for floats; cork has a low coefficient of thermal conductivity, so it is also used as thermal insulator; in addition, this material is a good sound and vibration isolator (Gil *et al.*, 2000; Pereira, 2007; Silva *et al.*, 2005).

A schematic representation of the axial section of cork oak stem with the different layers is showed in Figure 2.7.

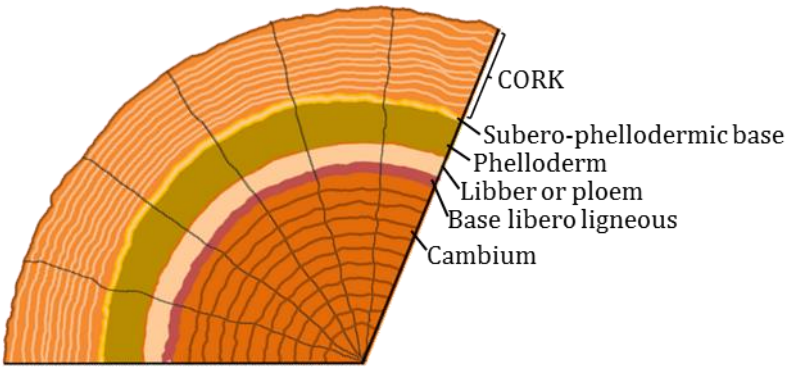


Figure 2.7 – Schematic representation of the axial section of a cork oak stem, showing the different layers

Cork has a distinctive cellular structure; being its cells, in average, closed hexagonal prisms kept in rows so that two contiguous cells share their hexagonal faces (Gil *et al.*, 2000) as shown in Figure 2.8, where 1 $cm^3$ of cork has about 42 million cells (Gil *et al.*, 2000, p. 303) that makes it very lightweight (Cork_Institute_of_America, 2008). The porosity has a close relationship with refers to the cork quality.

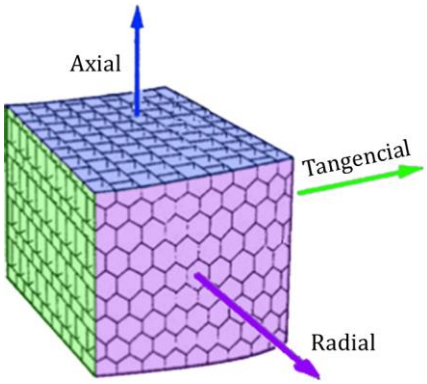


Figure 2.8 – Diagram of the cellular structure of cork (Gil *et al.*, 2000)

### 2.2.1 Chemical composition of cork

Cork is constituted by structural complex and extensive polymeric form components and non-structural components (Gil, 2006), and its chemical composition depends on several factors as the geographic and genetic origin, climate, soil and growth conditions, tree dimension and age, among many others (Silva *et al.*, 2005). Generally, cork is composed, as shown in Figure 2.9, by suberin (~40.8%), lignin (~23.8%), polysaccharides (~20.6%), and extractives (~14.7%). However, one has to take into account that the cork composition may also present some variations through the industrial processing (Conde *et al.*, 1999b), which is a consequence of different stage in the processing (stripping, "maturation" stage, boiling and rest).

The structural components of cork are suberin, lignin and polysaccharides; being the extractives a fraction of cork that can be removed without affecting its cell structure. The extractives are essentially polyphenols, long chain alkanols, triterpenes and, in minor quantities, long chain fatty acids. These non-polar cork fractions can be extracted directly with chloroform and dichloromethane. The extractives can influence the cork waterproofing properties, and also they can play protective functions against the attacks of biological organisms (Gil, 2006).

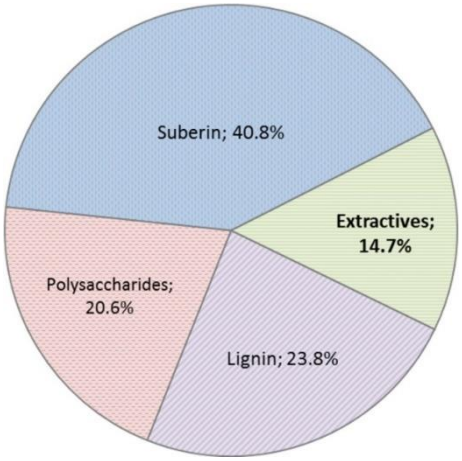


Figure 2.9 – Average chemical composition of cork.

Triterpenic compounds, that represent from about 28 up to 40% of the non-polar extract, have been studied as promising precursors for biomedical applications (Cichewicz *et al.*, 2004). However, the cork industry had been focused to remove the TCA and other contaminants (Lack *et al.*, 2009; Moura Bordado *et al.*, 2003; Taylor *et al.*, 2000), i.e., to guarantee the quality of both natural and technical cork stoppers; even small quantities of those contaminants are associated with "*cork taste*" in the wine, since those compounds have a very low sensory threshold that put in risk the essence of a good wine; the main client of cork stoppers is the wine industry.

In order to get the cork extractives, almost all published studies used conventional solvent extraction methods (Conde *et al.*, 1998, 1999a, 1999b; Pereira, 1988; Sousa *et al.*, 2006); of notice is the work of Castola *et al.* (2005) who used $CO_2$ at supercritical conditions for cork extraction and compared the results with those obtained with the Soxhlet technique. Nowadays, the supercritical fluid technology is applied with success in the cork industry through the processes developed by NATEX (Brunner, 2010; Lack *et al.*, 2009) with two plants for "cork purification" located in Spain; with a design pressure up to 150 bar and three extractors in each site, the plants were constructed in 2000 and 2004. Currently, a similar plant is under construction in France, with a design pressure of 130 bar, with also three extractors, each one with a volume of ca. 19 $m^3$. Nevertheless, all those plants have the aim to remove TCA and other contaminants that give rise to the "*cork taste*". To the best of the author's knowledge, there is no industrial process developed to extract high added-value

compounds from cork in an efficient and environmentally-friendly way as is proposed in the present work, i.e., adding a new value to cork without affecting its traditional uses. However, there are some studies on the purification of the friedelin obtained by alkaline hydrolysis, the conventional solvent extraction (LeFevre *et al.*, 2001; Pires *et al.*, 2008).

### 2.2.2 Applications of cork extractives

As previously described, the main triterpenic compound of the cork extractives are: friedelin, betulin, betulinic acid, cerine and β-sitosterol. It is to highlight that, in the last years, those compounds were studied and it was found some promising applications as isolated compounds.

Friedelin is a natural product that was isolated from cork for the first time in 1807 by Chevreul, according to his publication in the *Annales de Chimie.* Vol. 62, page 323 (LeFevre *et al.*, 2001). This compound is known as an analgesic and anti-inflammatory drug (Acton, 2013, p. 355). Ghosh *et al*. (2010) reported the antifungal activities of friedelin, that shows more activity when compared with cerine; they concluded also that friedelin should be a potential candidate drug in the treatment of some infectious diseases as consequence of its good antifungal activity *in-vitro*. Besides, it is one of the main tritepenic compounds in cork extractives; it can also be found in several others natural materials as *Azima tetracantha*, *Notonia Grandiflora*, *Vismia Laurentii*, *Calophyllum Brasiliense* (Duraipandiyan *et al.*, 2010). Antonisamy *et al*. (2011) investigated the properties of the friedelin isolated from *Azima tetracantha* Lam. Leaves, which have *in-vivo* anti-inflammatory, analgesic and antipyretic effects; Sunil *et al*. (2013) also concluded that the friedelin isolated from the *Azima tetracantha* Lam. leaves could be used to prevent the evolution of several oxidative stress-related diseases, since it possesses antioxidant and liver protective effects in *in-vitro* and *in-vivo* studies. Therefore, its biological activity makes it an extraordinary compound for further research in medicine (Antonisamy *et al.*, 2011).

With respect to betulinic acid, this has gained special attention, since it shows a variety of biological and medicinal properties. Moghaddam *et al*. (2012) made a review of the properties of betulinic acid focused on its pharmacological properties as anticancer, anti-HIV, anti-bacterial, antimalarial and some other biological activities when isolated from several plants; some researches envisage betulinic acid as a promise in the treatment of human cancers (Fulda, 2008). Birch tree (*Betula*) is an important source of betulinic acid, but mainly betulin which could be also used to synthetize betulinic acid. Also, it is detected in a wide range of species of plants (Moghaddam *et al.*, 2012; Mullauer *et al.*, 2010; Yogeeswari *et al.*, 2005). In the case of the betulin, it has also been found to have anti-bacterial, anti-inflammatory and wound-healing properties (Imlan, 2012). In its turn, β-sitosterol is used for heart disease and high cholesterol, since it reduces the total and bad cholesterol levels; FDA allows manufacturers to claim that foods containing β-sitosterol are for reducing the risk of coronary heart disease (WebMD, 2015). Table 2.1 summarizes the properties for the main triterpenes of cork extractives.

Table 2.1 – Properties and structures for the main triterpenes of cork extractives

| ID | Name<br>Formula | CAS Nº | MW<br>($g \cdot mol^{-1}$) | Tb<br>(K) | Tc<br>(K) | Pc<br>(bar) | Vc<br>($kg \cdot m^{-3}$) | Zc<br>(-) | Acentric Factor | Structure |
|---|---|---|---|---|---|---|---|---|---|---|
| 1 | Friedelin<br>$C_{30}H_{50}O$ | 559-74-0 | 426.72 | 731.3 | 923 | 10.19 | 294.0 | 0.193 | 0.66759 | 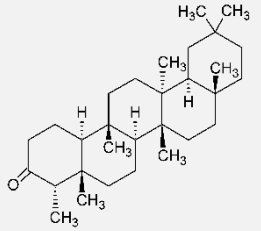 |
| 2 | Betulinic Acid<br>$C_{30}H_{48}O_3$ | 472-15-1 | 442.67 | 779.3 | 968 | 11.17 | 317.4 | 0.194 | 0.89885 | 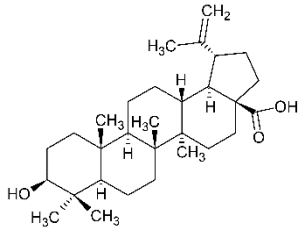 |
| 3 | Betulin<br>$C_{30}H_{50}O_2$ | 473-98-3 | 442.72 | 768.9 | 926 | 9.28 | 306.0 | 0.174 | 1.0959 | 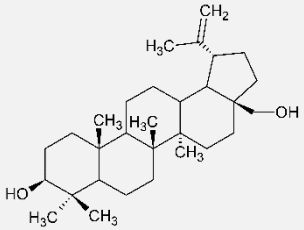 |
| 4 | Cerin<br>$C_{30}H_{50}O_2$ | 468-67-7 | 442.72 | 755.2 | 932 | 10.48 | 309.7 | 0.195 | 0.91968 | 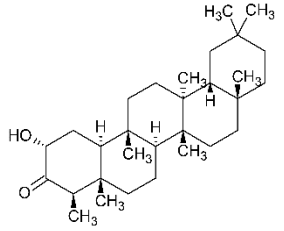 |

Table 2.1 – Properties and structures for the main triterpenes of cork extractives (*cont.*)

| ID | Name<br>Formula | CAS Nº | MW<br>($g \cdot mol^{-1}$) | Tb<br>(K) | Tc<br>(K) | Pc<br>(bar) | Vc<br>($kg \cdot m^{-3}$) | Zc<br>(-) | Acentric Factor | Structure |
|---|---|---|---|---|---|---|---|---|---|---|
| 5 | β-sitosterol<br>$C_{29}H_{50}O$ | 83-46-5 | 414.7 | 754 | 928 | 11.43 | 295.5 | 0.208 | 1.0188 | 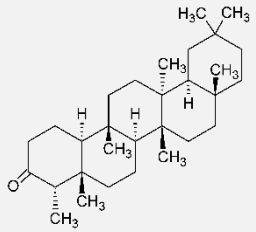 |

## 2.3 Manufacturing of cork – The granulated industrial cork

In Portugal, cork harvesting occurs each nine year. After the harvesting process, the cork planks are left out in the open air for a stabilization period of six months at least and are then sorted by quality and size. As a rule, the planks used for cork stoppers are displaced on stainless steel pallets, i.e., the planks that are in contact with the ground are never used for cork stoppers production. The remaining cork is processed to be used in the production of agglomerated cork and cork & rubber compounds with a variety of applications (Cork_Institute_of_America, 2008b).

Next, the planks to produce stoppers are boiled ca. 30 min in purified water, free of any microbiological contamination. Afterwards, they are submitted to a quality selection process and kept in controlled ambient conditions; during this step, the risk of mould growth is higher. After a stabilization time, the planks are ready to continue the production process.

Selected planks are punched, giving rise to the natural cork stoppers; this stoppers are selected manually or, recently, by image analysis; all stoppers unsuitable or discarded during production and the rest of the planks that were submitted to punching are taken to a grinding stage in order to be used subsequently in a variety of applications. In this stage, the material is granulated and separated by particle size and density according to its following applications, to technical cork stoppers and also can be used as agglomerates among many other applications. In order to add a new value and enlarge the markets to the cork industry, the raw material to be used in this work was constituted by the granulated and powder generated in this stage. Since the focus is to add value to cork without compromising its traditional uses as represented in Figure 2.10, it is to highlight that the total or even just a portion of the granulated can be extracted and returned to the actual process to be used in its traditional applications thus resulting in a new value to cork. In other words, the proposal is that the raw material does a by-pass to the traditional process, in order to add an efficient and environmentally-friendly extraction

process to get the compounds concealed in cork. It is to highlight that the cork powder can also be extracted; actually ca. 20 – 30% of the cork entering the mill ends as cork powder, currently burned to produce energy (Cordeiro *et al.*, 1998).

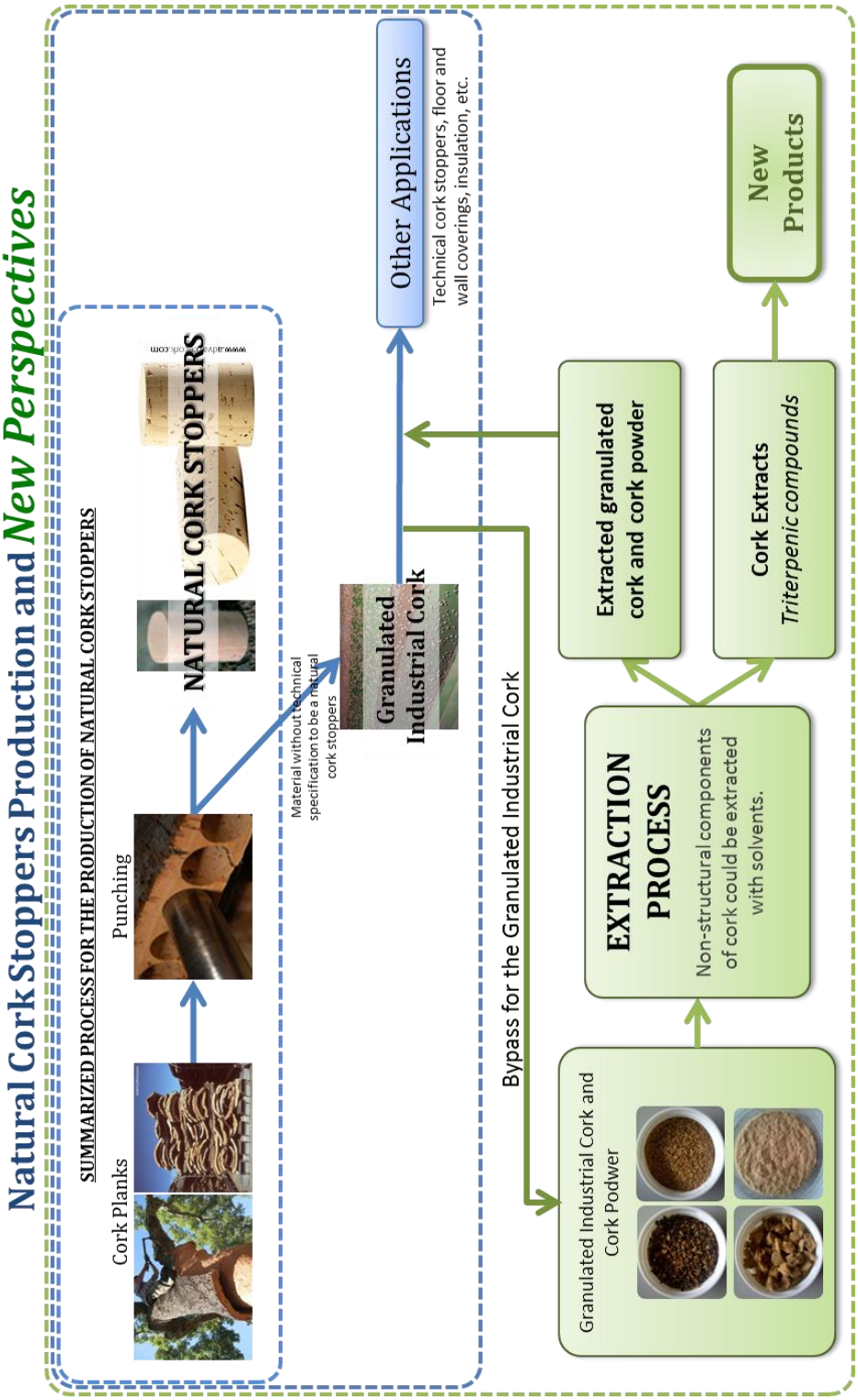


Figure 2.10 – New process step to add a new value to cork

# References


Acton, A. Q. (**2013**). "Terpenes—Advances in Research and Application." (S. Editions, Ed.) (2013 Ed). Atlanta, Georgia.

Amorim. (**2012**). "Corticeira Amorim's expanded insulation cork board in U.S. BuildingGreen's TOP 10 products." Retrieved February 1, 2015, from http://www.amorim.com/en/whats-new/news/Corticeira-Amorims-expanded-insulation-cork-board-in-US-BuildingGreens-TOP-10-products/700/

Amorim. (**2015**). "Nature without limits." Retrieved January 1, 2015, from http://www.amorimcork.com/en/natural-cork/cork-and-other-applications/

Antonisamy, P., Duraipandiyan, V., and Ignacimuthu, S. (**2011**). "Anti-inflammatory, analgesic and antipyretic effects of friedelin isolated from Azima tetracantha Lam. in mouse and rat models." *The Journal of Pharmacy and Pharmacology*, *63*(8), 1070–1077. doi:10.1111/j.2042-7158.2011.01300.x

APCOR. (**2009**). "Yearbook 2009." Associação Portuguesa da Cortiça.

APCOR. (**2015a**). "História da cortiça." Retrieved February 1, 2015, from http://apcor.pt/artigo/historia-cortica.htm

APCOR. (**2015b**). "History of Cork." Retrieved February 1, 2015, from http://www.apcor.pt/artigo/1.htm

Brunner, G. (**2010**). "Applications of Supercritical Fluids." *Annual Review of Chemical and Biomolecular Engineering, Vol 1*, *1*, 321–342. doi:10.1146/annurev-chembioeng-073009-101311

BuildingGreens. (**2013**). "Buildinggreens Top 10 Products 2013." Retrieved February 1, 2015, from https://www2.buildinggreen.com/buildinggreens-top-10-products-2013

Carvalho M., A. (**2002**). "A economia do sector da cortiça em Portugal." *Faculdade de Economia E Gestão*. Porto: Universidade Católica Portuguesa.

Castola, V., Marongiu, B., Bighelli, A., Floris, C., Laï, A., and Casanova, J. (**2005**). "Extractives of cork (Quercus suber L.): chemical composition of dichloromethane and supercritical CO2 extracts." *Industrial Crops and Products*, *21*(1), 65–69. doi:10.1016/j.indcrop.2003.12.007

Cichewicz, R. H., and Kouzi, S. A. (**2004**). "Chemistry, biological activity, and chemotherapeutic potential of betulinic acid for the prevention and treatment of cancer and HIV infection." *Medicinal Research Reviews*, *24*(1), 90–114. doi:10.1002/med.10053

Conde, E., Cadahía, E., Garcia-Vallejo, M. C., and Gonźalez-Adrados, J. R. (**1998**). "Chemical Characterization of Reproduction Cork from Spanish Quercus Suber." *Journal of Wood Chemistry and Technology*, *18*(4), 447–469. doi:10.1080/02773819809349592

Conde, E., Garcia-Vallejo, M. C., and Cadahía, E. (**1999a**). "Waxes composition of Quercus suber reproduction cork from different Spanish provenances." *Wood Science and Technology*, *33*(4), 271–283. doi:10.1007/s002260050115

Conde, E., Garcia-Vallejo, M. C., and Cadahía, E. (**1999b**). "Waxes composition of reproduction cork from Quercus suber and its variability throughout the industrial processing." *Wood Science and Technology*, *33*(3), 229–244. doi:10.1007/s002260050112

Cooke, G. (**1931**). "Cork and its uses." *Journal of Chemical Education*, *8*(8), 1463–1492.

Cordeiro, N., Belgacem, M. N., Silvestre, A. J. D., Neto, C. P., and Gandini, A. (**1998**). "Cork suberin as a new source of chemicals. 1. Isolation and chemical characterization of its composition." *International Journal of Biological Macromolecules*, *22*(2), 71–80. doi:10.1016/S0141-8130(97)00090-1

Cork_Forest_Conservation_Alliance. (**2015**). "History of Cork." Retrieved January 1, 2015, from http://www.corkforest.org/history-of-cork/

Cork_Information_Bureau. (**2010**). "CORK - HISTORY." Portugal.

Cork_Institute_of_America. (**2008**). "Cork History." Retrieved January 1, 2015, from http://www.corkinstitute.com/history.html

Cork_Institute_of_America. (**2008**). "Harvest." Retrieved January 1, 2015, from http://www.corkinstitute.com/harvest.html

Cork_Institute_of_America. (**2008**). "Properties." Retrieved February 1, 2015, from http://www.corkinstitute.com/properties.html

Corticeira_Amorim. (**2005**). "The art of cork." Mozelos: Corticeira Amorim.

"Definição de uma estratégia de marketing para o sector da cortiça." (**1992**).

Duraipandiyan, V., Gnanasekar, M., and Ignacimuthu, S. (**2010**). "Antifungal activity of triterpenoid isolated from Azima tetracantha leaves." *Folia Histochemica et Cytobiologica*, *48*(2), 311–313. doi:10.2478/v10042-010-0005-3

Fulda, S. (**2008**). "Betulinic acid for cancer treatment and prevention." *International Journal of Molecular Sciences*, *9*(6), 1096–1107. doi:10.3390/ijms9061096

Ghosh, P., Mandal, A., Chakraborty, M., and Saha, A. (**2010**). "Triterpenoids from Quercus suber and their antimicrobial and phytotoxic activities." *J. Chem Pharm. Res*, *2*(4), 714–721.

Gil, L. (**2006**). "A cortiça como material de construção. Manual Técnico." Portugal.

Gil, L., and Moiteiro, C. (**2000**). "Cork." In *Ullmann's Encyclopedia of Industrial Chemistry*. Wiley-VCH Verlag GmbH & Co. KGaA. doi:10.1002/14356007.f07_f01

Imlan. (**2012**). "Betulin." Retrieved February 1, 2015, from http://www.imlan.de/en/what-is-betulin.html

Lack, E., Seidlitz, H., Bakali, M., and Zobel, R. (**2009**). "Cork treatment - A new industrial application of supercritical fluids." *Proc. Int. Symp. Supercrit. Fluids,*. Retrieved from http://www.isasf.net/fileadmin/files/Docs/Arcachon/oraux/c04-CO42 Lack Manuskript.pdf

LeFevre, J. W., McNeill, K. I., and Moore, J. L. (**2001**). "Isolating Friedelin from Cork and Reducing It to Friedelinol and Epifriedelinol. A Project Involving NMR Spectrometry and Molecular Modeling." *Journal of Chemical Education*, *78*(4), 535. doi:10.1021/ed078p535

Moghaddam, M. G., Ahmad, F. B. H., and Samzadeh-kermani, A. (**2012**). "Biological Activity of Betulinic Acid: A Review." *Pharmacology & Pharmacy*, *3*, 119–123. doi:10.4236/pp.2012.32018

Moreira da Silva, R. P. (**2009**). "Avaliação do Ciclo de Vida Da Rolha de Cortiça Natural." Universidade do Porto.

Moura Bordado, J. C., Santos Marques, J. P., Pissarra Goncalves, M. A., Allegro, I. M., Mesquita, A. C., and Lopes Filipe, R. (**2003**). "New Process for treating cork stoppers or planks for the reduction of strange aromas, namely 2,4,6-Trichoroanisole." Portugal: WO 03/041927 A1.

Mullauer, F. B., Kessler, J. H., and Medema, J. P. (**2010**). "Betulinic acid, a natural compound with potent anticancer effects." *Anti-Cancer Drugs*, *21*(3), 215–227. doi:10.1097/CAD.0b013e3283357c62

Pereira, H. (**1988**). "Chemical composition and variability of cork from Quercus suber L." *Wood Science and Technology*, *22*(3), 211–218. doi:10.1007/bf00386015

Pereira, H. (**2007**). "Cork: biology production and uses" (1st ed.). Lisbon: Elsevier.

Pereira, H., Rosa, M. E., and Fortes, M. A. (**1987**). "The cellular structure of cork Quercus Suber L." *IAWA Bulletin*, *8*(3), 213–218.

Pestana, M., and Tinoco, I. (**2009**). "A Indústria e o Comércio da Cortiça em Portugal Durante o Século XX." *Silva Lusitana*, *17*(1), 1–26.

Pires, R. A., Martins, S., Chagas, J. A., and Reis, R. L. (**2008**). "Extraction and purification of friedelin." Portugal: WO 2009/072916 A1.

"Robert Hooke." (**2015**). Retrieved January 1, 2015, from https://en.wikipedia.org/wiki/File:RobertHookeMicrographia1665.jpg

Silva, S. P., Sabino, M. A., Fernandes, E. M., Correlo, V. M., Boesel, L. F., and Reis, R. L. (**2005**). "Cork: properties, capabilities and applications." *International Materials Reviews*, *50*(4), 345–365. doi:10.1179/174328005X41168

Sousa, A. F., Pinto, P. C. R. O., Silvestre, A. J. D., and Neto, C. P. (**2006**). "Triterpenic and other lipophilic components from industrial cork byproducts." *Journal of Agricultural and Food Chemistry*, *54*(18), 6888–6893. doi:10.1021/Jf060987+

Stecher, G. (**1914**). "Cork: Its origin and industrial uses." New York.

Sunil, C., Duraipandiyan, V., Ignacimuthu, S., and Al-Dhabi, N. A. (**2013**). "Antioxidant, free radical scavenging and liver protective effects of friedelin isolated from Azima tetracantha Lam. leaves." *Food Chemistry*, *139*(1–4), 860–865. doi:10.1016/j.foodchem.2012.12.041

Taber, G. M. (**2007**). "To cork or not to cork." London: Scribner.

Taylor, M. K., Young, T. M., Butzke, C. E., and Ebeler, S. E. (**2000**). "Supercritical Fluid Extraction of 2,4,6-Trichloroanisole from Cork Stoppers." *Journal of Agricultural and Food Chemistry*, *48*, 2208–2211. doi:10.1021/jf991045q

WebMD. (**2015**). "beta-sitosterol." Retrieved February 1, 2015, from http://www.webmd.com/vitamins-supplements/ingredientmono-939-beta-sitosterol.aspx?activeingredientid=939&activeingredientname=beta-sitosterol

WWF. (**2006**). "Cork screwed? Environmental and economic impacts of the cork stoppers market."

Yogeeswari, P., and Sriram, D. (**2005**). "Betulinic acid and its derivatives: a review on their biological properties." *Current Medicinal Chemistry*, *12*(6), 657–66. doi:10.2174/0929867053202214

*"plant a cork oak forest*
*for your grandchildren"*

# 3 Soxhlet Extraction

A conventional soxhlet extraction, the current benchmark technology, was performed in order to be a reference to yields and to the composition of cork extracts obtained by supercritical fluid extraction (SFE); also, an analytical method was developed for the identification and quantification of the cork extracts compounds.

Initially, the samples were characterized, determining their cork density, bulk density, particle size and moisture content. The granulated industrial cork and cork powder were soxhlet extracted, and cork extracts were derivatized prior to gas chromatography (GC) analysis.

## 3.1 Characterization of samples

Samples were constituted by granulated industrial cork of different particle sizes and densities, provided by António Almeida, Cortiças, S.A. (AAC) from their industrial facilities (in 2011). They were obtained by milling punched cork planks (Figure 3.1) that were used to produce single-piece natural cork stoppers, and also by cork material that did not meet the quality requirements for single-piece stoppers production. It is worth to note that the cork planks were previously submitted to a boiling-water treatment, which corresponds to one of the conventional industrial stages before the production of natural cork stoppers.

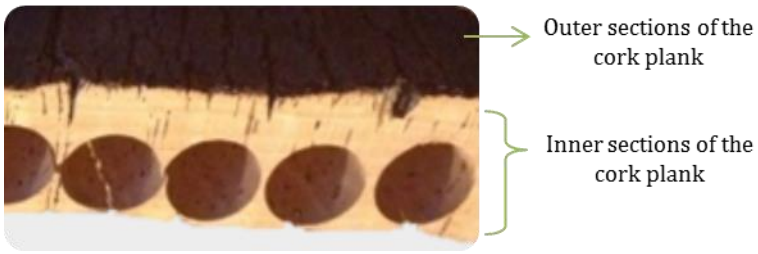


Figure 3.1 – Punched cork planks.

The samples were automatically separated, according to particle size, in the AAC facilities by their industrial milling equipment; altogether nine different samples cataloged from A1 to A9 and shown in Table 3.1 were obtained. Despite cork samples have different size, cork powder (<0.2 mm) and granulated from 0.5 to 6 mm, it is possible to note that cellular structures are similar as previously shown (Chapter 2); since cork has an anisotropic structure, the difference is related to the direction: axial, radial or tangential (Figure 2.8). It is to highlight that samples are constituted by granulated cork, then the directions shown in Figure 3.2 are random.

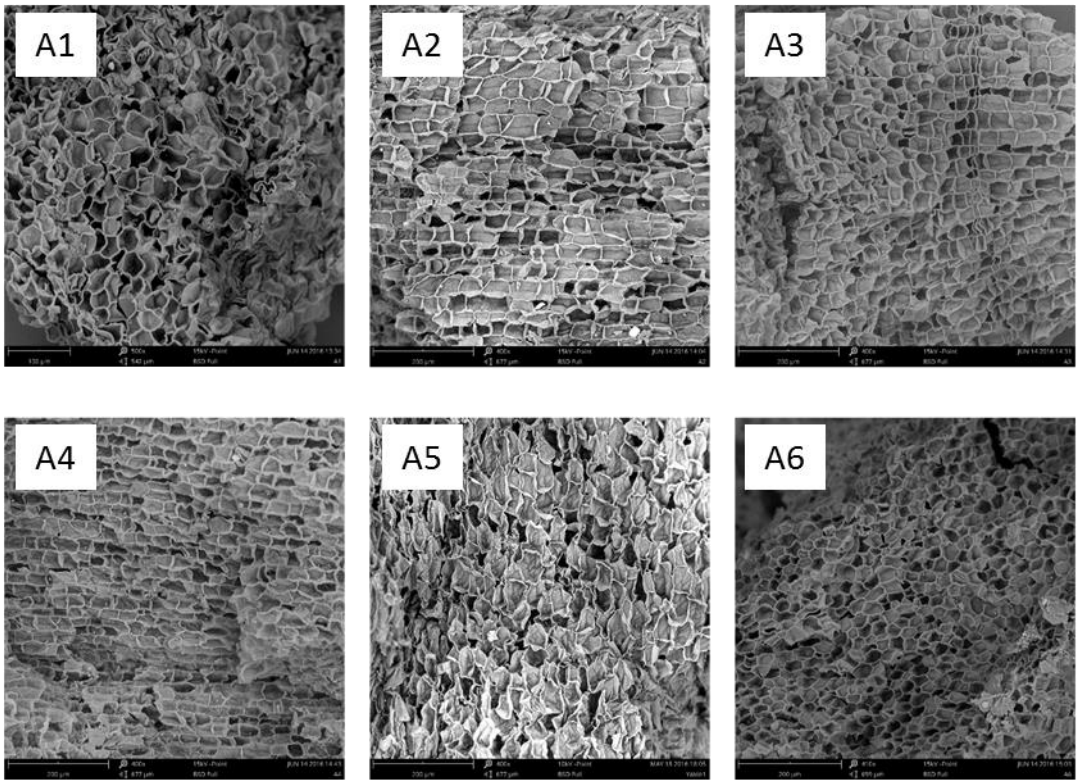


Figure 3.2 – SEM for samples A1 to A6 that correspond to inner section of plank.

Besides size, the samples can also be separated in two different types by visual inspection: (i) granulate from inner sections of the cork plank (A1-A6), and

(ii) from outer sections of the plank (A7 and A9), that are characterized by a darker color, as presented in Figure 3.3. It is to note that sample A8 corresponds to cork powder.

Table 3.1 – Particle size, bulk density, apparent density and moisture content of industrial granulated cork samples.

| Sample | Size Group (mm) | Average Particle size (mm) | Moisture (%) | Cork density ($kg \cdot m^{-3}$) | Bulk density ($kg \cdot m^{-3}$) | Apparent density ($kg \cdot m^{-3}$) |
|---|---|---|---|---|---|---|
| **A1** | 0.5 – 1 | 0.75 | 5.4 ± 0.1 | 710 ± 58 | 89 ± 6 | 209 |
| **A2** | 0.5 – 2 | 1.25 | 6.3 ± 0.1 | 334 ± 42 | 66 ± 5 | 159 |
| **A3** | 0.5 – 1 | 0.75 | 5.0 ± 0.1 | 546 ± 102 | 54 ± 3 | 141 |
| **A4** | 1 – 4 | 2.5 | 6.7 ± 0.1 | 326 ± 21 | 73 ± 5 | 173 |
| **A5** | 4 – 6 | 5 | 4.8 ± 0.1 | 266 ± 14 | 67 ± 4 | 166 |
| **A6** | 2 – 4 | 3 | 9.2 ± 0.1 | 267 ± 27 | 64 ± 3 | 170 |
| **A8*** | < 0.2 | < 0.2 | 5.2 ± 0.1 | 1160 ± 121 | 70 ± 11 | 233 |
| **A7**** | 0.5 – 2 | 1.25 | 13.7 ± 0.1 | 600 ± 31 | 160 ± 12 | 381 |
| **A9**** | 0.5 – 2 | 1.25 | 17.9 ± 0.3 | 998 ± 17 | 310 ± 16 | 762 |

* Cork powder
** Granulated industrial cork from the outer section of plank

### 3.1.1 Cork density, bulk density and particle size

The density depends on several factors as particle size and shape, specific density of individual particles and material composition (Lam *et al.*, 2008; Miranda *et al.*, 2012). The samples were automatically separated by size and density in the milling equipment. Table 3.1 shows, for each size group, the bulk density determined using a cylindrical container dividing the mass of the sample in the container by the volume of the container; to evaluate the cork (solid) density and the apparent density, helium pycnometry and mercury pycnometry were used, respectively.

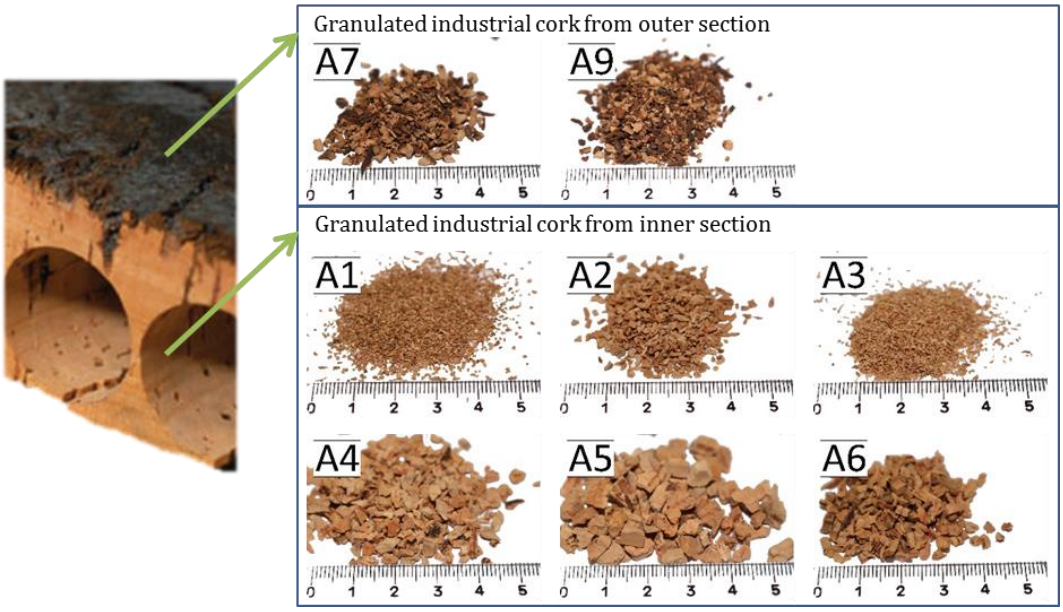


Figure 3.3 – Granulated industrial cork from two sections of cork planks: inner (A1 to A6) and outer (A7 and A9).

The region of the cork plank from where the sample comes represents the most important parameter that affects the bulk density of the granulated cork; the particles from the outer sections of the plank have larger bulk density values, between 160 and 310 $\mathrm{kg \cdot m^{-3}}$, which are at least two times the bulk density of the particles from the inner sections. With regard to the particles from inner sections, the bulk density is between 54 and 89 $\mathrm{kg \cdot m^{-3}}$. The internal particle porosity ($\varepsilon_p$) and the void fraction of packing (bulk porosity, $\varepsilon_b$) were calculated by Eq. 3.1.

$$\rho_{bulk} = \rho_{app}\left(1-\varepsilon_b\right) = \rho_{cork}\left(1-\varepsilon_p\right)\left(1-\varepsilon_b\right) \qquad \text{Eq. 3.1}$$

The total voidage ($\varepsilon_t$) in a packed bed (outside and inside particles) relates the void fraction of packing and internal porosity as described by,

$$\varepsilon_t = \varepsilon_b + \left(1-\varepsilon_b\right)\varepsilon_p \qquad \text{Eq. 3.2}$$

On average, for the granulated industrial cork from inner section, the total voidage is 0.81 ($\pm$ 0.07); this value excluded the cork powder and granulated cork from outer section. Figure 3.5 shows the total voidage ($\varepsilon_t$) of each sample.

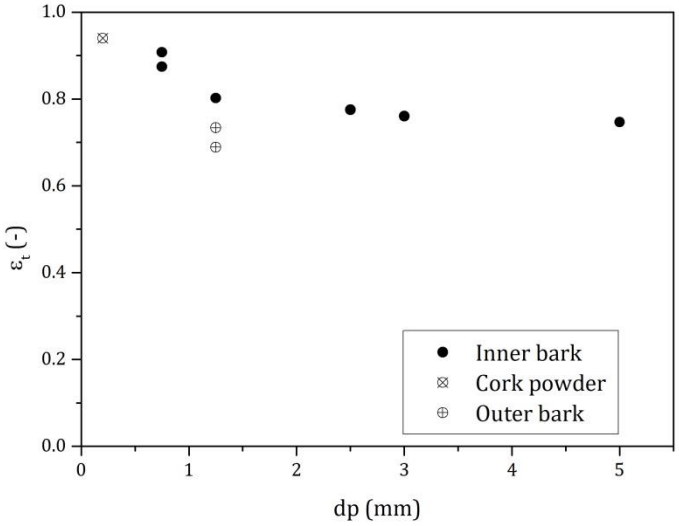


Figure 3.4 – Total void space ( $\varepsilon_t$ ) for each sample *vs*. average particle size.

Figure 3.5 represents the internal porosity ( $\varepsilon_p$ ) *vs*. average particle size, for granulated industrial cork and cork powder; on average, for particles with size bigger than 1 mm, the internal porosity is 0.39 ($\pm$ 0.10).

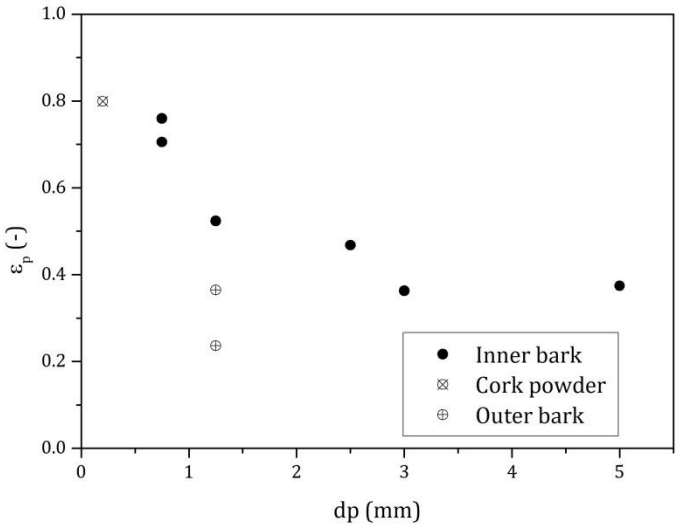


Figure 3.5 – Internal porosity ( $\varepsilon_p$ ) *vs*. average particle size.

## 3.2 Soxhlet extraction

Soxhlet extraction is a leaching technique for extraction from solid samples; it is a batch system continuously operated due to the solvent distillation and recirculation. In this extraction method, the sample is repeatedly in contact with

a fresh solvent, i.e., the solvent recirculates through the sample, which provides a great advantage (de Castro *et al.*, 2010).

The design of the Soxhlet was originally thought for lipids extraction from solid matrixes; nonetheless, this apparatus is not limited to lipids: if the component to extract is soluble in the solvent, this method can be applied. The first soxhlet extractor was proposed in 1879, by Franz Ritter von Soxhlet, in a research work dealing with the determination of milk fat (Jensen, 2007). Figure 3.6 shows a schematic representation of a soxhlet extractor.

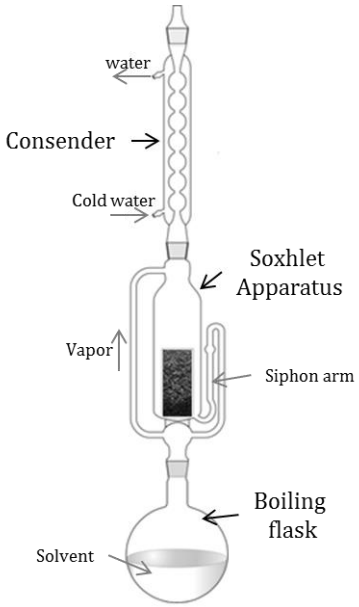


Figure 3.6 – Schematic representation of a soxhlet extractor.

Soxhlet extraction is a well-established technique that has been a standard for over a century. Currently, new leaching methods are still based on its primary references (de Castro *et al.*, 2010). Normally, soxhlet extraction is regarded as the "*benchmark technique*" for solid-liquid extraction against which all other extraction techniques are compared (Feilden, 2010), being the soxhlet recoveries regarded as high (Dean, 2009).

Until now, several studies were conducted to evaluate the chemical composition of cork (Castola *et al.*, 2002, 2005; Conde *et al.*, 1999; Pereira, 1988; Santos *et al.*, 2013; Sousa *et al.*, 2006), as mentioned in previous chapters; cork is constituted by extractives that can be easily removed by solvents without damaging its structure. In this sense, the total extractives of cork samples can be

obtained by sequential soxhlet extraction, using solvents of increasing polarity (Pereira, 1988; Sousa *et al.*, 2006).

Table 3.2 summarizes the yields obtained for the extraction of several cork samples; virgin cork, reproduction cork, and cork samples from different stages in the industrial process are included; the samples were milled to particle size lower than 1 mm and sequentially soxhlet extracted using as first solvent dichloromethane or chloroform.

The samples before industrial processing, i.e., virgin cork and reproduction cork, after harvesting, presented higher yields when extracted with dichloromethane, giving values of 79 $g_{extract} \cdot kg_{DryCork}^{-1}$ and 60 $g_{extract} \cdot kg_{DryCork}^{-1}$, respectively; otherwise, the industrial cork powder had the lowest yields.

It is to highlight that, according to Conde *et al.* (1999), the content of extractives in cork decreases throughout the industrial processing; the cork after the stripping had yields two times higher when compared with the samples after the boiling process.

As already mentioned, the samples used in this work were constituted by granulated industrial cork obtained from punched cork planks after the boiling-water treatment. These samples include from cork powder (<0.2 mm) until particles with 6 mm, and some samples (A7 and A9) also contain particles from the most external layer of the cork plank.

Table 3.2 – Yields obtained in the cork extract from several cork samples

| Material | Particle size | Solvent | *Yield* ($g_{extract} \cdot kg^{-1}_{DryCork}$) | Reference |
|---|---|---|---|---|
| Virgin Cork | 40 - 60 mesh | DCM | 79 | (Pereira, 1988) |
| Reproduction Cork | 40 - 60 mesh | DCM | 54 | (Pereira, 1988) |
| Cork powder from the outer bark *Q. suber* excluding the most external layer | Cork powder | DCM | 60 | (Castola *et al.*, 2002) |
| Natural cork planks – "amadia" grade | 40 - 60 mesh | DCM | 59.3 | (Santos *et al.*, 2013) |
| Cork powder from the outer bark of *Q. suber* excluding the most external layer | 40 - 60 mesh | DCM | 60 | (Castola *et al.*, 2005) |
| Cork powder from the outer bark of *Q. suber* excluding the most external layer - Industrial Processing - Stripping | 0.5 - 1 mm | Chloroform | 101.3 | (Conde *et al.*, 1999) |
| Cork powder from the outer bark of *Q. suber* excluding the most external layer - Industrial Processing - First rest | 0.5 - 1 mm | Chloroform | 80.8 | (Conde *et al.*, 1999) |
| Cork powder from the outer bark of *Q. suber* excluding the most external layer - Industrial Processing - Boiling open air rest | 0.5 - 1 mm | Chloroform | 49.1 | (Conde *et al.*, 1999) |
| Cork powder from the outer bark of *Q. suber* excluding the most external layer - Industrial Processing - Boiling + store rest | 0.5 - 1 mm | Chloroform | 53.2 | (Conde *et al.*, 1999) |
| Industrial cork powder | 40 - 60 mesh | DCM | 22.6 | (Santos *et al.*, 2013) |
| Industrial cork powder | 40 - 60 mesh | DCM | 26 | (Sousa *et al.*, 2006) |
| Cork powder from the outer bark of *Q. suber* e boiled cork planks obtained after a cork cooking stage | 40 - 60 mesh | DCM | 42 | (Sousa *et al.*, 2006) |
| Cork powder from the outer bark of *Q. suber* e, particles from inner sections of planks boiled cork planks obtained after a cork cooking stage | 40 - 60 mesh | DCM | 50 | (Sousa *et al.*, 2006) |
| Cork powder from the outer bark of *Q. suber* e, particles from outer sections of planks boiled cork planks obtained after a cork | 40 - 60 mesh | DCM | 27 | (Sousa *et al.*, 2006) |

The yields in Table 3.2 were assumed as an estimate/reference, since the composition of cork depends on several factors, such as climate and soil conditions, geographical and genetic origin, tree dimension, age and growth conditions (Silva *et al.*, 2005).

In this work, all samples were conventionally soxhlet extracted, and the procedure is shown in Figure 3.7. Table 3.3 presents the parameters for the soxhlet extraction. First, ca. 6–10 g of sample was weighed in a thimble; the ratio of solvent/solid matrix is 12–20 $\mathrm{mL}_{\mathrm{solvent}} \cdot \mathrm{g}_{\mathrm{Cork}}^{-1}$ ; in soxhlet extraction, the concentration of the extractable components in the solvent increases with time (after the first cycle); for each cycle, a new portion of the extractable fraction is extracted and this process is repeated as many times as necessary until it reaches the maximum extractable for the solvent. The total time of extraction was fixed as 8 h (approximately 50 cycles). All extractions were performed in triplicate, and three solvents with different polarities, hexane (HEX), dichloromethane (DCM) and acetone (ACE), were used; as the experimental procedure considers the screening of the effects of all variables, as particle size and sample density, i.e. cork samples A1 to A9 (see Table 3.1), a total of 81 extractions were done.

Table 3.3 – Parameters for the Soxhlet extraction

| | |
|---|---|
| **Samples:*** | **A1 up to A9** |
| **Solvents:** | Hexane (hex), dichloromethane (dcm) or acetone (ace) |
| **Mass of sample:** | 6 – 10 g |
| **Ratio of solvent/solid matrix:** | 12 – 20 $\mathrm{mL}_{\mathrm{solvent}} \cdot \mathrm{g}_{\mathrm{Cork}}^{-1}$ |
| **Extraction time** | 8 h (ca. 50 cycles) |

*To each solvent new samples were extracted and all extractions were performed in triplicate.

After soxhlet extraction, cork extracts were separated from each solvent by a rotary evaporator; as a consequence of the reduced pressure, the solvent evaporates at lower temperatures and guarantees that the extract is not over-heated. At the end, it is possible to quantify the total yield for each solvent and sample.

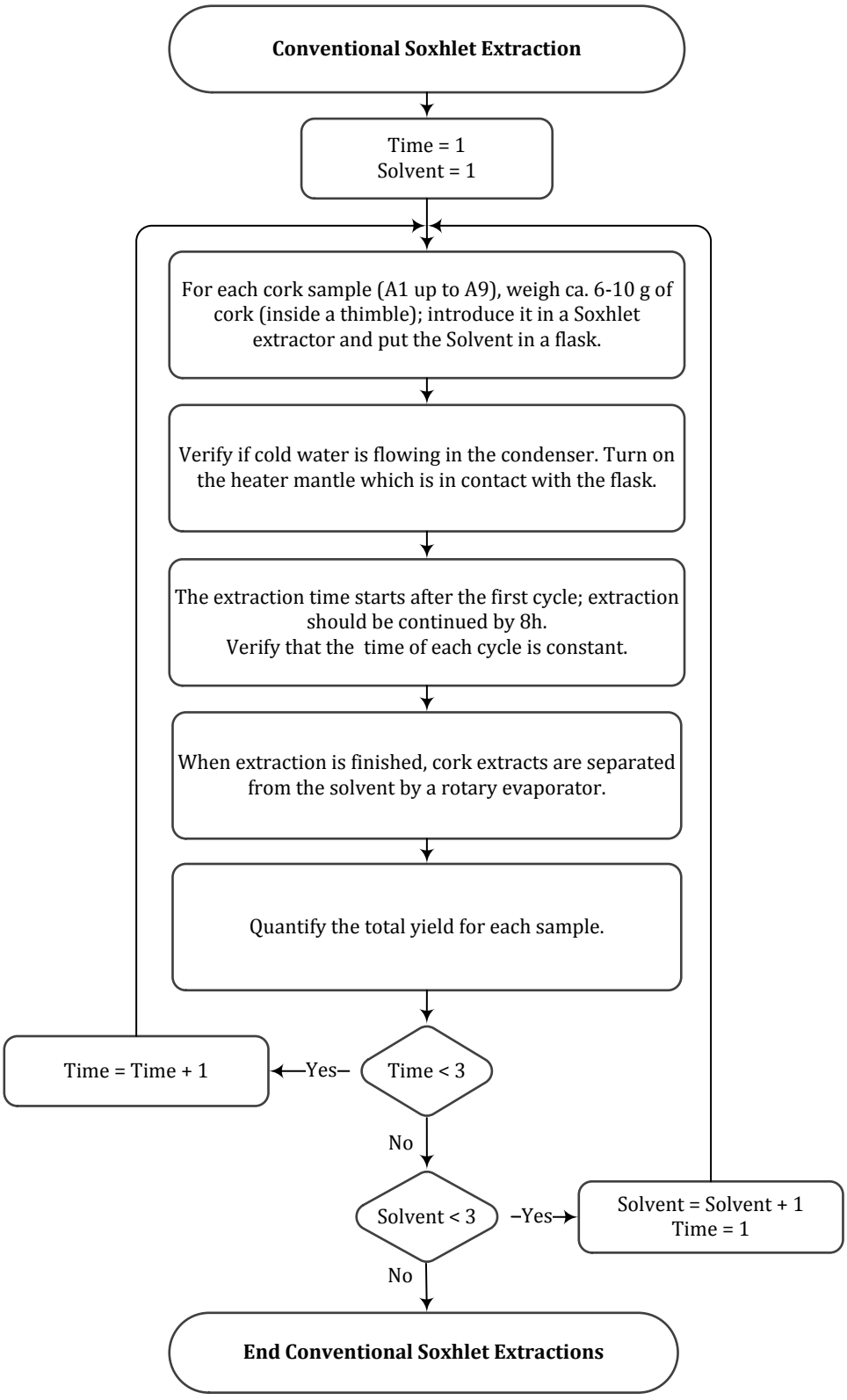


Figure 3.7 – Conventional method for soxhlet extraction.

In the next section (3.2.1 Yields), the effect of different parameters is evaluated with respect to the performance of the extraction.

### 3.2.1 Yields

The extraction yields (on a dry basis) obtained for each solvent are depicted in Figure 3.8 as a function of the average particle size. The influence of solvent polarity, particle size and density were analyzed in view of determining their effect on the yields.

For all samples (A1 to A9), the yield increases with the polarity of the solvent, regardless of the average particle size (or cork density). This increase was probably related with the increase of solvent power for a wider range of low molecular weight compounds present in the cork material.

The maximum yield (84 $g_{extract} \cdot kg^{-1}_{DryCork}$) was obtained for sample A1 using acetone as solvent; the value was ca. 17 and 42% higher than the ones obtained with dichloromethane and hexane, respectively, for the same sample.

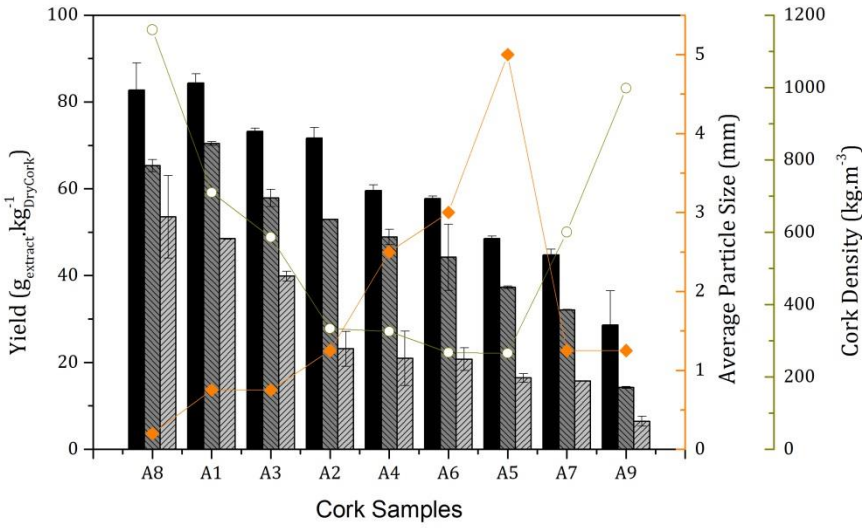


Figure 3.8 – Yields of conventional soxhlet extraction of industrial granulated cork as a function of particle size, for the three solvents tested: (black) acetone, (gray) dichloromethane, (light gray) hexane. (A8) cork powder, (A1 to A6) inner bark and (A7 and A9) outer bark samples. The diamonds represent the average particle size and the circles the cork density.

With respect to dichloromethane, the yields of samples from the inner section of cork planks (A1 to A6) were 37 to 70 $g_{extract} \cdot kg^{-1}_{DryCork}$; while the ones of samples from the outer section (A7 and A9) were 14 to 32 $g_{extract} \cdot kg^{-1}_{DryCork}$. Sousa *et al.* (2006) reported, for similar samples with a granulometric fraction of 40–

60 mesh (ca. 0.4 – 0.2 mm), a yield of 50 $g_{extract} \cdot kg^{-1}_{DryCork}$ for particles from the inner section of planks after the boiling process; whereas for samples from the outer section, the yield obtained was 27 $g_{extract} \cdot kg^{-1}_{DryCork}$. The results achieved by Sousa *et al.* (2006) were within the interval obtained in this work. Also, both works showed that the yields for the inner section were higher than those for the outer section.

It is to highlight that the maximum yields obtained in this work, for each individual solvent, were lower than the yields reached by Sousa *et al.* (2006); for sequential extraction (dichloromethane, methanol and water) these were 112 and 57 $g_{extract} \cdot kg^{-1}_{DryCork}$ for samples from the inner and the outer sections of the planks after the boiling process, respectively.

Regarding to industrial cork powder, Sousa *et al.* (2006) and Conde *et al.* (1999), achieved yields of 26 and 22.6 $g_{extract} \cdot kg^{-1}_{DryCork}$, respectively, using dichloromethane; however, those values were 60 and 65% lower than those obtained in this work for the same solvent and sample A8.

The influence of particle size in soxhlet extraction yields was also studied. Figure 3.8 shows that the yields decrease for all solvents, regardless of the cork density, when the particle size increases (within the inner bark samples: from A1 to A6). As previously referred, the highest yields were obtained for sample A1, the smallest particles (after cork powder). On the other hand, the lowest yields were obtained with sample A5 (excluding the samples from the outer section), i.e., the largest particles: 16 $g_{extract} \cdot kg^{-1}_{DryCork}$ (HEX), 37 $g_{extract} \cdot kg^{-1}_{DryCork}$ (DCM) and 48 $g_{extract} \cdot kg^{-1}_{DryCork}$ (ACE).

The cork samples from the outer section of cork planks had the lowest yields for all solvents used; despite having the same particle size, yields 50% higher for sample A7 than for sample A9 were obtained, in average.

The effect of particle size is more pronounced as the polarity of the solvent decreases, i.e., as it is more selective for nonpolar compounds. These differences

are probably related with the higher specific surface area of the smaller particles, promoting a better contact with the solvent and, consequently, leading to an easier diffusion and mass transfer of each soluble compound from the cork matrix into the solvent medium.

With respect to the effect of cork density, for particles from inner sections of the planks having the same particle size (A1 and A3), but with rather different densities (see Figure 3.8): for the three solvents used, a higher amount of soluble compounds was extracted from sample A1 (higher cork density) than from sample A3.

Particles corresponding to the outer sections of the planks (A7 and A9) have the opposite behavior: particles with higher cork density led to lower extraction yields. This behavior may be related with a lower content of low molecular weight compounds relatively to macromolecular components. Therefore, the effect of cork density in the outer region did not led to an increase on the extractives yield.

Wshen one compares granulated industrial cork of the same size group, but from different sections (inner – A2; and outer – A7 and A9), the yields obtained with inner particles are higher.

Until now, we described the yields of the soxhlet extraction; nevertheless, the previous results show that it is possible that only a layer of granulated can be extracted; in the following section, it is calculated the layer thickness of cork accessible to extraction, that could explain quantitatively the results obtained with different particle sizes.

## 3.3 Layer thickness of cork accessible to extraction

To know the total cork extractives, some studies (Pereira, 1988, 2013; Sousa *et al.*, 2006) were focused to determine the chemical composition of cork, where the samples were extracted sequentially with several solvents of increasing polarity and the sum of this sequential extraction will represent the total cork extractives. Table 3.4 shows the yield obtained for several cork samples (virgin

and reproduction cork, cork powder, natural boiled cork, etc.), where the total extractives were between 56 and 169 $g_{extract} \cdot kg^{-1}_{DryCork}$. In those studies, the cork samples were granulated to particle size lower than 1 mm.

Table 3.4 – Yields for sequential extractions of several cork samples.

| Material* | Total Extractives (%) | Solvent | | | Ref. |
|---|---|---|---|---|---|
| | | DCM | EtOH[1] or MeOH[2] | $H_2O$ | |
| Virgin Cork | **16.9** | 7.9 | 5.8[1] | 3.1 | (Pereira, 1988) |
| Industrial cork powder | **5.9** | 2.6 | 1.9[2] | 1.4 | (Sousa *et al.*, 2006) |
| Reproduction Cork | **16.2** | 5.8 | 5.9[1] | 4.5 | (Pereira, 2013) |
| Reproduction Cork | **14.2** | 5.4 | 4.8[1] | 4 | (Pereira, 1988) |
| Natural boiled cork planks obtained after a cork cooking stage | **8** | 4.7 | 2.2[2] | 1.1 | (Sousa *et al.*, 2006) |
| Inner from boiled cork planks obtained after a cork cooking stage | **11.2** | 5 | 3.6[2] | 2.6 | (Sousa *et al.*, 2006) |
| Outer from boiled cork planks obtained after a cork cooking stage | **5.6** | 2.7 | 1.8[2] | 1.1 | (Sousa *et al.*, 2006) |

* Particle size: 40-60 mesh.

The total of cork extractives depends on several factors, as previously described: growth conditions, genetic origin, age and tree dimension, etc. However, Table 3.4 will represent a bench mark to cork samples used in this work; as explained before, the samples were obtained after milling the punched cork planks, after a cork cooking stage, and they are constituted by granulated industrial cork with particle sizes until 6 mm. According to Table 3.4, it is assumed that the total extractives for the samples used in this work, from inner section of cork planks, was 112 $g_{extract} \cdot kg^{-1}_{DryCork}$.

In the soxhlet extraction, for hexane, dichloromethane or acetone, the maximum yield obtained, in this work, was 84 $g_{extract} \cdot kg^{-1}_{DryCork}$ (acetone); most probably, the cork samples used, after the extraction, still contain some extractives; and when the solvent polarity decreases, the fraction of extractives that remains in the sample is higher. It is to note that, since extraction was conducted until completion, the maximum yield achieved for each solvent represents the capacity for each one. Nevertheless, the decrease of yields when the particle size

for particles of same section increases can be explained if it is assumed that only an outer layer of cork is extracted.

Cork is an excellent liquid sealant used from ancient times until nowadays. It is then reasonable to assume that any liquid in contact with cork will penetrate just its outer layer, being prevented to attain the inner core due to the unique cork sealant properties. Assuming that each solvent extracts its maximum from the wetted region, it is possible to estimate the outer layer as a function of the extracting solvent.

To estimate this cork accessible shell to be extracted from each sample, i.e., the layer available to be extracted, it was assumed that the extractives are equally distributed inside the particle of each sample and all particles are spherical. Figure 3.9 shows dimensionless cork layer, for all solvents; in these calculations, it was assumed that cork powder was completely extracted, i.e., for cork powder $r_c = 0$, leading to the capacity of each solvent; as expected, when the particle size increases, the dimensionless thickness of the (outer) layer extracted decreases; however, it can be noted that for particles bigger than 1 mm this value decreases only slightly; then, it can be considered that this layer is nearly constant for each solvent; being for hexane around half the value extracted with the other two solvents, regardless of particle size. The dimensionless thickness, on average, is ca. 0.22, 0.20 and 0.11 for acetone, dichloromethane and hexane, respectively.

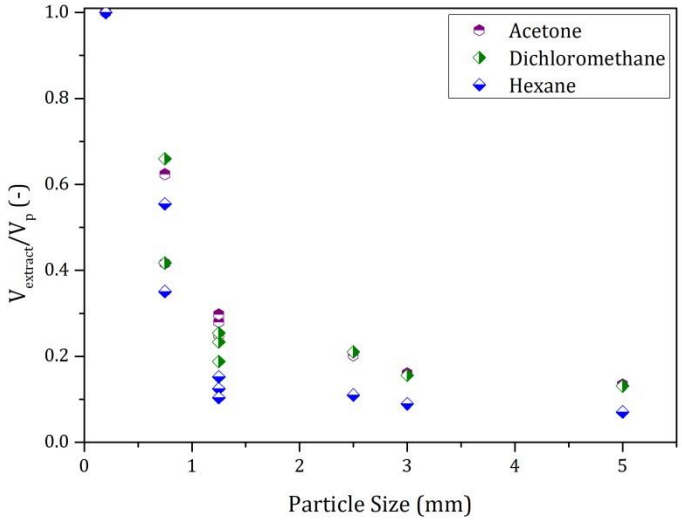


Figure 3.9 – Dimensionless thickness of the extractable outer cork layer *vs*. average particle size.

Until now, we described the yields of the soxhlet extraction (for each sample) and, according to the hypotheses presented above, the layer thickness that is accessible (particles from inner section) to remove cork extractives. It is also essential to know the composition of those extracts. The next section describes the methodology used for quantitative and qualitative analyses.

## 3.4 Quantification of betulin and betulinic acid

As described before (Chapter 2), the compounds that constitute the cork extracts have high boiling points. So, derivatization methods were used in order to obtain more volatile and thermally stable compounds and also to improve their detectability in GC (Sousa *et al.*, 2006).

The methodology used consisted in submitting to derivatization the cork extracts through silylation where an active hydrogen is replaced by an alkylsilyl group, such as trimethylsilyl (TMS). When compared to their parent compounds, the silyl derivatives are generally less polar, more volatile and more thermally stable.

Prior to GC analysis, ca. 20 mg of cork extract was trimethylsilylated according to Sousa *et al.* (2006) (see Figure 3.10). The extract was dissolved in pyridine

(250 µL) with internal standard (Cholesterol 2 $mg \cdot mL^{-1}$), and the components that contain hydroxyl and carboxyl groups were converted to their TMS ethers and esters, respectively, by adding BSTFA (N,O-bis(trimethylsilyl) trifluoroacetamide) (250 µL) and Chlorotrimethylsilane (50 µL). The mixture remained for 30 min at 70°C. After derivatization, the TMS derivatives were analyzed by GC.

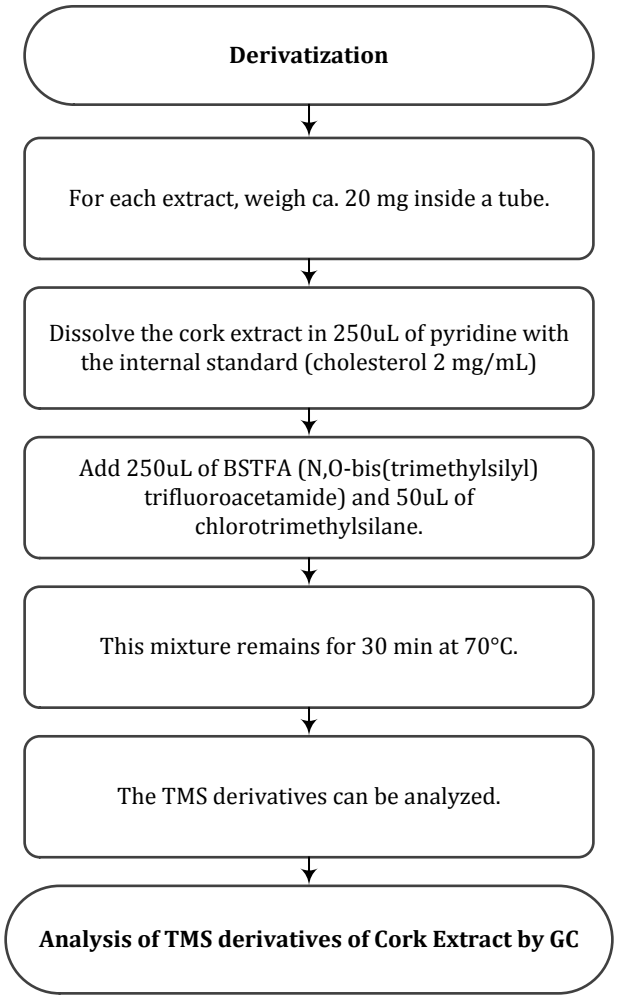


Figure 3.10 – Procedure for derivatization of cork extracts before GC Analysis.

For GC Analysis, a GC (Chrompack CP-9003) equipped with a FID and a capillary column DB-1 (30 m x 0.32 mm inner diameter and 0.25 µm film thickness) from Agilent Technologies was used to get the separation of cork extracts; helium was used as carrier gas (1 $cm^{3} \cdot min^{-1}$); and a temperature program was defined to achieve a good separation of the compounds; the detector and injector temperatures were set at 300°C and the temperature program was defined as

follows: 80°C during the first 5 min, an increase from 80°C to 280°C with a heating rate of 4 $^{\circ}C \cdot min^{-1}$; and 20 min at 280°C.

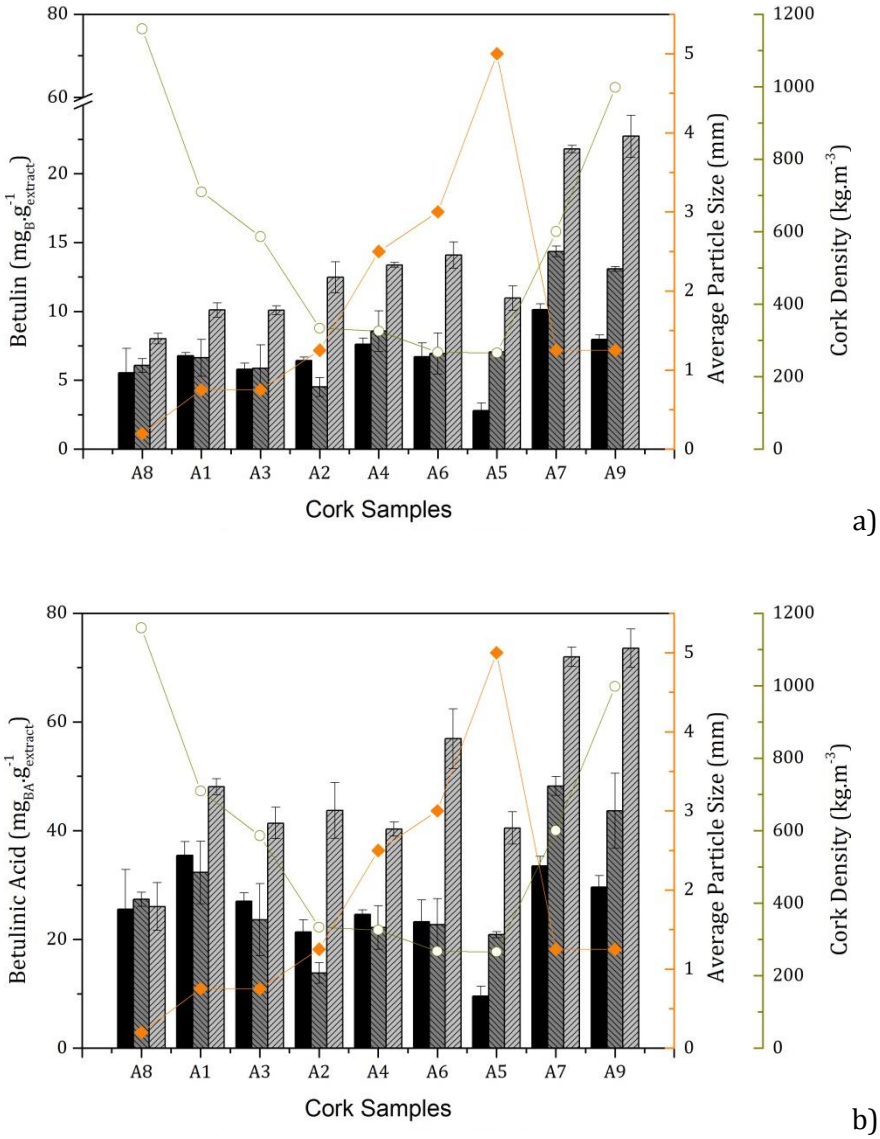


Figure 3.11 – Betulin (a) and betulinic acid (b) content in each extract sample *vs*. particle size, for the three solvents tested. (A8) cork powder, (A1 to A6) inner bark and (A7 and A9) outer bark samples. Solvents: (black) acetone, (gray) dichloromethane, (light gray) hexane. The diamonds represent the average particle size and the circles the cork density.

Figure 3.11 shows the betulin and betulinic acid contents in the extracts for each sample and the three solvents (hexane, dichloromethane and acetone) tested. As can be observed, the betulin content is 2.5 to 4.6 times lower than the content of betulinic acid for all extracts.

Solvent polarity, size group, and plank region affect the amounts of these two target compounds in the extracts, but in a different manner when compared to their influence on the yields (Figure 3.8), demonstrating that all these parameters affect the extraction selectivity.

Although the yields obtained with hexane were the lowest, the extracts for this non-polar solvent have the highest content of betulin (23 $\mathrm{mg}\cdot\mathrm{g}_{\mathrm{extract}}^{-1}$ – sample A9) and betulinic acid (74 $\mathrm{mg}\cdot\mathrm{g}_{\mathrm{extract}}^{-1}$ – sample A9) when compared with the other two solvents (Figure 3.11), making hexane more selective to the target compounds, which is in accordance with its low polarity nature.

To the author's best knowledge, there is no literature data with respect to hexane extractions. However, Sousa *et al.* (2006) presented results for dichoromethane extracts: 70 $\mathrm{mg}_{\mathrm{Betulinic\ Acid}}\cdot\mathrm{g}_{\mathrm{extract}}^{-1}$ and 13 $\mathrm{mg}_{\mathrm{Betulin}}\cdot\mathrm{g}_{\mathrm{extract}}^{-1}$ (betulinic acid in extract was 5.3 times higher than betulin), for samples from the outer section of cork planks after the boiling process; while Castola *et al.* (2005) obtained, for a similar sample, 73 $\mathrm{mg}_{\mathrm{Betulinic\ Acid}}\cdot\mathrm{g}_{\mathrm{extract}}^{-1}$ and 27 $\mathrm{mg}_{\mathrm{Betulin}}\cdot\mathrm{g}_{\mathrm{extract}}^{-1}$ (betulinic acid in extract was 2.7 times higher than betulin); in this work the best results obtained for dichoromethane were with sample A7: 48 $\mathrm{mg}_{\mathrm{Betulinic\ Acid}}\cdot\mathrm{g}_{\mathrm{extract}}^{-1}$ and 14 $\mathrm{mg}_{\mathrm{Betulin}}\cdot\mathrm{g}_{\mathrm{extract}}^{-1}$, and for hexane were 71 $\mathrm{mg}_{\mathrm{Betulinic\ Acid}}\cdot\mathrm{g}_{\mathrm{extract}}^{-1}$ and 21 $\mathrm{mg}_{\mathrm{Betulin}}\cdot\mathrm{g}_{\mathrm{extract}}^{-1}$ for the same sample; in average, the content of betulinic acid in cork extracts were 3.3 times higher when compared with betulin, which are in line with the literature presented.

With respect to the plank region, the behavior is also very interesting: although, again, the yields obtained for outer bark sections are the lowest, their extracts are the richest in betulinic acid and betulin. This behavior was also observed for other barks (eg., *Eucalyptus urograndis, Eucalyptus grandis, Eucalyptus maidenii, Eucalyptus globulus and Eucalyptus nitens*), where high amounts of triterpenoids in the outer fraction are reported (Domingues *et al.*, 2012; Domingues, Patinha, *et al.*, 2011; Domingues, Sousa, *et al.*, 2011; Freire *et al.*, 2002).

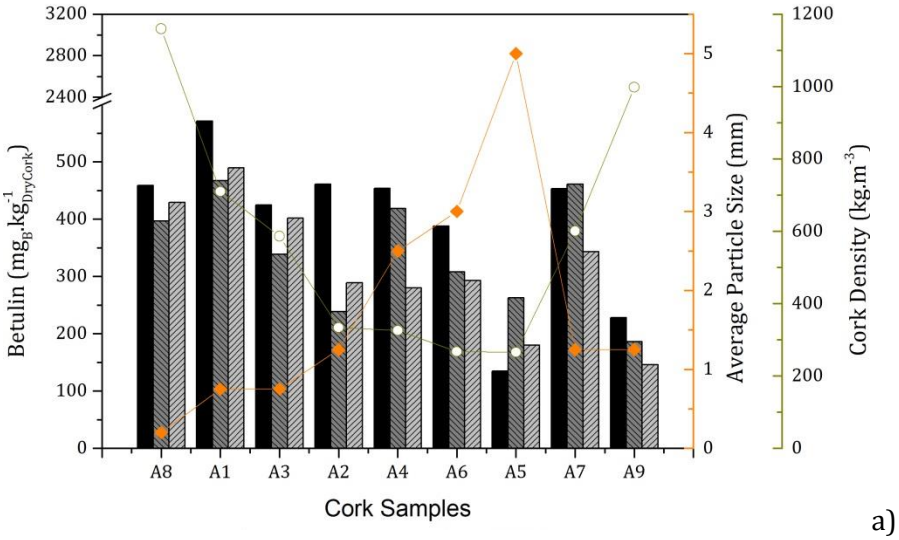


a)

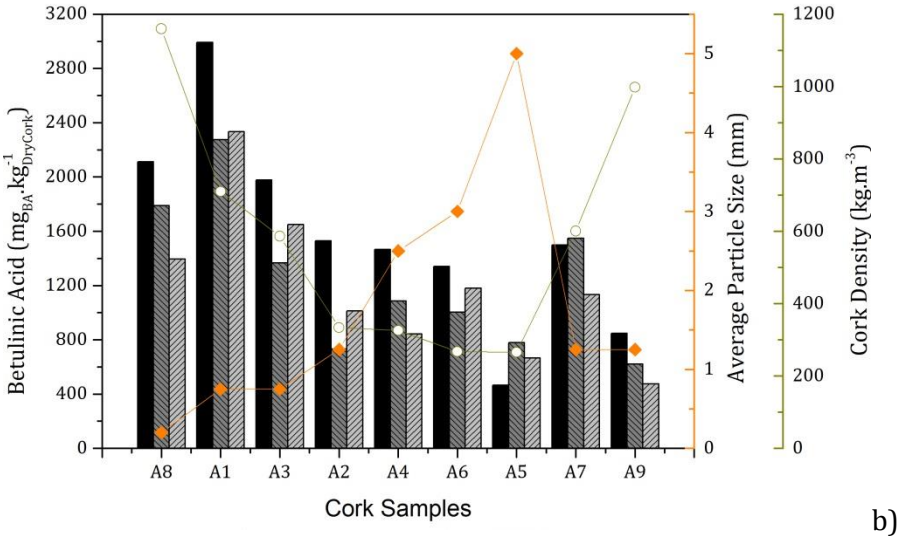


b)

Figure 3.12 – Betulin (a) and betulinic acid (b) contents in each sample *vs*. particle size, for the three solvents tested. (A8) cork powder, (A1 to A6) inner bark and (A7 and A9) outer bark samples. Solvents: (black) acetone, (gray) dichloromethane, (light gray) hexane. The diamonds represent the average particle size and the circles the cork density.

Figure 3.12 shows a global analysis, i.e., the betulinic acid and betulin contents but on a dry cork basis. As can be observed, for the three solvents tested, there is a similar trend: (i) the contents of betulin and betulinic acid in cork decrease as the particle size increases, with sample A1 being the richest in both compounds (2991 $mg_{Betulinic\ Acid} \cdot kg^{-1}_{DryCork}$ and 571 $mg_{Betulin} \cdot kg^{-1}_{DryCork}$, for acetone); (ii) for the same particle size and inner section (A1 and A3), samples with higher cork density are richer in betulinic acid and betulin (iii); for the same

particle size and outer section (A7 and A9), samples with lower cork density are richer in betulinic acid and betulin.

It is also important to remark that, although the yields obtained with sample A7 (outer bark section) are lower than with all the other inner section samples and cork powder, with respect to betulinic acid and, specially, betulin content (on a dry cork basis), its behavior is different: the values obtained are not only comparable to, but sometimes higher, than the ones obtained with inner section cork samples.

# Notation

| | | |
|---|---|---|
| $Yield$ | content of extractives in cork | $g_{extract} \cdot kg_{DryCork}^{-1}$ |
| $R_p$ | particle radius | m |
| $r_c$ | radius of core | m |

# List of Acronyms

| | |
|---|---|
| ACE | Acetone |
| AAC | António Almeida, Cortiças, S.A |
| $CO_2$ | Carbon Dioxide |
| DCM | Dichloromethane |
| EtOH | Ethanol |
| FID | Flame Ionization Detector |
| GC | Gas Chromatography |
| HEX | Hexane |
| MeOH | Methanol |
| SEM | Scanning Electron Microscope |
| SFE | Supercritical Fluid Extraction |

# References


Castola, V., Bighelli, A., Rezzi, S., Melloni, G., Gladiali, S., Desjobert, J.-M., and Casanova, J. (**2002**). "Composition and chemical variability of the triterpene fraction of dichloromethane extracts of cork (Quercus suber L.)." *Industrial Crops and Products*, *15*(1), 15–22. doi:10.1016/S0926-6690(01)00091-7

Castola, V., Marongiu, B., Bighelli, A., Floris, C., Laï, A., and Casanova, J. (**2005**). "Extractives of cork (Quercus suber L.): chemical composition of dichloromethane and supercritical CO2 extracts." *Industrial Crops and Products*, *21*(1), 65–69. doi:10.1016/j.indcrop.2003.12.007

Conde, E., Garcia-Vallejo, M. C., and Cadahía, E. (**1999**). "Waxes composition of reproduction cork from Quercus suber and its variability throughout the industrial processing." *Wood Science and Technology*, *33*(3), 229–244. doi:10.1007/s002260050112

de Castro, M. D. L., and Priego-Capote, F. (**2010**). "Soxhlet extraction: Past and present panacea." *Journal of Chromatography A*, *1217*(16), 2383–2389. doi:10.1016/j.chroma.2009.11.027

Dean, J. R. (**2009**). "Extraction Techniques in Analytical Sciences." Wiley.

Domingues, R. M. A., Oliveira, E. L. G., Freire, C. S. R., Couto, R. M., Simões, P. C., Neto, C. P., … Silva, C. M. (**2012**). "Supercritical Fluid Extraction of Eucalyptus globulus Bark-A Promising Approach for Triterpenoid Production." *International Journal of Molecular Sciences*, *13*(6), 7648–62. doi:10.3390/ijms13067648

Domingues, R. M. A., Patinha, D. J. S., Sousa, G. D. A., Villaverde, J. J., Silva, C. M., Freire, C. S. R., … Pascoal Neto, C. (**2011**). "Eucalyptus biomass residues from agro-forest and pulping industries as sources of high-value triterpenic compounds." *Cellulose Chemistry and Technology*, *45*(7–8), 475–481.

Domingues, R. M. A., Sousa, G. D. A., Silva, C. M., Freire, C. S. R., Silvestre, A. J. D., and Neto, C. P. (**2011**). "High value triterpenic compounds from the outer barks of several Eucalyptus species cultivated in Brazil and in Portugal." *Industrial Crops and Products*, *33*(1), 158–164. doi:10.1016/j.indcrop.2010.10.006

Feilden, A. (**2010**). "Update on Undertaking Extractable and Leachable Testing." Smithers Rapra Technology. Retrieved from http://www.knovel.com/web/portal/browse/display?_EXT_KNOVEL_DISPLAY_bookid=4202

Freire, C. S. R., Silvestre, A. J. D., Neto, C. P., and Cavaleiro, J. A. S. (**2002**). "Lipophilic extractives of the inner and outer barks of Eucalyptus globulus." *Holzforschung*, *56*(4), 372–379.

Jensen, W. B. (**2007**). "The origin of the soxhlet extractor." *Journal of Chemical Education*, *84*(12), 1913–1914.

Lam, P. S., Sokhansanj, S., Bi, X., Lim, C. J., Naimi, L. J., Hoque, M., … Narayan, S. (**2008**). "Bulk density of wet and dry wheat straw and switchgrass particles." *Applied Engineering in Agriculture*, *24*(3), 351–358.

Miranda, I., Gominho, J., Mirra, I., and Pereira, H. (**2012**). "Chemical characterization of barks from Picea abies and Pinus sylvestris after fractioning into different particle sizes." *Industrial Crops and Products*, *36*(1), 395–400. doi:10.1016/j.indcrop.2011.10.035

Pereira, H. (**1988**). "Chemical composition and variability of cork from Quercus suber L."

*Wood Science and Technology*, *22*(3), 211–218. doi:10.1007/bf00386015

Pereira, H. (**2013**). "Variability of the Chemical Composition of Cork." *BioResources*, *8*(2), 2246–2256.

Santos, S. A. O., Villaverde, J. J., Sousa, A. F., Coelho, J. F., Neto, C. P., and Silvestre, A. J. D. (**2013**). "Phenolic composition and antioxidant activity of industrial cork by-products." *Industrial Crops and Products*, *47*, 262–269. doi:10.1016/j.indcrop.2013.03.015

Silva, S. P., Sabino, M. A., Fernandes, E. M., Correlo, V. M., Boesel, L. F., and Reis, R. L. (**2005**). "Cork: properties, capabilities and applications." *International Materials Reviews*, *50*(4), 345–365. doi:10.1179/174328005X41168

Sousa, A. F., Pinto, P. C. R. O., Silvestre, A. J. D., and Neto, C. P. (**2006**). "Triterpenic and other lipophilic components from industrial cork byproducts." *Journal of Agricultural and Food Chemistry*, *54*(18), 6888–6893. doi:10.1021/Jf060987+

*"Cork is a gift of Nature and a key factor for Sustainable Development"*
*(Corticeira Amorim)*

# 4 Supercritical Fluid Extraction & Experimental Setup

In the extraction process, the solute should have a higher affinity for the solvent in order to improve its separation. If the extraction is performed when the solvent is above its critical pressure and temperature, the process can be designated as supercritical fluid extraction (SFE).

The SFE aroused enormous interest a consequence of its advantages, since the physical properties in this region promote the separation, its density is similar to the liquid and its lack of surface tension allows to come in contact with the solid to improve the extraction process; also its viscosity is in the same order of magnitude of that of gases.

Nowadays, there are two major areas of application for the supercritical extraction process, the counter current extraction of a liquid stream, and the extraction of solutes from the interior of solid matrices. From the solid matrices, the extraction is determined by the proportion of soluble components and their distribution in the matrix, as particle size and solid nature (Coulson *et al.*, 2002). Usually, this process can be considered in three stages: first the solute is dissolved by the solvent, then it diffuses through the pores to the outside of the particle, and finally the solute in solution is transferred to the fluid (Coulson *et al.*, 2002).

This work is focused in the extraction of granulated industrial cork as described in Chapter 3; to perform the extraction of samples using as solvent $CO_2$ at supercritical conditions, an experimental setup at bench scale was designed, constructed and operated.

## 4.1 Supercritical Fluid Extraction (SFE)

As previously described, when the solvent is over its critical point the extraction can be called as SFE. Figure 4.1 displays the typical values of density, diffusivity and viscosity in the different phases being that the properties in this region promote the separation; the density of the supercritical fluids is similar to those of liquids, that allows to dissolve larger amounts of solute which benefits the extraction (Francis, 1999). The molecular diffusivity of solute in a gas (at ambient pressure) is about four orders of magnitude higher than in liquid; however, close to supercritical conditions the diffusivity is typically 1-2 orders of magnitude larger than in the liquid phase which results in lower mass transfer resistance. Moreover, the viscosity of a supercritical fluid is about one order of magnitude lower than that of its liquid (Seader *et al.*, 2006).

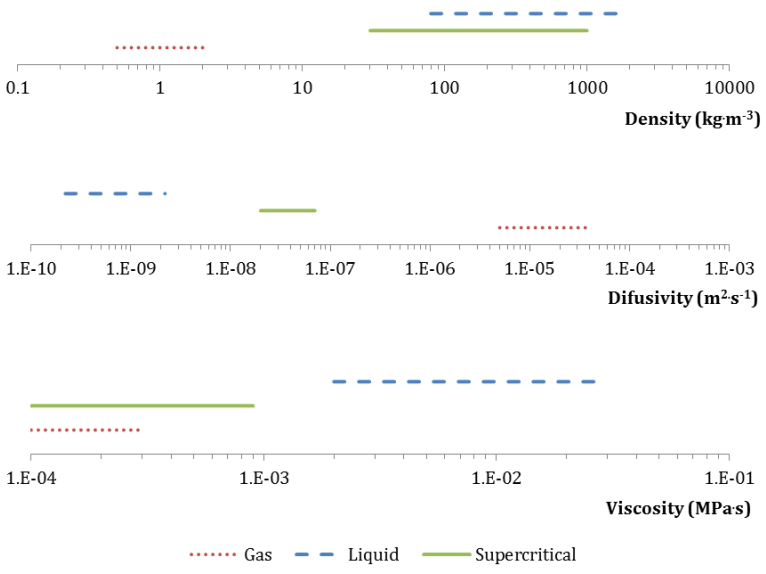


Figure 4.1 – Physical properties of different phases; adapted fromFrancis *et al.* (1999).

To select the solvent, it should be taken into account the solute affinity and the compatibility with the process as well as its cost and availability. Table 4.1 lists

some compounds which have received special attention as solvents in supercritical conditions.

Table 4.1 – Critical constants of the main solvents considered in supercritical extraction. Data from Perry (2008)

| **Solvent** | | **Molecular weight,** $\left(\mathrm{g \cdot mol^{-1}}\right)$ | **Critical temperature,** $T_c$ (K) | **Critical pressure,** $p_c$ (MPa) | **Critical density,** $\rho_c$ $\left(\mathrm{kg \cdot m^{-3}}\right)$ | $Z_c$ (–) |
|---|---|---|---|---|---|---|
| **Acetone** | ($C_3H_6O$) | 58.079 | 508.2 | 4.701 | 278 | 0.233 |
| **Ammonia** | ($NH_3$) | 17.031 | 405.6 | 11.28 | 235 | 0.242 |
| **Carbon dioxide** | ($CO_2$) | 44.010 | 304.2 | 7.383 | 468 | 0.274 |
| **Ethane** | ($C_2H_6$) | 30.069 | 305.3 | 4.872 | 207 | 0.279 |
| **Ethanol** | ($C_2H_5OH$) | 46.068 | 514.0 | 6.137 | 274 | 0.241 |
| **Ethylene** | ($C_2H_4$) | 28.053 | 282.3 | 5.041 | 214 | 0.281 |
| **N-hexane** | ($C_6H_{14}$) | 86.175 | 507.6 | 3.025 | 232 | 0.266 |
| **Methane** | ($CH_4$) | 16.042 | 190.5 | 4.599 | 163 | 0.286 |
| **Methanol** | ($CH_3OH$) | 32.042 | 512.5 | 8.084 | 274 | 0.222 |
| **Propane** | ($C_3H_8$) | 44.096 | 369.8 | 4.248 | 220 | 0.276 |
| **Propylene** | ($C_3H_6$) | 42.080 | 364.8 | 4.600 | 227 | 0.280 |
| **Water** | ($H_2O$) | 18.015 | 647.1 | 22.06 | 322 | 0.229 |

Besides solvent phase, in the extraction process there are some other factors that may influence the separation, as the particle size, since smaller particles provide a large interfacial area between the solid and the fluid phase which increases transfer rate; however, by decreasing the particle size, the pressure drop within the bed increases. Operating parameters have also relevance, e.g., increasing the extraction temperature commonly raises the solubility and the diffusion coefficient, and as consequence the extraction rate.

In Table 4.1 $CO_2$ should be highlighted, since the supercritical $CO_2$ is recognized by the FDA (U.S. Food and Drug Administration) as a GRAS (Generally Recognized As Safe), i.e., a safe solvent, because it leaves no trace on the products (extracts) neither on the raw material. It is not flammable, non-corrosive, inert and non-toxic. Likewise, it enables the treatment of the raw material in near-ambient temperatures, since its critical temperature is around

31°C, which becomes relevant in the treatment of substances that are thermally labile, as numerous natural products (Azevedo *et al.*, 2009). Figure 4.2 depicts the $CO_2$ phase diagram, according to the equations to estimate the melting pressure ( $p_{mel}$ ), Eq. 4.1, the sublimation pressure( $p_{sub}$ ), Eq. 4.2, and the vapour pressure ( $p_{vap}$ ), Eq. 4.3, that were established by Span and Wagner (1994).

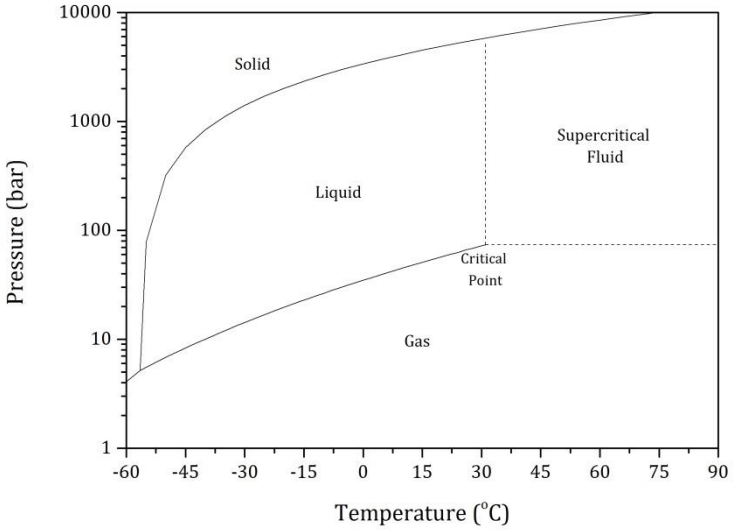


Figure 4.2 – $CO_2$ Phase Diagram.

$$\frac{p_{mel}}{p_t} = 1 + a_{1,mel}\left(\frac{T}{T_t} - 1\right) + a_{2,mel}\left(\frac{T}{T_t} - 1\right)^2 \quad ; \quad 217\ K < T < 222\ K \qquad \text{Eq. 4.1}$$

$$\ln\left(\frac{p_{sub}}{p_t}\right) = \frac{T_t}{T}\left\{a_{1,sub}\left(1 - \frac{T}{T_t}\right) + a_{2,sub}\left(1 - \frac{T}{T_t}\right)^{1.9} + a_{3,sub}\left(1 - \frac{T}{T_t}\right)^{2.9}\right\} \qquad \text{Eq. 4.2}$$

$$\ln\left(\frac{p_{vap}}{p_c}\right) = \frac{T_c}{T}\left\{\sum_{i=1}^{4} a_{i,vap}\left(1 - \frac{T}{T_c}\right)^{t_{i,vap}}\right\} \qquad \text{Eq. 4.3}$$

Where $T$ is the temperature in kelvin and $p_t = 0.51795$ MPa , $T_t = 216.592$ K , $p_c = 7.383$ MPa and $T_c = 304.2$ K , the values of the other constants $a_{i,j}$ and $t_{i,vap}$ are displayed in Table 4.2.

Table 4.2 – Constants for the equations of melting (Eq. 4.1) sublimation (Eq. 4.2) and vapour pressures (Eq. 4.3).

| | **Melting** ( $j = \text{mel}$ ) | **Sublimation** ( $j = \text{sub}$ ) | **Vapour** ( $j = \text{v}ap$ ) |
|---|---|---|---|
| $a_{1,j}$ | 1955.5390 | -14.740846 | -7.0602087 |
| $a_{2,j}$ | 2055.4593 | 2.4327015 | 1.9391218 |
| $a_{3,j}$ | – | -5.3061778 | -1.6463597 |
| $a_{4,j}$ | – | – | -3.2995634 |
| $t_{1,j}$ | – | – | 1.0 |
| $t_{2,j}$ | – | – | 1.5 |
| $t_{3,j}$ | – | – | 2.0 |
| $t_{4,j}$ | – | – | 4.0 |

To calculate the density of $CO_2$ at supercritical conditions we used the equation developed by Span and Wagner (1994), and the result is represented in Figure 4.3, the PVT diagram.

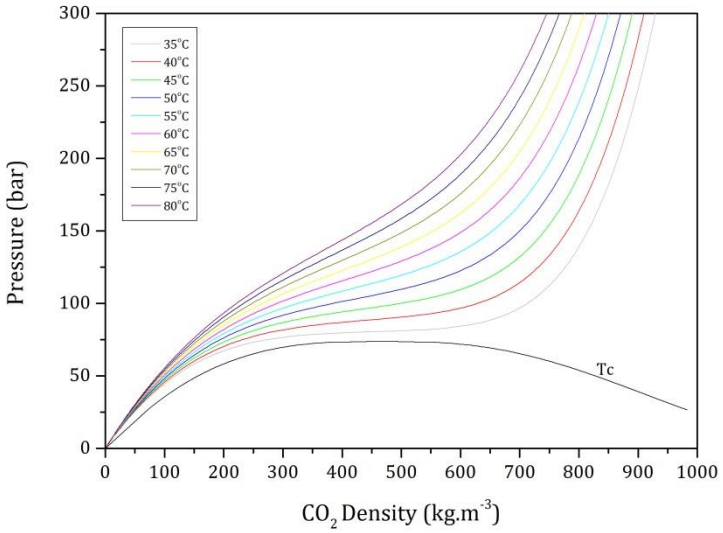


Figure 4.3 – PVT diagram of $CO_2$.

Above the critical point, small variations in temperature and pressure produce large changes in density; in the same way, when the temperature is kept constant, the density increases when pressure increases; on the other hand, keeping constant the pressure, the density decreases if the temperature

increases, e.g., at 100 bar and 40°C, the $CO_2$ density is 629 $kg \cdot m^{-3}$, and decreases about 54% until 290 $kg \cdot m^{-3}$ at 60°C. Table 4.3 shows the values of the density of $CO_2$ in a range from 31 up to 80°C and from its critical pressure up to 300 bar.

Table 4.3. – Density of $CO_2$ $(kg \cdot m^{-3})$ for the critical point and above it.

| Pressure (bar) / Temperature (°C) | 31 | 40 | 60 | 80 |
|---|---|---|---|---|
| **73.8** | 468* | 222 | 168 | 144 |
| **100** | 761 | 629 | 290 | 222 |
| **150** | 841 | 780 | 604 | 427 |
| **200** | 886 | 744 | 724 | 594 |
| **250** | 918 | 879 | 787 | 686 |
| **300** | 944 | 910 | 830 | 746 |

* Critical density

Besides density, in the supercritical region, the solubility and selectivity are also sensitive to changes in pressure and temperature; this makes possible dissolving non-volatile compounds at moderate temperatures (31°C) (Noyes, 1994), since $CO_2$ has a low critical temperature. The $CO_2$ presents good solvent properties for non-polar molecules (Modey *et al.*, 1996); however, to dissolve polar compounds, adding a co-solvent can increase the solubility.

In industry, the use of supercritical $CO_2$ has been arousing great interest, for example, in the extraction of caffeine and some high value-added products, such as flavorings, fragrances and food supplements (Lozowski, 2010). Table 4.4 shows some commercial-scale supercritical $CO_2$ extraction plants or processes, indicating the location and manufacturer.

Table 4.4 – Commercial-scale supercritical $CO_2$ extraction plants and processes.

| Process | Location | Manufacturer |
|---|---|---|
| **Coffee decaffeination*** | Houston, Tex., U.S. | Maximus Coffee Group LP (General Foods) |
| | Bremen, Germany | Kaffe HAG AG |
| | Bremen, Germany | Hermsen |
| | Poszillo, Italy | SKW-Trostberg AG |
| **Tea decaffeination*** | Munchmuenster, Germany | SKW-Trostberg AG |

Table 4.4 – Commercial-scale supercritical $CO_2$ extraction plants and processes.

| Process | Location | Manufacturer |
|---|---|---|
| **Tea/coffee decaffeination, hop and other plant extract** | Germany | Evonik |
| **Fatty acids from spent barley*** | Dusseldorf, Germany | Marbery, GmbH |
| **Vitamin and oil, phytosterol, fatty acid methyl ester, ginger oil*** | Wuhan, Hubei, China | Wuhan Kaidi Fine Chemical Industrial Co. |
| **Nicotine extraction*** | Hopewell, Va., U.S. | Philip Morris |
| **Natural insecticide/pesticide*** | High Wycombe, U.K. | Agropharm |
| **Hops extraction*** | Wolnzach, Germany | Hopfenextraktion, HVG |
| | Yakina, Washington, U.S. | Hops Extraction Corp. of America |
| | Melbourne, Australia | Carlton & United Beverages Ltd |
| | West Midiands, U.K. | Botanix |
| **Extraction plant for hops and nutraceuticals** | New Zealand | Natex |
| **Species/flavours/aromas/natural products/colors*** | Munchmuenster, Germany | SKW-Trostberg AG |
| | Rehlingen, Germany | Flavex GmbH |
| | Edmonton, Canada | Norac Technologies |
| | Tsukaba, Japan | Ogawa Flavours and Fragances |
| | Milwaukee, Wisc., U.S. | Sensient Technologies |
| | Japan | Kirin Food-Tech Co. |
| **Extraction plant for spices and herbs** | India | Natex |
| **Extraction plants** | Germany | NatCO2 |
| **Botanical extract** | Czech Republic | Flaveco Trade |
| **Rice treatment plant** | Taiwan | Natex |
| **Cork purification plant** | Spain | Natex |

* Adapted from Lozowski (2010)

It should to be noted that, actually, Natex developed a process (the DIAM process) to clean the granulated cork, being its main goal getting a clean technical cork stopper; however, in this process the pressure only reaches up to 100 bar since it was only focused to remove the TCA (2,4,6-trichloroanisole), i.e., there is no mention to extract the high added-value compounds concealed in granulated cork (NATEX, 2011).

## 4.2 Design and construction of a bench-scale supercritical fluid extraction (SFE) setup

The experimental setup for the supercritical fluid extraction used in this work was designed and built by the author. Figure 4.4 shows the proposed layout; it was divided in three zones according to its operating conditions, each one corresponding to a specific stage of the process: feed, extraction and separation.

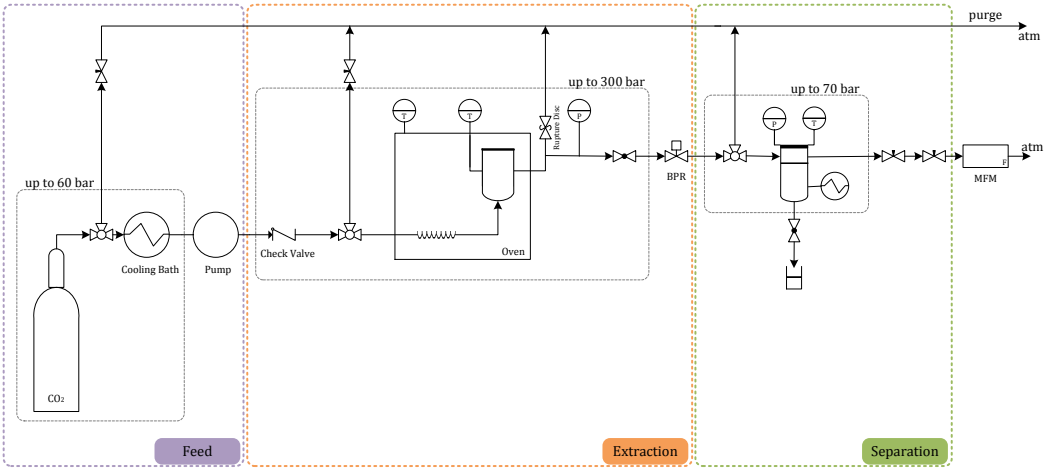


Figure 4.4 – Schematic representation of SFE setup

The $CO_2$ is supplied through a cylinder at the liquid/gas equilibrium pressure (e.g., pressure 50 bar at 15°C); this cylinder is equipped with a dip tube through which the $CO_2$ leaves the bottle in the liquid phase and the pump head is also cooled to ensure liquid phase at the pump inlet. After the pump, extraction zone, the pressure can achieve 300 bar according to the operating conditions. An oven keeps the temperature constant in this zone. The $CO_2$ under supercritical conditions dissolves the extractable compounds concealed in the cork. The pressure is reduced in the next stage (separation section) through a pressure-reducing valve, and the cork extracts are separated from the $CO_2$, now in the gas phase; the cork extracts remain in the separator while the $CO_2$ is released to the environment. It should be highlighted that, in a large scale process, the $CO_2$ should be recirculated.

The SFE setup was designed to work in both static mode being the inlet and outlet of the extractor closed by a specific period of time; and in continuous mode with a constant flow rate of $CO_2$; in both cases, the temperature and

pressure are kept constant. The parts of the extraction and separation zones were designed and built specifically to this project in order to operate at pressures up to 300 and 100 bar, respectively as will be referred in the following sections.

After defining the requirements of the entire setup, it was evaluated the possibility to use some equipment already available in the laboratory, as a high pressure isocratic pump adapted to $CO_2$, and cooling bath with recirculation, etc.

The experimental setup will be described in detail in the next sections, indicating the components of each section and a 3D drawing was done in order to simplify its construction/assembling, since it helps the visualization of the real position of each part.

### 4.2.1 Feed section

The function of this section is the supply and conditioning of the $CO_2$ (solvent). The $CO_2$ supply (>99% purity) is made by a cylinder under pressure with a dip tube to take liquid $CO_2$, as shown in Figure 4.5; afterwards, the solvent goes through a switching (3-way) valve, to the pump or the bypass (purge).

The maximum pressure, in this section, corresponds to the equilibrium $CO_2$ pressure inside the cylinder (see Phase diagram of $CO_2$ – Figure 4.2). The pump head is cooled to ensure liquid phase at its inlet. The isocratic pump (JASCO PU-2080) was already available in the laboratory; it works at constant flow or constant pressure; in the constant flow mode, the maximum pressure is about 50 MPa at a flow rate lower than 5 $mL \cdot min^{-1}$; if the flow rate is higher than 5 $mL \cdot min^{-1}$, the maximum pressure is ca. 35 MPa. This pump has two check valves, one at the inlet and the other at the outlet to guarantee that the flow has only one direction; after the pump, the $CO_2$ continues to the extraction section as described below.

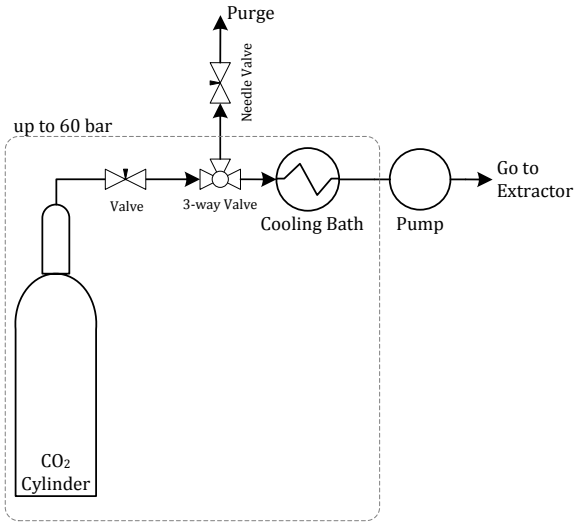


Figure 4.5 – Schematic representation of the feed section.

The schematic 3D drawing of this section is presented in Figure 4.6, where a recirculating bath is used to cool the pump head.

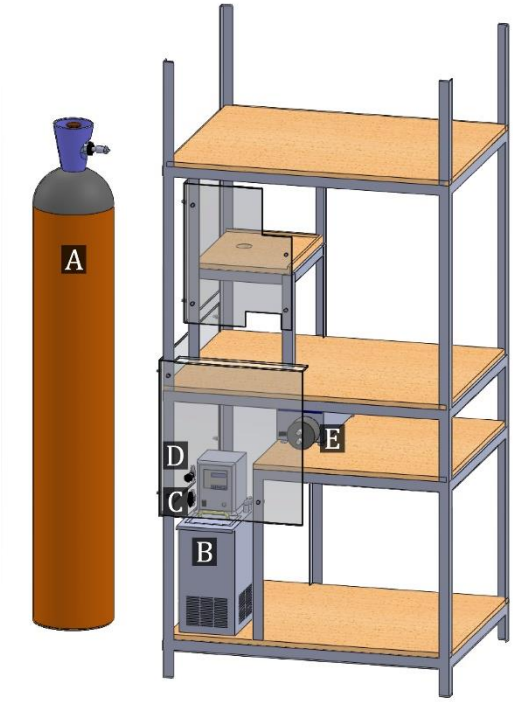


Legend:

A – $CO_2$ Cylinder

B – Recirculating bath

C - Switching (3-way) valve

D – Needle valve (purge)

E – Isocratic $CO_2$ Pump with cooled head

Figure 4.6 – Schematic 3D drawing of feed section of the experimental SFE setup.

### 4.2.2 Extraction section

The extraction section corresponds to the heart of the setup. Here, the pressure can reach 300 bar, while the temperature can be between 40 and 80°C; small changes in the operating conditions can result in very large changes in the

properties of supercritical fluids, so their control is essential; this is why the extractor is located inside an oven to keep constant its temperature while the pressure is monitored by a pressure transducer and controlled using a back pressure regulator (BPR) that opens or closes according to the defined set-point in order to keep the pressure constant. It should be highlighted that the BPR can originate a high pressure drop and, in order to compensate the refrigeration by the free (Joule-Thomson) expansion, it is heated using heating tapes to avoid clogging the BPR and tubing with ice. As a matter of fact, all equipment parts that can cause high pressure drops in the system are heated.

Figure 4.7 displays the layout of this section; a check valve was placed after the $CO_2$ pump, and a combination of three on-off valves are used after it, their configuration turning possible the introduction of a bypass to the extractor or even the release of the pressure from the extractor which would not be possible with a simple 3-way valve (as represented previously in Figure 4.4 ).

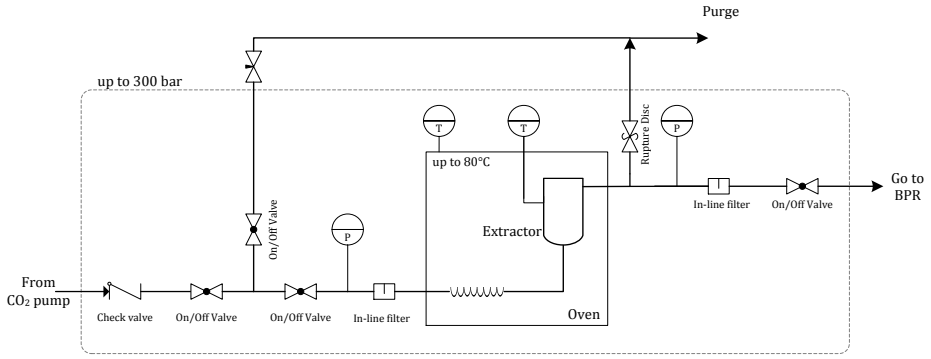


Figure 4.7 – Schematic representation of the extraction section of the SFE setup

The 3D drawing of the extractor is presented in Figure 4.8a; it can withstand pressures up to 300 bar, its cover (Figure 4.8b) was designed to facilitate its opening and closing and to avoid the use of the lathe. Also to facilitate the charging, the raw material to extract was placed inside a basket as can be seen in Figure 4.8c.

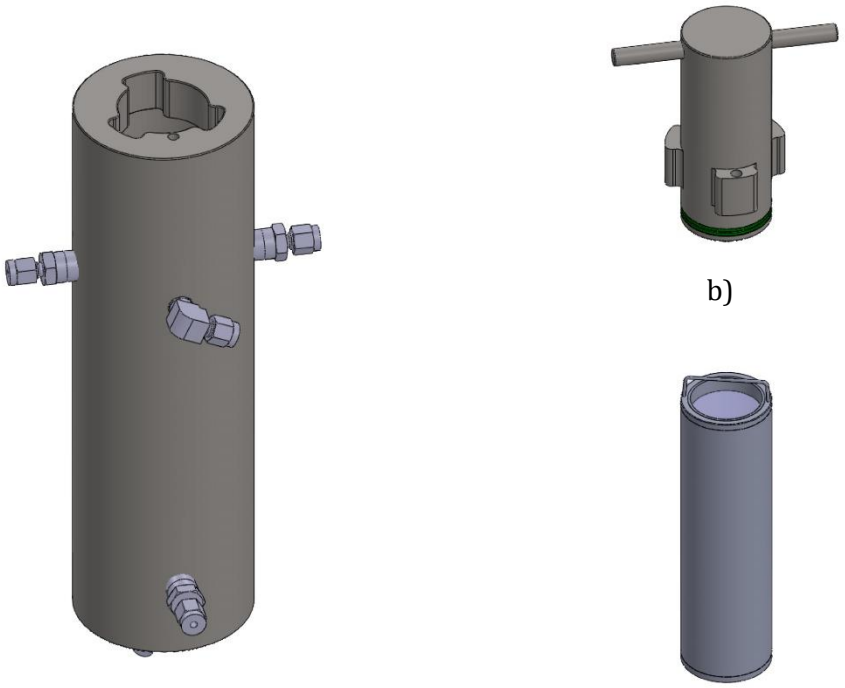


Figure 4.8 - 3D drawing of a) the extractor, b) its cover and c) the raw material basket.

The extractor is located inside the oven, after charged with sample. To prevent that some particles enter or leave the extractor, an in-line filter was used. Also, a rupture disc was placed in the exit of the extractor as safety, i.e., to avoid unexpected increases of pressure. And just before the BPR an on-off valve was placed to allow the isolation of the extractor, since both the inlet and the outlet have one on-off valve. In the same way, it should be referred that the valve at the outlet must be closed until the system reaches the pressure of the extraction experiment. Figure 4.9 displays a 3D drawing of this section.

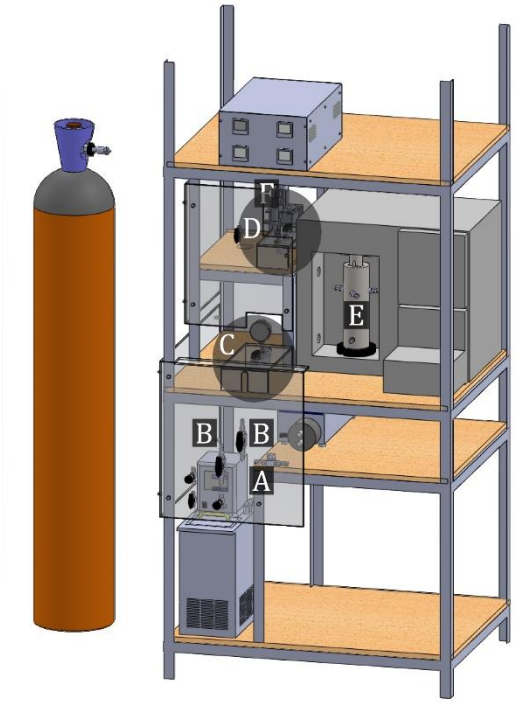


Legend:

A – Check valve

B – on-off valve

C – Section that includes:

B – on-off valve,

G – pressure gauge,

H – in-line filter,

D – Section that includes:

B – on-off valve

H – in-line filter,

I – pressure transducer,

J –rupture disc,

E – Extractor

F – BPR

zoom of section C

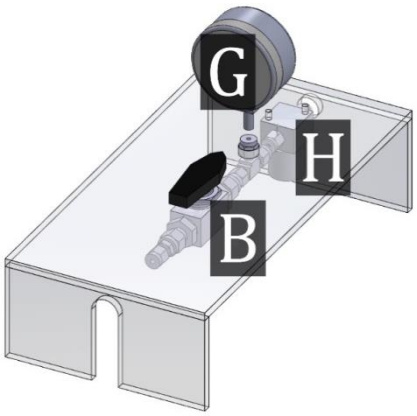


zoom of section D

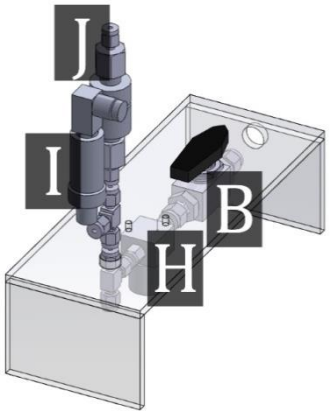


Figure 4.9 – Schematic 3D drawing of the extraction section of the experimental SFE setup.

In the following section, the extracts from cork are separated from the solvent ($CO_2$).

### 4.2.3 Separation section

In this section, the cork extracts are separated from the solvent; the $CO_2$ is in the gas phase due to the drop of the pressure, so the solvent loses its solubility in these new conditions. Figure 4.10 displays the layout of this particular section.

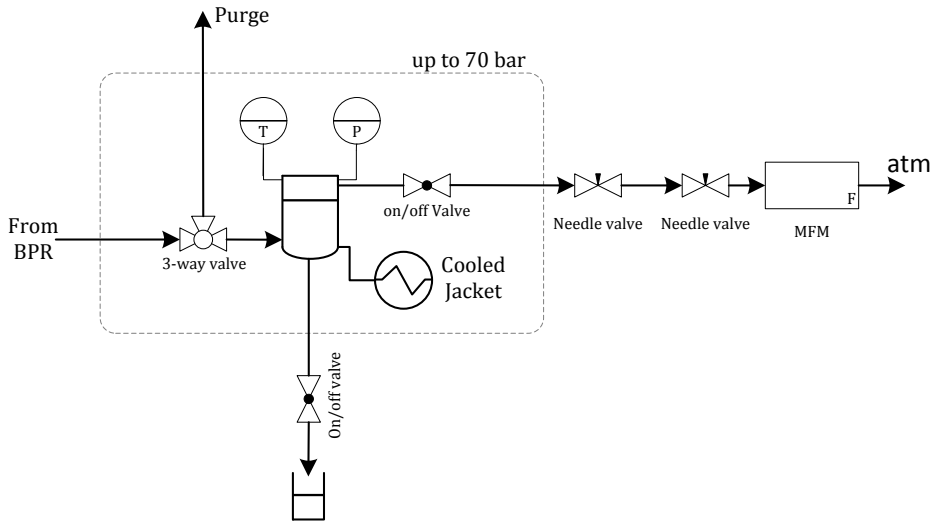


Figure 4.10 – Schematic representation of the separation section of the SFE setup.

The separator has a jacket to keep constant its temperature. Figure 4.11 shows the 3D drawing of this equipment; it can work up to 100 bar, and the design of the cover was similar to that of the extractor (Figure 4.11b).

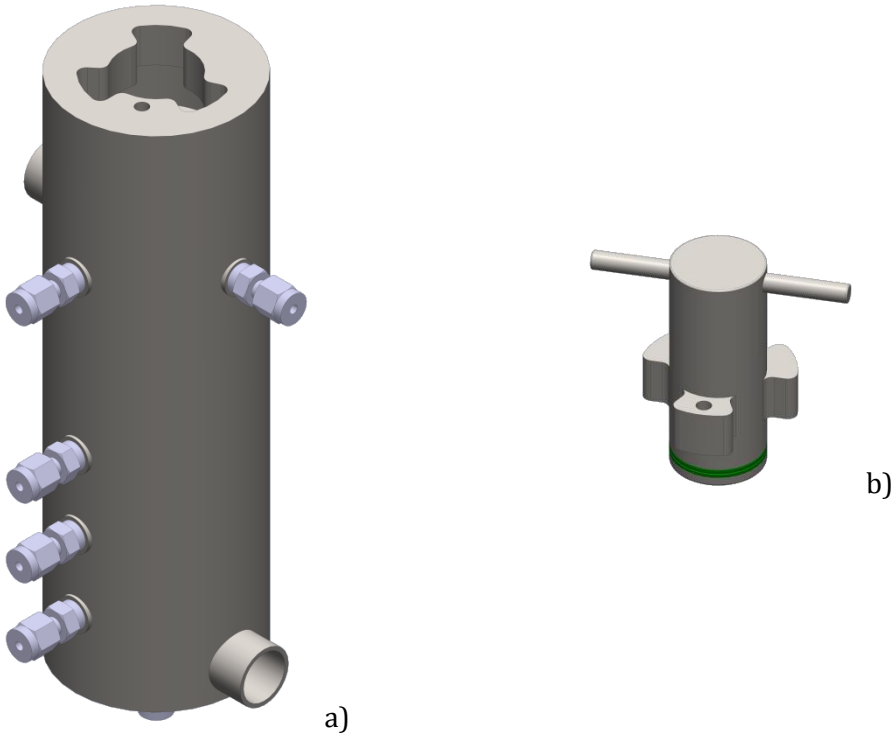


Figure 4.11 – 3D drawing of a) the separator and b) its cover.

In this section, the temperature and pressure were monitored by a thermocouple and a pressure transducer, respectively. The $CO_2$ is quantified using a mass flow meter (MFM). Prior to the MFM, two needle valves are used to reduce the pressure to atmospheric; those valves also have heating tapes. After the MFM the solvent is released to the environment. Figure 4.12 exhibits the 3D scheme of this particular section.

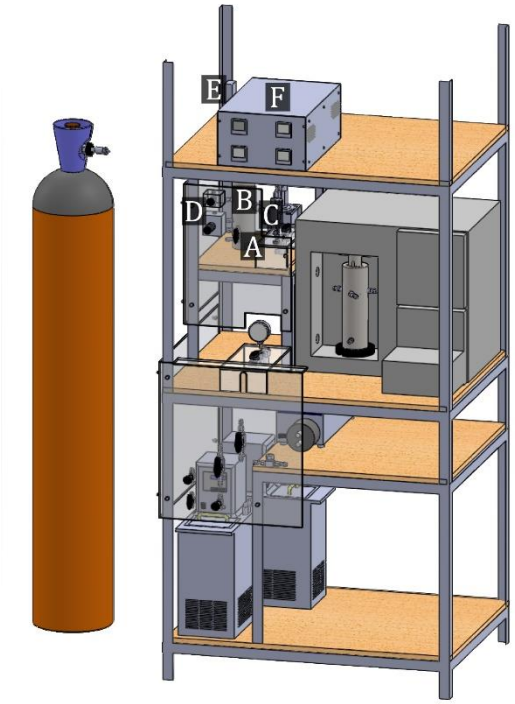


Legend:

A – switching (three-way) valve

B – Separator with jacket

C – Pressure gauge / pressure transducer

D – Needle valve

E – MFM

F – Control box

Figure 4.12 – Schematic 3D drawing of the separation section of the experimental SFE setup.

### 4.2.4 Purge

Throughout the entire experimental setup, valves were placed before pump, extractor and separator that allow to release the pressure of the system.

After showing each component of the setup, Figure 4.13 shows a 3D drawing of the entire SFE unit and a photo of the real setup after assembling.

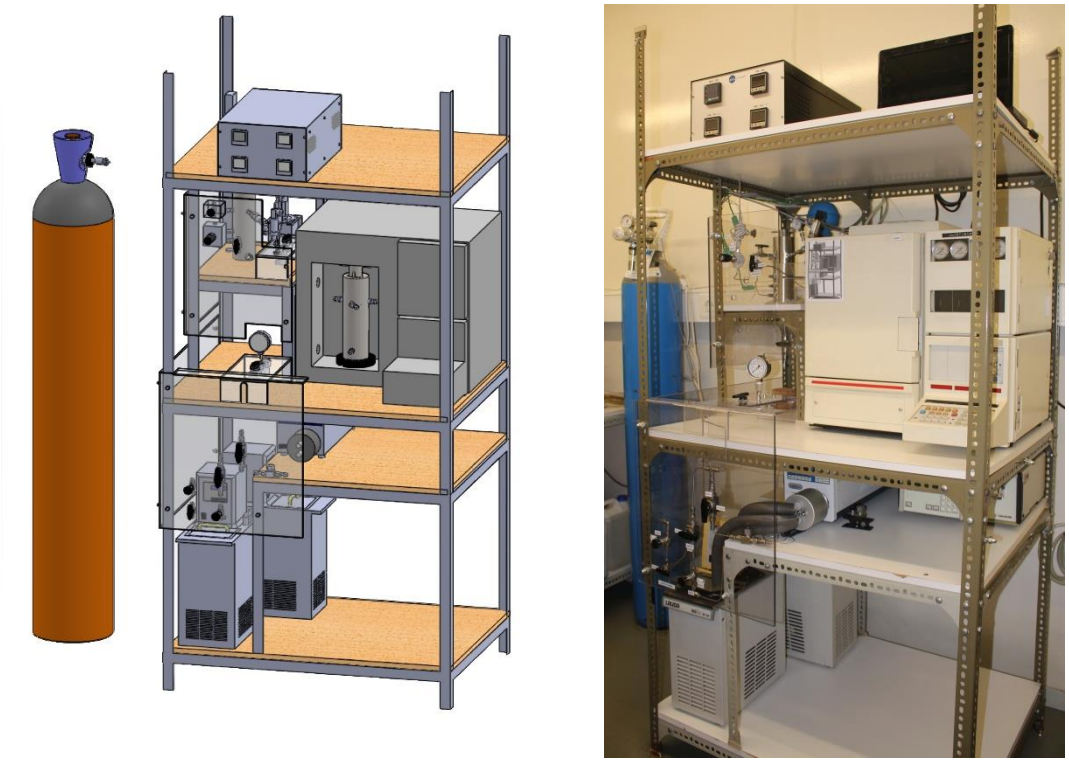

Figure 4.13 – Schematic 3D drawing and photo of the SFE setup after assembling.

Table 4.5 depicts a material list for all equipment used in this setup, indicating the respective main feature as well as brief descriptions of the equipment in all sections.

Table 4.5 – List of material in the supercritical fluid extraction setup

| Section | Equipment | Requirements | Description |
|---|---|---|---|
| Feed | $CO_2$ Cylinder | $CO_2$ supply (> 99.99 %) to the extraction. | $CO_2$ cylinder with a dip tube to take liquid $CO_2$. Cylinder from Ar Liquide Portugal (>99.99%). |
| | Bath | To cool the $CO_2$ before entering the pump, its temperature was about -1°C. | This bath was available in the laboratory. Mc: Lauda; model: eco-line RE 104. Operating temperature range: -10 to 120°C. |
| | Tube | In this section, the maximum pressure was defined by the equilibrium pressure of $CO_2$ inside the cylinder (i.e., up to 60 bar). | Mc: Swagelok, Type: 1/8"; material: stainless steel; working pressure: up to 8500 psig. |
| | $CO_2$ pump | To increase the pressure to extraction requirements. The pressure should be higher than the critical pressure up to 300 bar. | Isocratic pump to high pressure; this pump was already available in the laboratory; it was adapted to $CO_2$ with a cooled head. Mc: Jasco; model: PU-2080. |
| Extraction | Check valve | Ensures there is no flow return to pump head. | Mc: Swagelok; type: lift check valves; material: stainless steel; temperature: 93°C - working pressure: 355 bar. |
| | Oven | To keep constant the extraction temperature in the entire process. | It was used an old GC oven available in the lab. The internal dimension of the oven: 215 x 355 x 125 mm. |
| | Filters | Prevent that some particles from cork samples goes to the follow equipment as the BPR. | Mc: Swagelok; type: tee-type filters; material: stainless steel; temperature: up to 93°C - working pressure: up to 355 bar. |
| | Valves | Control the $CO_2$ supply to the extractor and also the output of the extractor. | Mc: Swagelok; type: multipurpose ball valves (on-off); material: Stainless Steel, temperature: up to 93°C - working pressure: up to 355 bar. |
| | Rupture disc | To avoid over pressurization peaks in the system (extractor); if the pressure rises over 300 bar the disc breaks to release the pressure. | The disc breaks when the pressure reaches ca. 400 bar. |
| | Pressure Gauges | Monitor the pressure before the extractor in the range of working pressure. | Mc: Swagelok, model: general-purpose stainless steel gauge with adjustable pointer. Pressure range: 0 – 400 bar. |

Table 4.5 – List of material in the supercritical fluid extraction setup (continued)

| Section | Equipment | Requirements | Description |
|---|---|---|---|
| Extraction | Pressure transducer | The pressure is monitored and recorded during the entire extraction process. | Mc: Omega; range: 0 – 7500 psig. |
| | Thermocouple | Monitors the temperature inside the extractor. Temperature: room temperature up to 80°C. | Thermocouple Type K. |
| | Extractor | This piece must work until 300 bar and 80°C. It should be possible to measure internally its temperature and pressure. The material to extract (e.g. cork samples) should be easily charged. | Material: stainless steel, working temperature - pressure: up to 80°C – 300 bar. Basket dimensions: diameter 30 mm and height 130 mm (internal dimensions). |
| | Tube | In this section, the maximum working pressure can reach 300 bar, while the maximum temperature can be 80°C. | Mc: Swagelok; type: 1/8"; material: stainless steel; working pressure: up to 8500 psig |
| | Back Pressure Regulator (BPR) | This valve has an automatic control to open or close in way to keep constant the pressure inside the extractor. Also, this valve has a Cv that allows a large pressure drop. | Mc: Research Control Valves; model: RC200. Including the electric actuators. |
| Separation | Bath | To keep constant the temperature inside the separator. | This bath was available in the lab. Mc: Lauda; model: eco-line RE 104. Operating temperature range: -10 to 120°C |
| | Separator | This piece should work at pressures up to 100 bar; it should be possible to measure the temperature and pressure inside it; also, the separator is equipped with a jacket to keep constant the temperature. | Material: stainless steel, working temperature - pressure: up to 80°C – 100 bar. |
| | Thermocouple | Monitors the temperature inside the extractor. | Thermocouple Type K. |
| | Valves | Through these valves, it is possible to supply the separator or to purge system. The valves should work up to 100 bar. | Mc: Swagelok; type: one 3-way valve / on-off; material: stainless steel; pressure-temperature rating: up to 172 bar at 93°C. |

Table 4.5 – List of material in the supercritical fluid extraction setup (continued)

| Section | Equipment | Requirements | Description |
|---|---|---|---|
| Separation | Pressure transducer | To monitor and record the pressure in the separator in the entire process. | Mc: Omega; range: 0 – 3200 psig. |
| | Tube | In this section, the pressure decreases until atmospheric pressure; being the maximum pressure lower than feed. | Mc: Swagelok; type: 1/8"; material: stainless steel, working pressure: 8500 psig |
| | Mass Flow Meter (MFM) | To record the mass of $CO_2$ (at atmospheric pressure) used in the process. | Mc: Bronkhorst; model: F-111B |

### 4.2.5 Program – SFE

As previously referred, to keep constant the pressure, the BPR is open/closed; also the temperature and pressure through the entire process should be monitored and recorded using a program developed in Labview, being the drivers of the data acquisition module (ADAM 4000 Series) developed for this particular application by Paralab, and all the program/interface was adapted by the author.

Figure 4.14 shows the computer display, in real time, of the pressure and temperature in the extractor and separator, the $CO_2$ flow rate at each instant of time as well as its cumulative value. The pressure in the BPR is controlled according to the defined pressure set-point. In this same window, there is also a region denominated “Heating Zone” where the set-point temperature in the BPR and the two needle valves (after the separator) are defined. It is to remark that this window presents the instantaneous operating conditions, while the process window (Figure 4.15) shows the temperature and pressure histories, i.e., the temperature and pressure of the extraction and separator since the starting time; and also the total mass of $CO_2$ that was used. Moreover, it is possible to register the cork sample type, its mass and some other observations concerning each extraction experiment. The program allows to record all pressures and temperatures at the time intervals defined by the user.

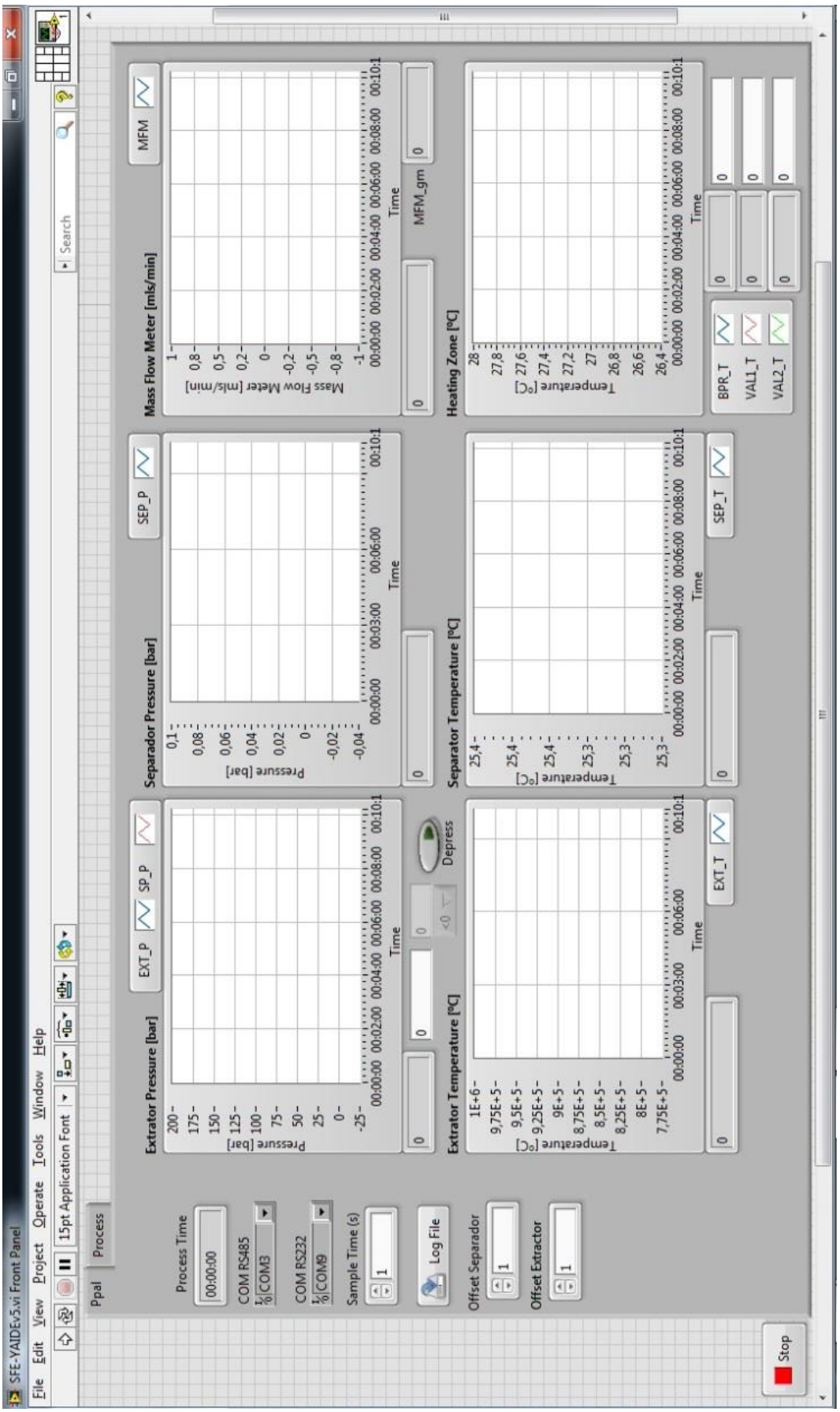


Figure 4.14 – Principal windows of the SFE Program.

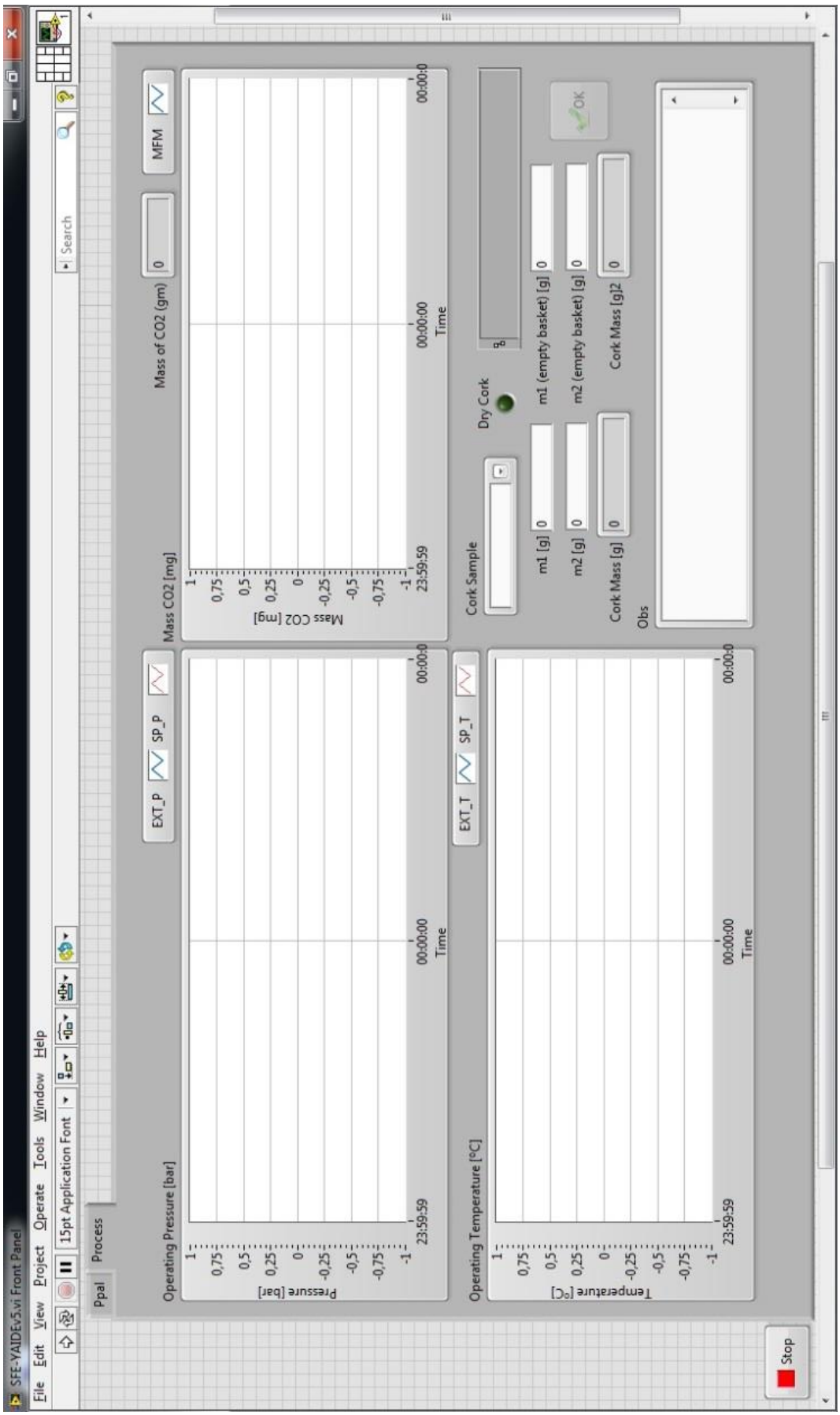


Figure 4.15 – Process windows of the SFE Program

## 4.3 Startup, operation and shutdown of the SFE bench scale setup

After the design and assembling of the setup, the next phase was to test it, which was essential in order to check for leaks and some other problems that can arise. At the end of the tests, it was possible to perform the first experiment; in this section a typical startup, running and shutdown is described for a simple experiment on the bench scale setup in batch or dynamic operations.

### 4.3.1 Start-up of SFE setup

First, for both batch and dynamic operations, the raw material (granulated or cork powder) should be weighed and placed inside the sample basket, and this inside the extractor and the extractor closed; all connections must be checked and the valves until the exit of the extractor as well as all purge valves must be in closed position. Next, turn on the control box, and run the program "*SFE*" that was developed by the author in Labview (as previously described); it is to refer that before running, both the communication ports of the RS485 (acquisition module ADAM 4000 Series) and the RS232 (MFM) interfaces should be indicated; when the program is running, it is possible to monitor all the variables of the process; to start the recording, the user must press the button "Log File" in the tab named "Ppal" of the program user interface as shown in Figure 4.14; after pressing that button, it must be indicated in the new window the name and localization of the new file (to record all data in the run); it is to refer that the interval of time to record each variable was previously defined in "Sample Time (s)", the default value being one second. In tab "Process" of the program, can be registered the type of sample and mass of cork used as well as other observations; remember that to save this information it is necessary to press the button "OK" in this new window. It is noteworthy that through this program, it is possible to define a set point value to the pressure, in the BPR, that is directly related with the pressure in the extractor, as well as the temperature in the valves with heating tapes.

Then, turn on the cooling baths defining a set-point to each one; after the cooling bath that cools the pump head reaches the value of its set-point, the $CO_2$

cylinder is opened, and all the valves from the cylinder exit until the inlet of the extractor must be opened (keep closed the purge valves); switch on the $CO_2$ pump (note that the valve at the exit of the extractor should be closed until reaching the pressure for the extraction). Then, switch off the pump and close all valves and: (i) verify that there are not leaks in the system, i.e. no pressure drop is observed in the extractor and (ii) wait for the system to stabilize at the temperature and pressure required to the extractions. Until now, the procedure is similar to both modes of operation, batch and continuous/dynamic.

### 4.3.2 Operation of the SFE setup

To operate in batch mode, the system remains closed, since the extraction time is one of the main parameters of the extraction; then, the solvent inside is not refreshed being the total mass of $CO_2$ defined by the volume occupied at the previously fixed pressure and temperature. For this operating mode, and in order to evaluate the transfer of solute to the solvent, the extraction time can be changed and also the temperature and/or pressure of the process.

For the dynamic operation, after the stabilization period, the pressure set-point on the BPR must be fixed, and the pump switched-on, fixing the $CO_2$ flow rate for the experiment; the valves will be opened, including the exit-valve of the extractor, and the valves of the separation section. It is to note that it is possible to monitor and record all operating conditions (pressure and temperature) in the extraction and separation sections at each time through the program *"SFE"*, according to the previous definition by the user.

The pressure set-point of the BPR and the temperature set-point for each valve in the denominated "heating zone" (as defined in the previous section) can be fixed in the program "*SFE"*; however, it must be remembered that although it is possible to monitor the temperature in the recirculating baths, the change of their set-points should be directly done in the respective bath; the same is true for the temperature in the oven, where the extractor is located; the $CO_2$ flow rate can only be changed directly in the pump. The program helps to visualize all the operating conditions in a simple window, but you have to remember that

in this particular case, it is not possible to perform an experiment by remote control, since we have no control of the $CO_2$ pump, neither of the open/close for all valves. Summarizing for this particular case, the program *"SFE"* monitors and records all variables of the experiment, but to operate this setup at bench-scale it is fundamental to stay in the laboratory, and remember that when working at high pressure it is necessary to focus the attention on the experiment. For example, if you perform an experiment at 40°C and 120 bar ($CO_2$ density of 717.8 $kg \cdot m^{-3}$), with an extractor of ca. 200 $cm^3$, and a flow rate of 6 $g \cdot min^{-1}$ of $CO_2$, if suddenly the exit of the extractor is closed, maintaining the same rate of flow, in 5 min the pressure inside the extractor can reach ca. 234 bar (at the same temperature); then it is crucial to know what happens at any time, since in short time we can have large variations in the operating variables.

### 4.3.3 Shutdown of the SFE

To finish, switch–off the $CO_2$ pump and close the $CO_2$ cylinder as well as the valve at the exit pump, and remember to change the pressure set-point of the BPR. Also, you can switch-off the cooling bath used for the pump head. When the system reaches the atmospheric pressure, stop the acquisition in the program "*SFE*". And also turn off the oven and the thermostatic bath used to cool the jacket of the separator.

To collect the cork extractives, it is necessary to pass a solvent to remove all extracts in the separator and even any that remains in the BPR, since this extract is solid at atmospheric conditions; at the exit of the extractor it will be made a connection to the co-solvent pump to remove all the extract in the system. It is to note that the separator has an on/off valve at the bottom and the solvent passes from the exit of the extractor to the separator, the extract being collected in solution at the bottom of the separator. After this step, the solvent used to collect the cork extractives must be removed; it can be used a rotary evaporator as described previously in Chapter 3.

After collecting the extract, and before beginning a new experiment, it must be guaranteed that there is no solvent or trace of the extractives in the setup, in order to not influence the following experiments.

## 4.4 Experimental Results

The SFE of cork starts with the cork sample that gave the higher yield (on a dry mass basis) in Chapter 3, when using the soxhlet extraction (sample A1).

First, the experiments were performed in the batch mode, i.e., the pressure and temperature were kept constant; however, these experiments were limited by equilibrium and it was not possible to quantify their low yields. So, the following extractions were implemented in the continuous mode. In the first place, the temperature was kept constant at 41°C in a wide range of pressures from 170 up to 243 bar; the best yield obtained was 19.7 $g_{extract} \cdot kg_{DryCork}^{-1}$ for pressures of 213 and 215 bar; however, there is not a large difference between the values obtained in this range of pressure since the minimum achieved was 14.2 $g_{extract} \cdot kg_{DryCork}^{-1}$ for 197 and 243 bar as represented in Figure 4.16.

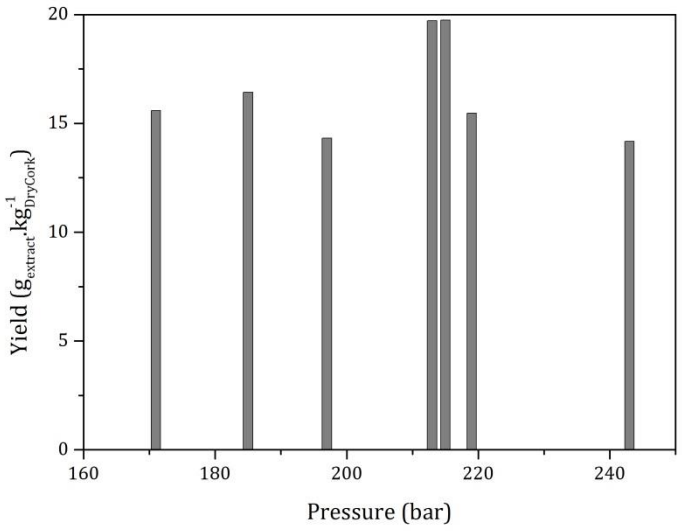


Figure 4.16 – Yields obtained with sample A1 (granulated industrial cork – particle size 0.75 mm) for the SFE at 41°C in a range of pressures from 170 up to 243 bar.

To evaluate the effect of temperature in the extraction, three different temperatures were tested keeping constant the pressure at ca. 210 bar; Figure

4.17 shows that the best result was obtained at 41°C (19.7 $g_{extract} \cdot kg^{-1}_{DryCork}$), while the minimum was 12.2 $g_{extract} \cdot kg^{-1}_{DryCork}$ at 59°C.

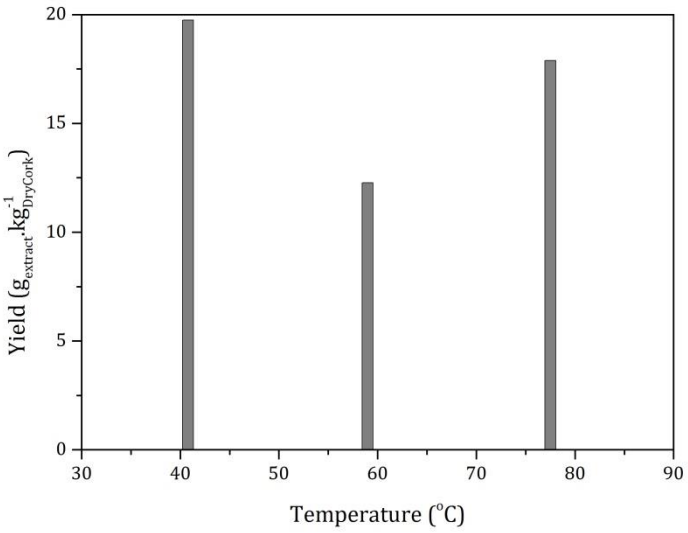


Figure 4.17 – Yields obtained with sample A1 (granulated industrial cork – particle size 0.75 mm) for the SFE at 41, 59 and 78°C and ca. 210 bar.

## 4.5 Conventional extraction *vs.* SFE

Comparing the results obtained for the conventional soxhlet extraction (sample A1), with acetone the yield was 84.3 $g_{extract} \cdot kg^{-1}_{DryCork}$ (Chapter 3), that is ca. 4.3 times higher than the maximum of the SFE using $CO_2$ without co-solvent; and for the lowest polar solvent, hexane, the yield was 48.5 $g_{extract} \cdot kg^{-1}_{DryCork}$ which is only 2.5 times higher when compared with the result for the $CO_2$ at supercritical conditions as shown in Figure 4.18

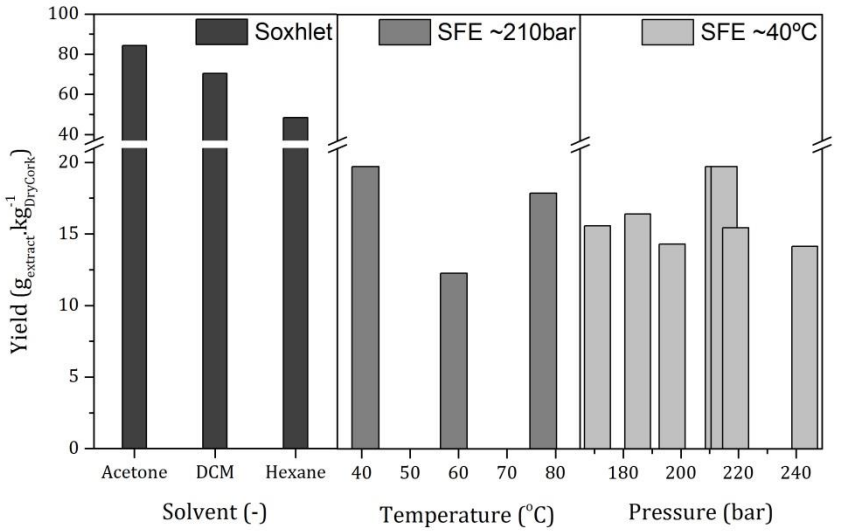


Figure 4.18 – Yields of the conventional solvent extraction *vs.* SFE (41, 59 and 78°C at ~210 bar). For granulated industrial cork with particle size 0.75 mm (sample A1)

Although the yields obtained for the SFE were lower than for the conventional extraction, SFE has a large advantage, since the granulated and cork powder extracted are not contaminated with organic solvent. A quantitative analysis of the compositions of the extracts showed an increase of the target compound when the polarity of the solvent used decreases, i.e. although the yield is lower for hexane, its extract has a higher content of betulin and betulinic acid, being up to 1.5 times higher. It is also to refer that the betulinic acid content of the soxhlet extracts is, in average, 4.8 times higher than that of betulin; the results of the SFE reveals a similar content of betulin and betulinic acid in the extract. Figure 4.19 depicts that the contents of betulin and betulinic acid in the extract are ca. 2.1 and 8.7 times lower than those achieved with the conventional extraction, respectively.

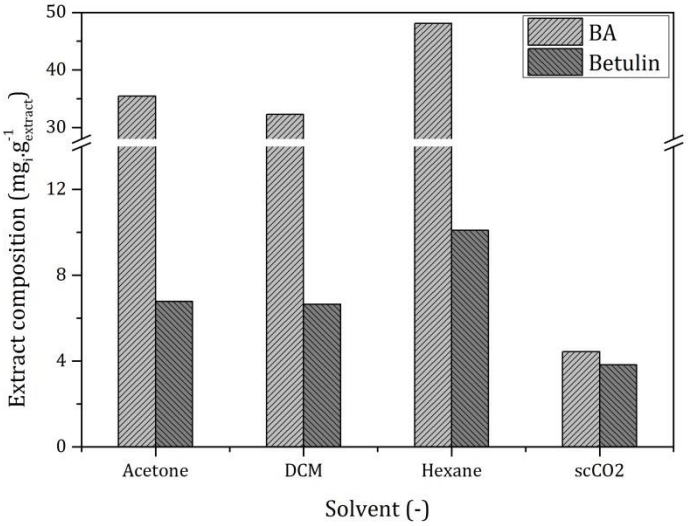


Figure 4.19 – Betulin and betulinic acid (BA) contents in the different extracts, soxhlet extraction (acetone, dichloromethane and hexane) and SFE.

## 4.6 SFE setup improvement to add co-solvent

The experimental setup previously described was prepared to use only one solvent, the $CO_2$; however, in order to increase the yields and also the range of components extracted, it was required to add a new solvent to increase the polarity of the mixture and to increase the separation of the cork extractives compounds. Then, the experimental setup was adapted to add a co-solvent to the $CO_2$. Figure 4.20 shows the new layout of the setup: there is a new pump, that increases the pressure of the new solvent to mix with the $CO_2$.

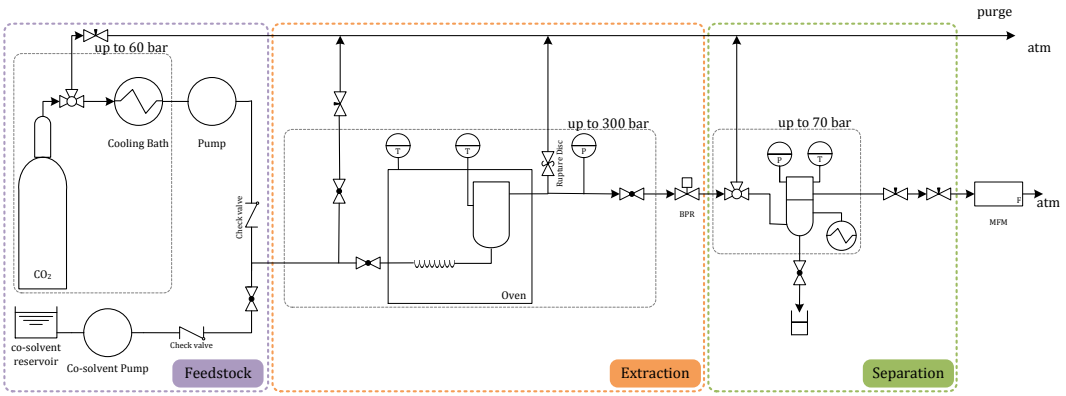


Figure 4.20 – Flowsheet of SFE setup with co-solvent.

It should be noted that this new layout involves some adaptations of the original setup, as the above referred new pump to the co-solvent, an on-off valve for the

new stream, and a check valve for the co-solvent. Figure 4.21 shows the new 3D drawing.

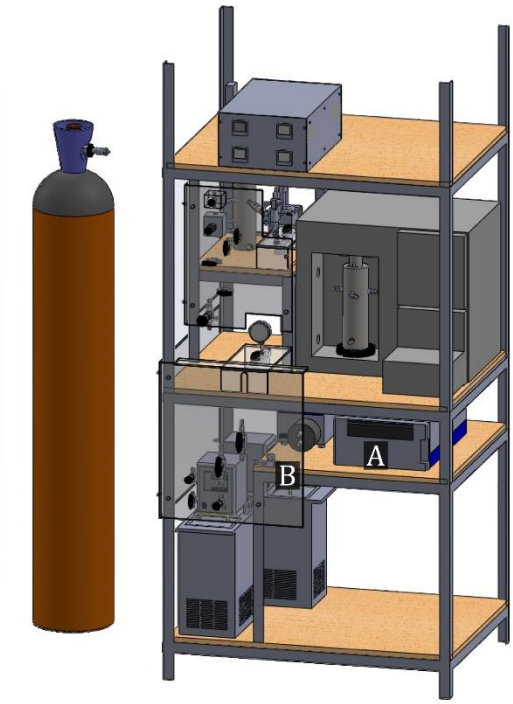


Legend:

A – co-solvent pump

B – Check valve

Figure 4.21 – Schematic 3D drawing of the SFE setup using co-solvent.

In which concerns to the list of material, this adaptation modified both the feed and extraction zones: in the feed zone a new pump is included, the co-solvent-pump, to increase the pressure of the co-solvent until matching with the $CO_2$ pressure; this pump was an isocratic pump, brand: Jasco, model PU-4180; concerning the extraction zone, a new check valve was added, brand: Swagelok, type Poppet 6000 psig (413 barg) check valve; material: stainless steel; this valve ensures there is no flow returning to the pump head.

In this new configuration, it is to take into account that the new solvent (co-solvent) must remain in the separator, i.e., it is not released to the environment as the $CO_2$; therefore, it is important to know the total volume of co-solvent to be used and redefine the new operating conditions for the separation section. Also, with this new configuration it is possible to perform samples collection during the extraction time, since the extract remains in the co-solvent.

In the next section, it will be presented the results for SFE when a co-solvent was added to $CO_2$ at supercritical conditions.

## 4.7 Experimental results, sc$CO_2$ and Ethanol

As showed in the previous chapter (Chapter 3), for soxhlet extraction, the yield increases with the solvent polarity, regardless of the particle size; in this sense, the best yield obtained for supercritical fluid extraction (SFE), using carbon dioxide at supercritical conditions, was 4.3 times lower than the obtained for soxhlet extraction (acetone). To obtain a better performance with SFE a co-solvent was added.

To determine the solvent to use to increase the polarity of the solvent mixture in SFE, a new solvent, ethanol, was tested by soxhlet extraction; with this new solvent, the yield was 1.1 times higher than the obtained with acetone, for sample A1 (Figure 4.22).

Since the yield obtained with ethanol was higher, it was chosen as the co-solvent in SFE. The experiments using co-solvent were carried out at ~215 bar and 41°C, the operating conditions that gave the best performance when using only $CO_2$ at supercritical conditions (see section 4.4). Figure 4.22 compares the yields obtained for soxhlet extraction and SFE with and without co-solvent. The yields were 1.9 and 1.4 times higher than the obtained in the same operating conditions (at 41°C and ~210 bar) without co-solvent, for a mixture with 10% and 5% of ethanol, respectively. It is interesting to note that the extraction capacity for the mixture, ethanol and $CO_2$ at supercritical conditions, is almost a linear combination of the capacity obtained individually for each solvent; e.g., when a mixture with 10% of ethanol is used, a good estimate for the yield is given with 10% of the yield obtained for soxhlet extraction with ethanol and 90% of the yield obtained in the SFE without co-solvent, for the same operating conditions.

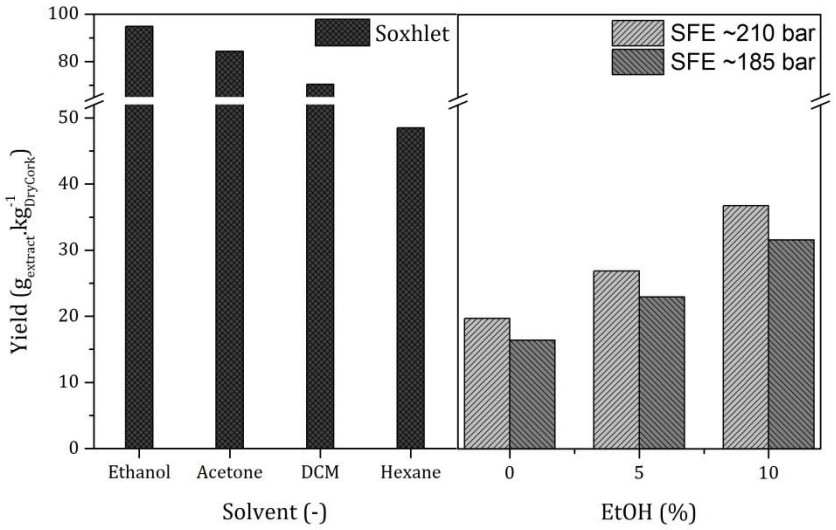


Figure 4.22 – Yields of the conventional solvent extraction *vs.* SFE at 41°C and ~185 bar and ~210 bar with different concentrations of ethanol (10%, 5% and 0%). For granulated industrial cork with particle size 0.75 mm (sample A1).

Despite the addition of co-solvent increases the yields obtained as shown in Figure 4.22, it is to highlight that in the supercritical fluid extraction without co-solvent, both the cork and the extracts are obtained in a solvent-free condition. With respect to the composition of the extract, when the polarity of the SFE mixture increases, the capacity of the extraction for the target compound also increases. Figure 4.23 a) presents the contents of betulin and betulinic acid in the extract (sample A1), for the soxhlet extraction and SFE; when a 5% of ethanol was used in the SFE, the results indicate that the target components in the extract are comparable with the best results obtained in the soxhlet extraction; and the contents of betulin and betulinic acid in the extract were 12.3 and 3.4 times higher than obtained without co-solvent, respectively.

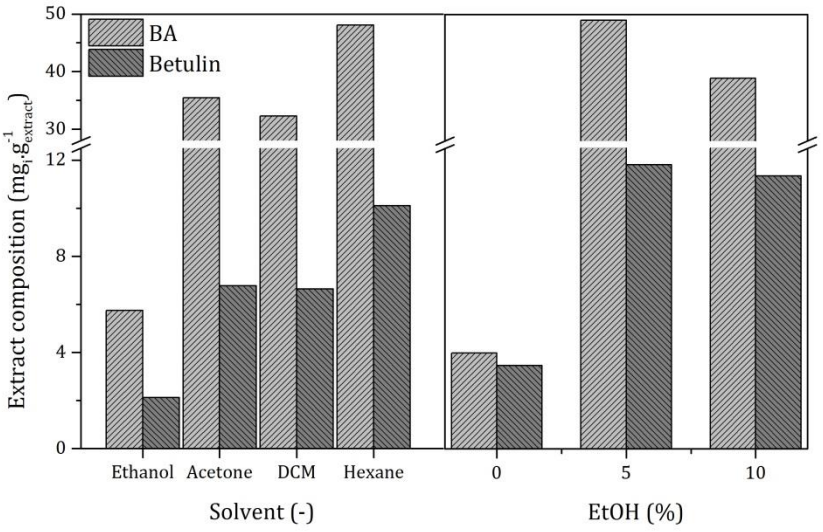


a)

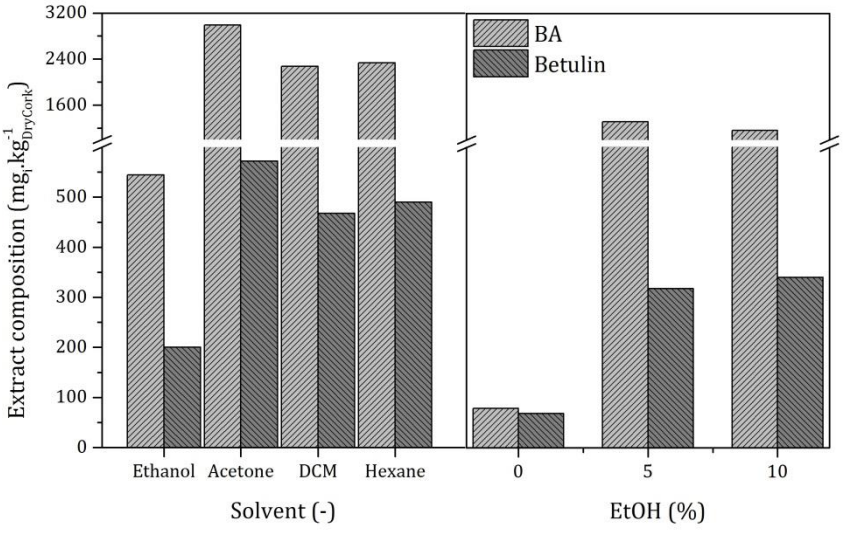


b)

Figure 4.23 – Contents of betulin and betulinic acid (BA): a) in the extracts and b) in the cork. For granulated industrial cork with particle size 0.75 mm (sample A1). For the conventional solvent extraction and SFE at 41°C and ~210 bar with different concentrations of ethanol (0, 5 and 10%).

# Notation

| | | |
|---|---|---|
| $a_{i,j}$ | constants of Eq. 4.1, Eq. 4.2 and Eq. 4.3 (Value Table 4.2) | – |
| $MW$ | molecular weight | $g \cdot mol^{-1}$ |
| $p_c$ | critical pressure | MPa |
| $p_{mel}$ | melting pressure | MPa |
| $p_t$ | triple point pressure | MPa |
| $p_{sub}$ | sublimation pressure | MPa |
| $p_{vap}$ | vapour pressure | MPa |
| $\rho_c$ | critical density | $kg \cdot m^{-3}$ |
| $\rho_{CO_2}$ | carbon dioxide density | $kg \cdot m^{-3}$ |
| $T$ | temperature | K |
| $T_c$ | critical temperature | K |
| $t_{i,vap}$ | constants of Eq. 4.3 (Value Table 4.2) | – |
| $Z_c$ | compressibility factor | – |

# List of Acronyms

| | |
|---|---|
| BPR | Back Pressure Regulator |
| $CO_2$ | Carbon Dioxide |
| FDA | U.S. Food and Drug Administration |
| GRAS | Generally Recognized As Safe |
| MFM | Mass flow meter |
| SFE | Supercritical Fluid Extraction |
| TCA | 2,4,6-trichloroanisole |

# References


Azevedo, E. G. de, and Alves, A. M. de F. B. (**2009**). "Engenharia de processos de separação." *Ensino da Ciência e da Tecnologia 27* (1.ª ed). Lisboa: IST Press. Retrieved from http://eos.fe.up.pt:1801/webclient/DeliveryManager?custom_att_2=simple_viewer&metadata_request=false&pid=50939

Coulson, J. M., Richardson, J. F., Harker, J. H., and Backhurst, J. R. (**2002**). "Chemical engineering." *Coulson & Richardson's Chemical Engineering* (5th ed, Vol. 2). Oxford: Butterworth Heinemann.

Francis, F. J. (**1999**). "Wiley Encyclopedia of Food Science and Technology (2nd Edition) Volumes 1-4." John Wiley & Sons. Retrieved from http://www.knovel.com/web/portal/browse/display?_EXT_KNOVEL_DISPLAY_bookid=681

Green, D. W., and Perry, R. H. (**2008**). "Perry's Chemical Engineerrs' HandBook" (8th ed). McGraw Hill. doi:10.1036/0071422943

Lozowski, D. (**2010**). "Supercritical CO2: A Green Solvent." *Chemical Engineering*, *117*(2), 15–18.

Modey, W. K., Mulholland, D. A., and Raynor, M. W. (**1996**). "Analytical Supercritical Fluid Extraction of Natural Products." *Phytochemical Analysis*, *7*, 1–15. doi:10.1002/(SICI)1099-1565(199601)7:1<1::AID-PCA275>3.0.CO;2-U

NATEX. (**2011**). "New Application."

Noyes, R. (**1994**). "Unit Operations in Environmental Engineering." William Andrew Publishing/Noyes. Retrieved from http://www.knovel.com/web/portal/browse/display?_EXT_KNOVEL_DISPLAY_bookid=1292

Seader, J. D., and Henley, E. J. (**2006**). "Separation process principles" (2nd ed.). New York: John Wiley.

Span, R., and Wagner, W. (**1994**). "A New Equation of State for Carbon Dioxide Covering the Fluid Region from the Triple-Point Temperature to 1100 K at Pressures up to 800 MPa." *J. Phys. Chem. Ref. Data*, *25*(6), 1509–1596. doi:10.1063/1.555991

*"The cork industry is truly unique for its sustainability." (WWF)*

# 5 Modelling Extraction Process

In order to predict the experimental results, phenomenological models of the extraction of bioactives from cork will be developed, and applied to both soxhlet and supercritical fluid extractions. In the extraction from a solid, mass transfer takes place when a solute is removed from the solid matrix by the fluid phase, i.e., the solvent. The physical characteristics of the particles and their bonds with the solute as well as the changes of the process variables have direct influence on the extraction.

There are several models to describe the extraction process, Figure 5.1 summarizes the main considerations to define a specific model wherein each assumption determines where and when can it be applied (Cocero *et al.*, 2001a, 2001b; de Melo *et al.*, 2014; Esquível *et al.*, 1999; Martinez *et al.*, 2003; Naik *et al.*, 1989; Oliveira *et al.*, 2011; Tan *et al.*, 1989). The equilibrium, for example, is a function of temperature and pressure as well as of the composition of the solute in the solid matrix and the saturation concentration in the solvent; it is important to know the particles configurations, since their sizes, geometries and surface area will have direct influence on mass transfer; moreover, the velocity profile of the solvent in the packed-bed determines the mass transfer process. Also, the diffusivity and solubility have influence in the process.

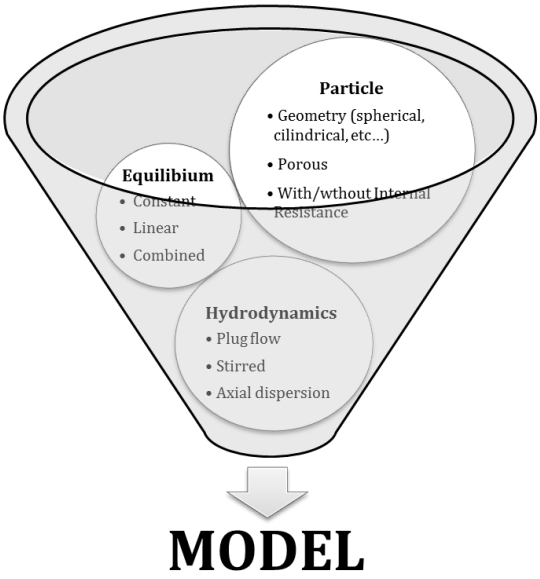


Figure 5.1 – Considerations to describe a model for extraction processes (e.g., supercritical fluid extraction).

As previously referred, each group of assumptions defines an extraction model, so there are several classifications; e.g. (Cocero *et al.*, 2001a, 2001b) defined two basic models, (i) desorption models; assuming that the solute is removed by a desorption process, they developed a model with two parameters to describe the process (equilibrium and mass transfer coefficients), (ii) shortcut methods; these methods consider that the extraction curve can be simulated by the residence time distribution (RTD), i.e. the process is described by the flow pattern. On the other hand, de Melo *et al.* (2014) consider two main classes of models, (i) empirical and simplified models; and (ii) comprehensive phenomenological models (shrinking core, broken plus intact cells and a combination of both).

In this chapter, two phenomenological models are described, a diffusional model and a shrinking core model with the aim to describe the experimental results.

The contact system will be considered to be a fixed bed for both soxhlet and supercritical fluid extractions. The soxhlet case deserves a special explanation. As a matter of fact, it is in reality an extraction process constituted by several successive batch steps. Nonetheless, it is well known that batch and plug flow

systems can be considered equivalent if the operating time of the batch system is equal to the space time (mean residence time) of the plug flow system. In the operation of the soxhlet, the solvent is vaporized and condenses around the particles operating then the extraction; when the system is full of liquid, it is emptied and the solvent (now with the extracted matter) is returned to the boiler to be vaporized. And this process is repeated as many times as wanted, always with "fresh" (recently vaporized) solvent, fixing the total extraction time. In the models to be developed in the following, the time from the beginning of each extraction step (start of the filling up with solvent) until the end of the same step (emptying of the extraction system), which is the operating time of each batch, is taken as the space time of the fixed bed system which is modelled.

## 5.1 Desorption Model

In this model, it is proposed that the solute is removed from a solid matrix in a packed-bed through a desorption process; the main assumptions which refer to the fluid phase are:

- ✓ The flow rate, density and viscosity of the solvent are kept constant through the process.
- ✓ There is no gradient of temperature in the bed or it can be neglected.
- ✓ Density and porosity of bed are constant.
- ✓ Solute in the matrix is completely soluble in the fluid phase, i.e. in the solvent.

The mass balance for the fluid phase is given by:

$$\frac{\partial C_i}{\partial t} = D_{ax} \frac{\partial^2 C_i}{\partial z^2} - u_i \frac{\partial C_i}{\partial z} - k_f a_p \frac{(1-\varepsilon)}{\varepsilon}\left(C_s^*\Big|_{Rp} - C_i\right) \qquad \text{Eq. 5.1}$$

Where, $C_i$ is the concentration of solute in the fluid phase, $C_s^*\Big|_{Rp}$ is the surface equilibrium concentration, $t$ corresponds to the time of extraction, $z$ is the length in the axial direction, $R_p$ is the radius of particle, $D_{ax}$ is the axial dispersion coefficient, $u_i$ is the interstitial velocity, $k_f$ is the mass transfer

coefficient, $a_p$ is the particle specific surface area (area/volume) and $\varepsilon$ is the porosity or void fraction of the packed-bed. To solve Eq. 5.1 it is necessary to know the initial and boundary conditions. The initial condition is given by,

$$t = 0 \; ; \; C_i = 0 \quad \forall \quad z \qquad \text{Eq. 5.2}$$

While the boundary conditions, the conditions at the inlet and outlet of bed are given by,

$$z = 0 \; ; \; -D_{ax} \left. \frac{dC_i}{dz} \right|_{z=0} = u_i \left( C_{i,\text{feed}} - C_{i,z=0^+} \right)$$

$$z = L \; ; \; \left. \frac{dC_i}{dz} \right|_{z=L} = 0 \qquad \text{Eq. 5.3}$$

Where $L$ is the length of the bed.

Introducing the following dimensionless variables and time constants:

$$\theta = \frac{t}{\tau} \; ; \; Z = \frac{z}{L} \; ; \; \xi = \frac{r}{R_p}$$

$$x_i = \frac{C_i}{C^*_{s0}} \; ; \; x^*_s = \frac{C^*_{s,i}}{C^*_{s0}} \; ; \; C^*_{s0} = C_{s0} \frac{(1-\varepsilon)}{\varepsilon} \qquad \text{Eq. 5.4}$$

$$\tau = \frac{L}{u_i} \; ; \; \tau_f = \frac{1}{k_f a_p} \frac{\varepsilon}{(1-\varepsilon)} \; ; \; \tau_d = \frac{R_p^{\,2}}{D_h}$$

With the following model parameters,

$$N_f = \frac{\tau}{\tau_f} \; ; \; N_d = \frac{\tau}{\tau_d} \; ; \; Bi_m = \frac{N_f}{N_d} \; ; \; Pe = \frac{u_i L}{D_{ax}} \qquad \text{Eq. 5.5}$$

Eq. 5.1 becomes in dimensionless form:

$$\frac{\partial x_i}{\partial \theta} = \frac{1}{Pe} \frac{\partial^2 x_i}{\partial Z^2} - \frac{\partial x_i}{\partial Z} - N_f \left( x^*_s \Big|_{\xi=1} - x_i \right) \qquad \text{Eq. 5.6}$$

With the initial condition,

$$\theta = 0; \quad x_i = 0 \quad \forall \quad Z \qquad \text{Eq. 5.7}$$

And the following boundary conditions,

$$Z = 0 \; ; \; -\frac{1}{Pe}\frac{dx_i}{dZ}\bigg|_{Z=0} = \left(x_{i,\text{feed}} - x_{i,Z=0^+}\right)$$

$$Z = 1 \; ; \; \frac{dx_i}{dZ}\bigg|_{Z=1} = 0 \qquad \text{Eq. 5.8}$$

In this chapter, two considerations were assumed with respect to the material balance to the solid phase; first, it was considered a "diffusional model", in which the solute is uniformly distributed throughout the matrix and it diffuses through the particle until its surface being then transferred to the fluid phase. The second model studied was the "shrinking core model", in which it is considered that the solute is removed by layers and it is only in a portion of the matrix (core).

Taking into account the results of chapter 3 and the respective interpretation, it will be considered that only an outer layer of each particle will be extracted. This layer, as shown before depends on the particle size and on the solvent.

### 5.1.1 Diffusional model

Considering spherical particles, the mass balance for the solid is given by the Eq. 5.9,

$$\frac{dC_{s,i}}{dt} = \frac{D_h}{r^2}\frac{\partial}{\partial r}\left(r^2\frac{\partial C_{s,i}}{\partial r}\right) \qquad \text{Eq. 5.9}$$

Where, $C_{s,i}$ is the concentration of solute in the particle, $t$ corresponds to the time of extraction, $r$ is the radial position, $R_p$ is the radius of particle, $D_h$ is the effective diffusivity. The initial condition to solve Eq. 5.9 is given by,

$$t = 0; \quad C_{s,i} = C_{s,0} \quad \forall \quad z \;\&\; r \qquad \text{Eq. 5.10}$$

With the following boundary conditions,

$$r = r_c \; ; \; \left. \frac{\partial C_{s,i}}{\partial r} \right|_{r=0} = 0$$

$$r = R_p \; ; \; -D_h \left. \frac{\partial C_{s,i}}{\partial r} \right|_{r=R_p} = k_f \left( C^*_{s,i}\big|_{Rp} - C_i \right) \qquad \text{Eq. 5.11}$$

Introducing dimensionless variables, Eq. 5.9 becomes,

$$\frac{dx_{s,i}}{d\theta} = \frac{N_d}{\xi^2} \frac{\partial}{\partial \xi} \left( \xi^2 \frac{\partial x_{s,i}}{\partial \xi} \right) \qquad \text{Eq. 5.12}$$

With the initial condition,

$$\theta = 0 \; ; \qquad x_{s,i} = 1 \qquad \text{Eq. 5.13}$$

And the boundary conditions,

$$\xi = r_c \Rightarrow \left. \frac{\partial x_{s,i}}{\partial \xi} \right|_{\xi=0} = 0$$

$$\xi = 1 \Rightarrow -3 \left. \frac{\partial x_i}{\partial \xi} \right|_{\xi=1} = \frac{N_f}{N_d} \left( x_s\big|_{\xi=1} - x_i \right) \qquad \text{Eq. 5.14}$$

In order to evaluate the effects of the dimensionless parameters on the process behaviour, the Péclet number was changed; $N_d$ and $N_f$ were also varied; these two last parameters represent the numbers of mass transfer units by diffusion inside the particles and in the film surrounding particles, respectively. Table 5.1 shows the minimum and maximum of those numbers used in the simulation runs. In the following simulations, the particles are assumed to be totally extracted, i.e., $r_c = \xi_c = 0$.

Table 5.1 – Dimensionless numbers

| | **Minimum** | **Maximum** |
|---|---|---|
| **Péclet (*Pe*)** | 0.01 | 1000 |
| $N_d$ | 0.01 | 10 |
| $N_f$ | 0.01 | 10 |

Assuming that the solute is uniformly distributed throughout the particle and that it is totally removed, Figure 5.2 shows for several Péclet numbers (*Pe*), using the diffusional model, the histories of the cumulative amount of solute in the fluid phase (at the exit of the packed-bed). This Figure represents the effects of different *Pe* when the other parameters are unchanged; in this particular case, $Bi_m$ was kept as 1, i.e. the diffusion in the particle and in the film surrounding particles have the same influence in the extraction process.

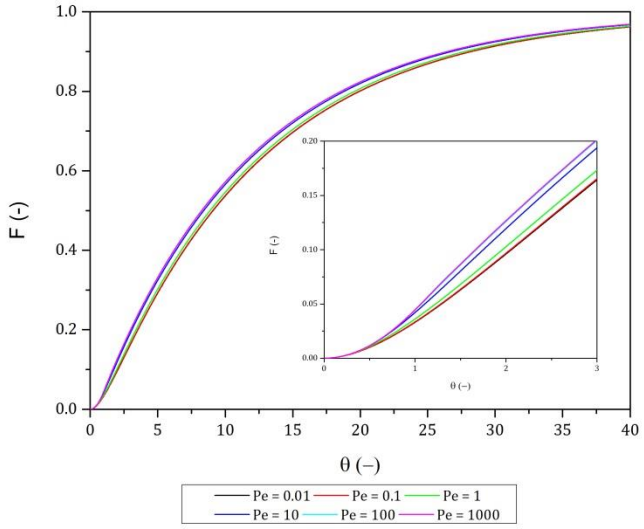


a)

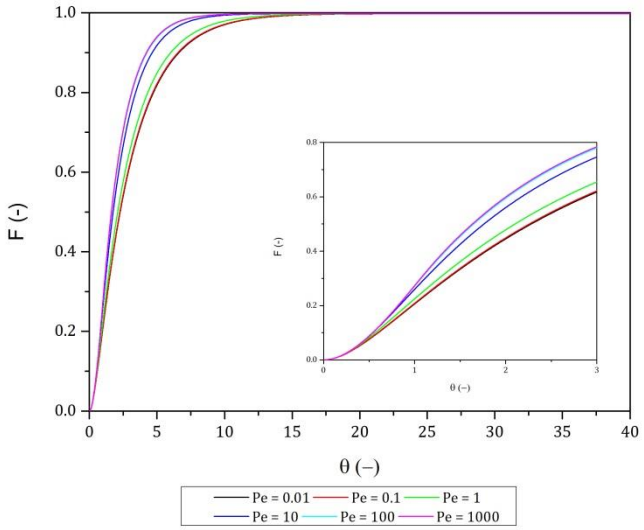


b)

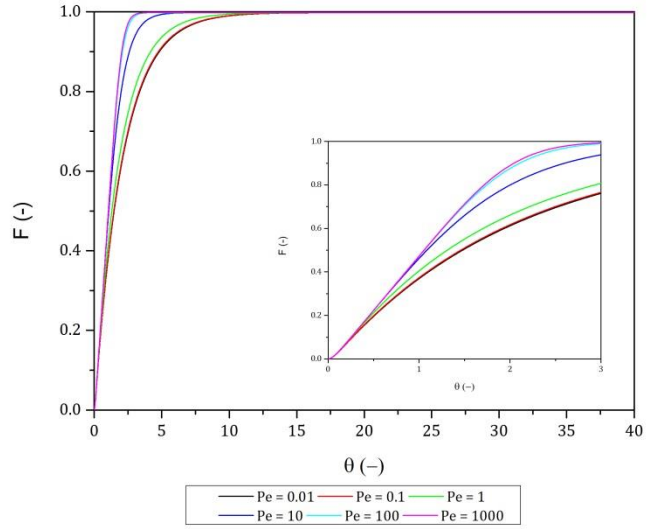


c)

Figure 5.2 – Histories of amount of solute in the fluid phase at the outlet of the packed-bed for different Péclet number values (0.01 to 1000) and $Bi_m$ = 1. (a) $N_f$= $N_d$= 0.1; (b) $N_f$= $N_d$= 1; (c) $N_f$= $N_d$= 10

Figure 5.2 reports the results obtained for different (18) runs; when Péclet increases, the transfer rate of solute from the solid to the fluid phase increases for all runs; despite Biot is kept constant and equal to 1, the transfer of solute takes a longer time when $N_d$ and $N_f$ are lower (Figure 5.2a). Also, Figure 5.2 shows that it is not noticeable a difference in the transfer of solute to fluid phase when *Pe* is higher than 100; Figure 5.3 shows the influence of $N_d$ and $N_f$, when *Pe* was kept as 100 and the number of mass transfer units by diffusion, in the particle, has no influence in the extraction process ($N_d$ = 10), while the number of mass transfer units in the film surrounding particles was changed from 0.01 until 10, i.e., the mass transfer coefficient ($k_f$) decreases three orders of magnitude; as expected, when $N_f$ increases the transfer from the solid to the fluid phase increases. When the dimensionless time is 5 and $N_f$ is 10, it was extracted the totality of the solute from the solid phase, while only 94%, 35% and 4% were extracted when $N_f$ is 1, 0.1 and 0.01, respectively.

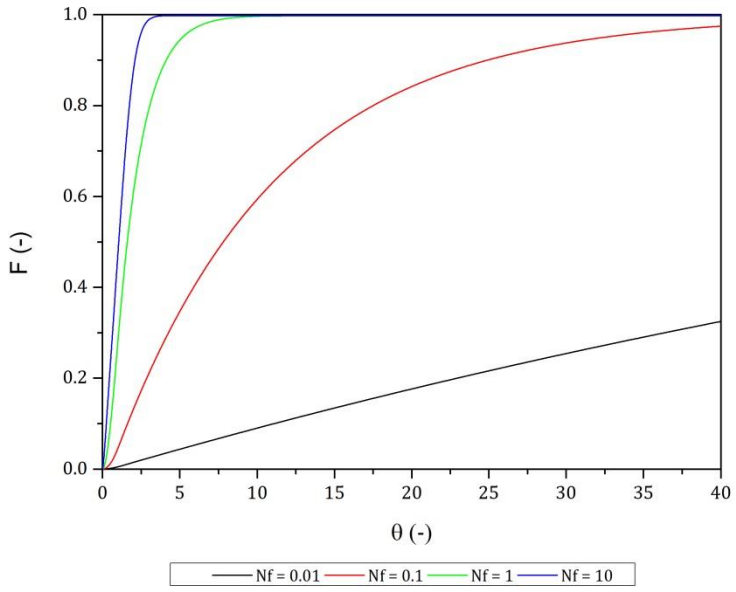


Figure 5.3 – Histories of amount of solute in the fluid phase at the outlet of the packed-bed. $N_f$ = 0.01 to 10; $N_d$ = 10 and Péclet number is 100.

If the effect of the film surrounding particles is negligible, it is possible to study the effect of diffusion in the particle. Figure 5.4 shows the effect of $N_d$. For *Pe* = 100, $N_f$ = 10 and $N_d$ = 10 or 1; when the dimensionless time is 5, the particle was totally extracted while for $N_d$ = 0.1 and 0.01 the amounts extracted are 96% and 55%, respectively.

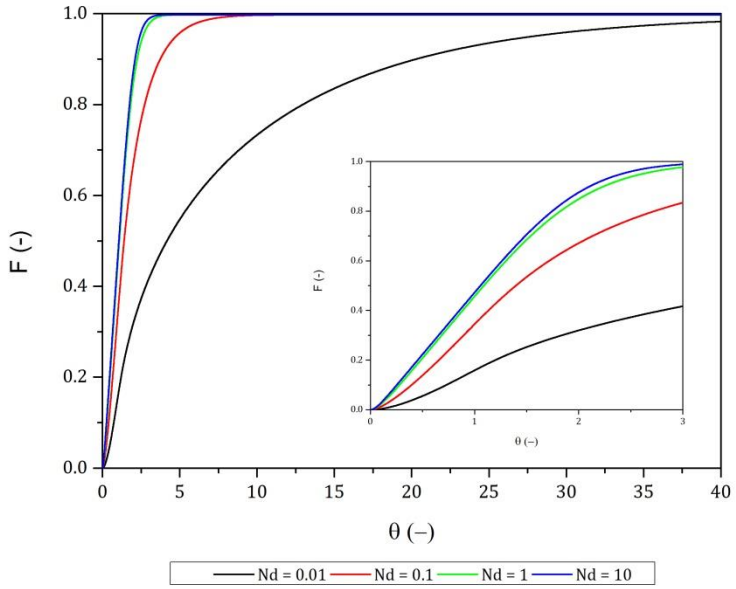


Figure 5.4 – Histories of amount of solute in the fluid phase at the outlet of the packed-bed. $N_d$ = 0.01 to 10; $N_f$ = 10 and Péclet number is 100

Until now, it was assumed that the solute was uniformly distributed in the particle and that it was totally removed ($\xi_c = 0$). However, as conjectured in Chapter 3 based on the soxhlet results, it is possible that the solute is available until a specific radius of the particle (considering spherical particles), i.e., only an outer layer is accessible for solvent; Figure 5.5 indicates the percentage of the total volume of particle used with respect to the radius of particle until where the solute is available $\left(V_{used} / V_p = \left(1 - \xi_c{}^3\right)\right)$. This Figure indicates the maximum value for the amount of solute that is transferred to the fluid phase ($F$); e.g., if $\xi_c = 0$ the particles are totally extracted then $F = 1$; but if $\xi_c = 0.50$, the maximum value to $F$ will be 0.785.

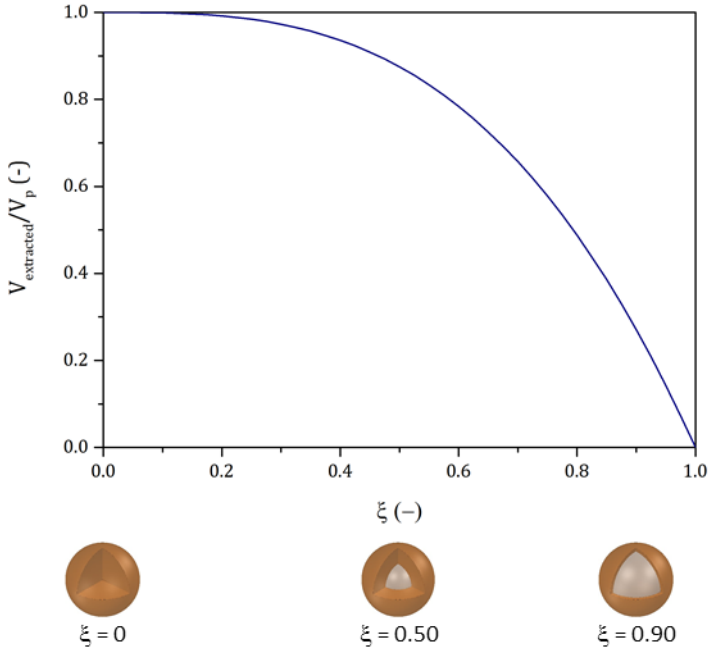


Figure 5.5 – Volume used according to internal radius $\left(\xi_c = r_c / R_p\right)$

In this section, the diffusional model was described, as well as the influence of some parameters in the extraction process; in the following, the shrinking core model will be considered.

### 5.1.2 Shrinking core model

In this case, spherical particles are also assumed; however, the solute is removed by layers; since everything is happening in the "extraction front", the outer region is considered to be in steady state, i.e., there is no accumulation in this region and the mass balance is given by

$$\frac{\partial}{\partial r}\left(r^2 \frac{\partial C_{s,i}}{\partial r}\right) = 0 \qquad \text{Eq. 5.15}$$

The solute extracted from the core is transferred to the fluid phase; the core radius changes over time as described by the following equation:

$$\frac{r_c}{R_p^2}\frac{\partial r_c}{\partial t} = -\frac{D_h}{C_{s,0}}\frac{\partial C_s}{\partial r}\bigg|_{R_p} \qquad \text{Eq. 5.16}$$

The initial conditions for the previous equations are,

$$t = 0 \qquad C_{s,i} = C_{s,0} \quad \forall \quad z \;\&\; r$$

$$r_c = R_p \quad \forall \quad z \qquad \text{Eq. 5.17}$$

While the boundary conditions are,

$$r = r_c \qquad C_{s,i} = C_{s,0} \quad \forall \quad z$$

$$r = R_p \qquad -D_h \left.\frac{\partial C_{s,i}}{\partial r}\right|_{r=R_p} = k_f \left(C^*_{s,i}\Big|_{Rp} - C_i\right) \qquad \text{Eq. 5.18}$$

The mass balance equations, after introducing dimensionless variables, become

$$\frac{\partial}{\partial \xi}\left(\xi^2 \frac{\partial x_s}{\partial \xi}\right) = 0 \qquad \text{Eq. 5.19}$$

And,

$$\xi_c^{\,2} \frac{\partial \xi_c}{\partial \theta} = N_d \left.\frac{\partial x_s}{\partial \xi}\right|_{\xi=1} \qquad \text{Eq. 5.20}$$

With the initial conditions

$$\theta = 0 \qquad x_{s,i} = 1$$

$$\xi_c = 1 \qquad \text{Eq. 5.21}$$

The boundary conditions are given by

$$\xi = \xi_c \Rightarrow x_s = 1$$

$$\xi = 1 \Rightarrow -3 \left.\frac{\partial x_{s,i}}{\partial \xi}\right|_{\xi=1} = \frac{N_f}{N_d}\left(x_i - x_s\Big|_{\xi=1}\right) \qquad \text{Eq. 5.22}$$

Similarly to the previous analysis for the diffusional model, for the shrinking-core model the influences of Péclet, $N_d$ and $N_f$ were studied. In this model, the

transfer of the solute occurs by layers and the core radius changes over time until eventually reaching the centre of the particle. Figure 5.6 represents the histories of the cumulative amount of solute in the fluid phase at the outlet of the packed-bed; the effect of the Péclet number was evaluated, while $N_d$ and $N_f$ were kept constant. As in the diffusional model, when $N_d$ and $N_f$ are lower, the mass transfer decreases, despite the *Pe* number.

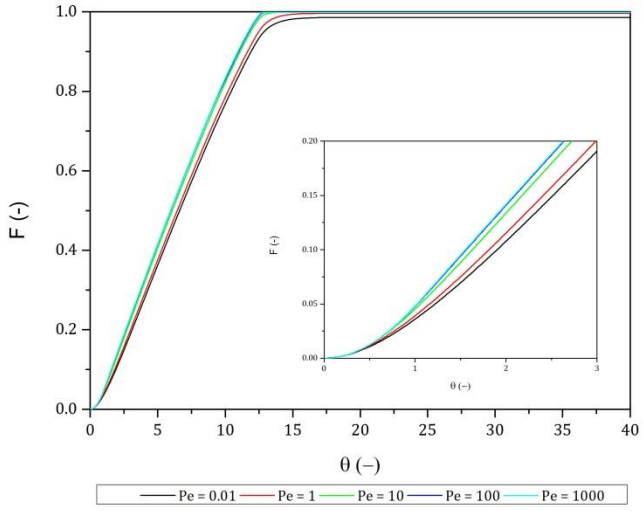


a)

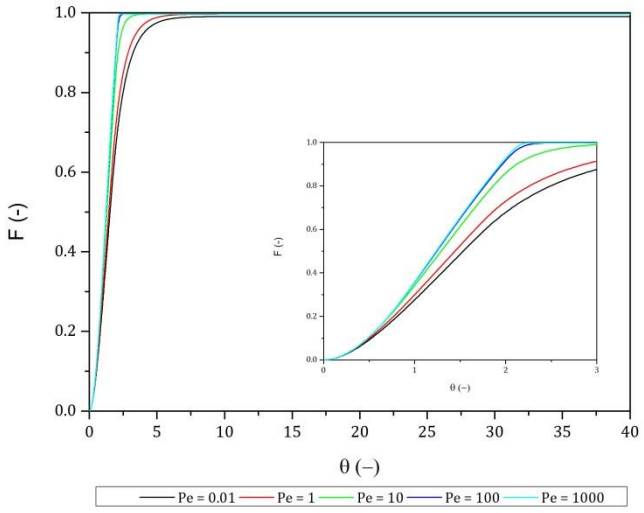


b)

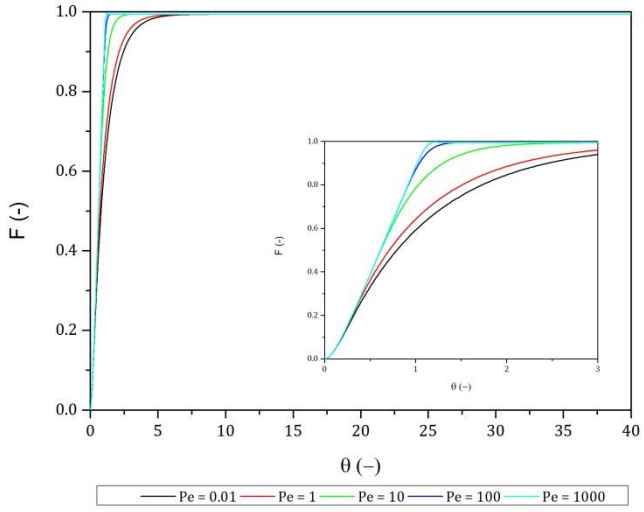


c)

Figure 5.6 – Histories of the amount of solute in the fluid phase at outlet of the packed-bed for several Péclet number values (0.01, 1 and 1000) and $Bi_m$ = 1. (a) $N_f$= $N_d$= 0.1; (b) $N_f$= $N_d$= 1; (c) $N_f$= $N_d$= 10

The effects of $N_d$ and $N_f$ showed in Figure 5.7 and Figure 5.8 were similar to the obtained in the diffusional model (Figure 5.3 and Figure 5.4, respectively). It is possible to note that for the same parameter, the transfer of the solute from the solid to the fluid phase is higher in the shrinking core model. When the term of diffusion inside the particle was considered negligible, i.e. $N_d = 10$, the particle was fully extracted when the dimensionless time was 1.6, 2.5 and 11.6, for $N_f = 10$, 1 and 0.1, respectively.

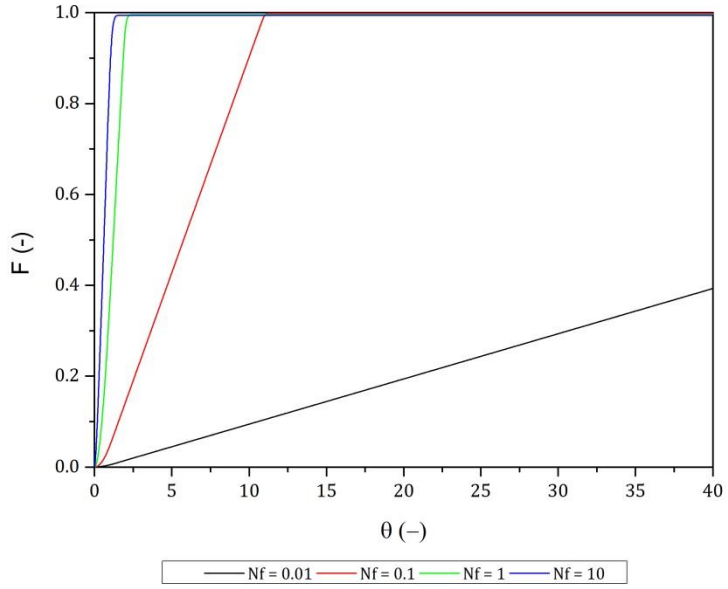


Figure 5.7 – Histories of amount of solute in fluid phase at the outlet of the packed-bed. $N_f = 0.01$ to 10; $N_d = 10$ and Péclet number is 100.

When the film surrounding the particles is not the limiting step of the extraction process, it is possible to study the effect of diffusion inside the particle. Figure 5.8 shows the effect of $N_d$, considering $Pe = 100$ and $N_f = 10$. When the dimensionless time is 5, the particle was totally extracted for $N_d = 0.1$ until 1, while for $N_d = 0.01$ the amount extracted was only 67%.

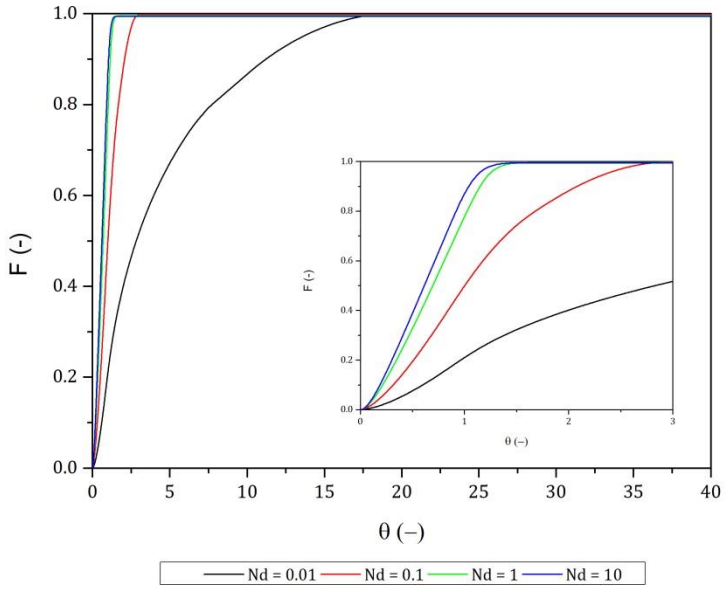


Figure 5.8 – Histories of amount of solute in fluid phase at the outlet of the packed-bed. $N_d$ = 0.01 to 10; $N_f$ = 10 and Péclet number is 100.

For both models, diffusional and shrinking core, Figure 5.9 compares the particular case of negligible film resistance ($N_d$ = 10) and with Péclet = 100; this Figure shows that for the shrinking core model (dashed lines), the transfer is faster than in the diffusional model (full lines); although the shrinking core model assumed that the solute is removed by layers, it should be noted that it was considered that in both models all the particles were fully extracted.

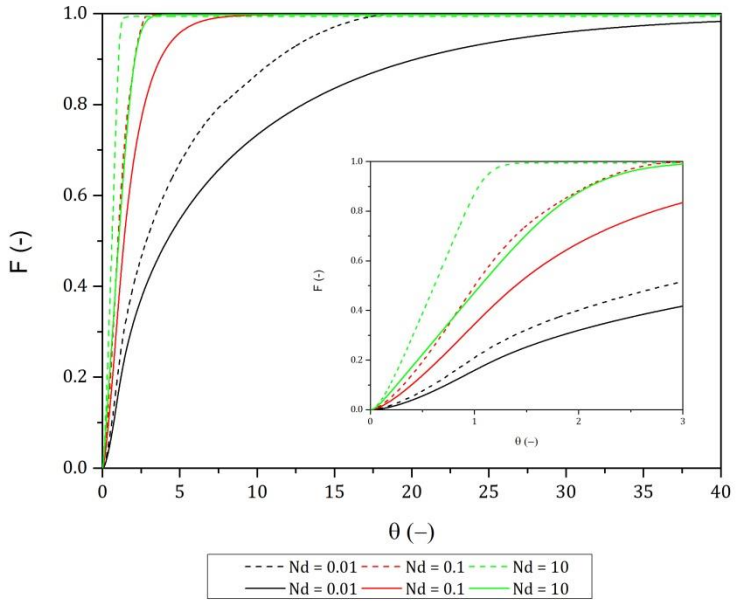


Figure 5.9 – Histories of amount of solute in fluid phase at the outlet of the packed-bed. $N_d$ = 0.01; 0.1 and 10; $N_f$ = 10 and Péclet number is 100. Diffusional model is represented by solid lines and shrinking core model by dashes lines

Figure 5.10 shows the effect of the film resistance around the particles for each model, considering $N_d$ = 10 and $Pe$ = 100.

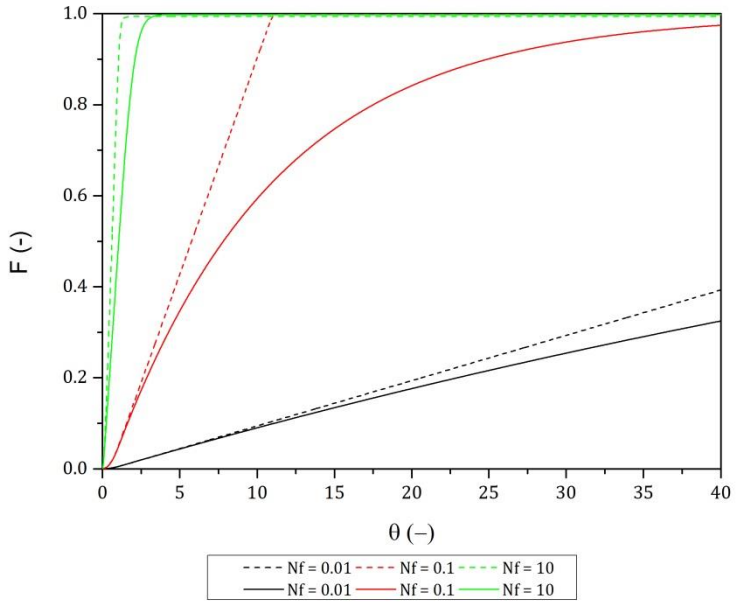


Figure 5.10 – Histories of amount of solute in fluid phase at the outlet of the packed-bed. $N_f$ = 0.01; 0.1 and 10; $N_d$ = 10 and Péclet number is 100. Diffusional model is represented by solid lines and shrinking core model by dashed lines

In the following section, the models described previously will be compared with the experimental data, for both soxhlet extraction and supercritical fluid extraction (with or without ethanol as co-solvent).

## 5.2 Validation of models

In previous chapters (Chapter 3 and 4), the yields were represented as mass of extract by mass of cork; but in chapter 3, section 3.3 (layer thickness of cork accessible to extraction), it was found that when the particle size increases, for the granulated industrial cork, only the external layer is accessible to the solvent, i.e., it is not fully extracted according with the result obtained. As the total volume of cork is not extracted it was essential to represent the yields in terms of volume of cork used; Figure 5.11 shows the yields of the conventional soxhlet extraction (mass extract by volume of dry cork). It was considered that the cork powder was fully extracted and the yield obtained for powder represents the maximum extraction capacity for each solvent. Also, it is possible to note that when the particle size increases, only a layer was extracted;

however, for particles higher than ~1 mm, as a consequence of cork being a liquid sealant, the layer is almost constant regardless of particle size, and it only depends on the type of solvent.

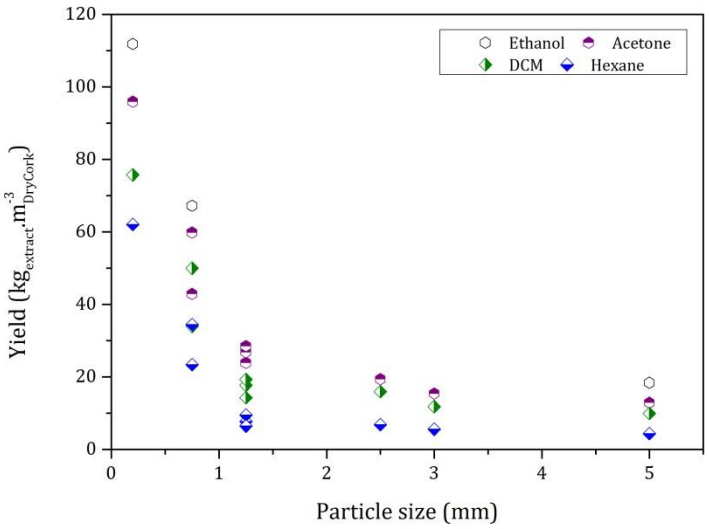


Figure 5.11 – Yields of conventional soxhlet extraction of industrial granulated cork as a function of particle size, for the different solvents tested: (hexagon-open) ethanol, (hexagon-half up) acetone, (diamond-half right) dichloromethane, (diamond-half down) hexane.

The previous Figure represents the fraction of volume extracted; being the cork powder fully extracted according to the capacity of each solvent. Figure 5.12 shows the dimensionless (extractable) core radius as a function of particle size; cork powder was totally extracted, i.e., $r_c / R_p = \xi_c = 0$, if the particle size increases only a fraction of the particle is extracted $(\xi_c \neq 0)$.

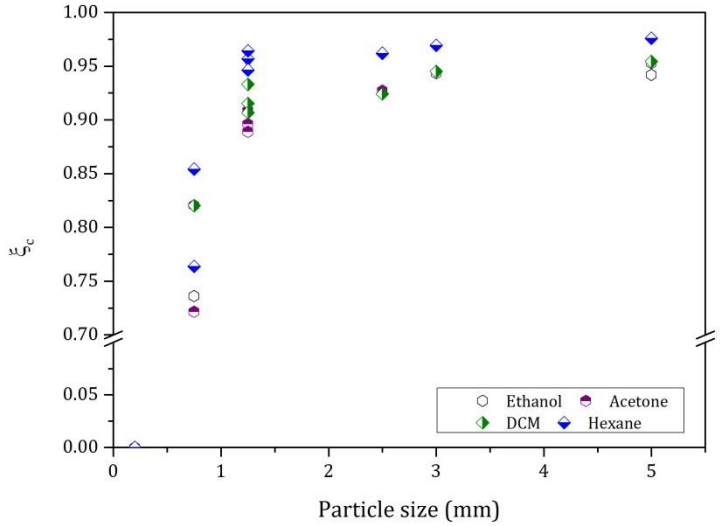


Figure 5.12 – Dimensionless core radius *vs.* particle size, for the different solvents tested: (hexagon-open) ethanol, (hexagon-half up) acetone, (diamond-half right) dichloromethane, (diamond-half down) hexane.

To evaluate the effect of particle size on the extraction process, experiments for three different particle sizes (powder, 0.75 mm and 5 mm) were performed and ethanol was used as solvent. Figure 5.13 shows the histories of cumulative amount of solute extracted; cork powder presents a higher yield at the end of extraction; in that Figure the full lines represent the diffusional model while the dash-dot lines represent the shrinking core model; for both models, the film resistance around particles is considered negligible ($N_f = 10$) and the particle Péclet number is taken as $Pe_p = 2$, while the internal effective diffusivity ($D_h$) was $1.7 \times 10^{-8}$ cm $\cdot s^{-1}$. For the particles sizes 0.75 mm (sample A1) and 5 mm (sample A5), the diffusional model described reasonably well the experimental results; however, the histories of cumulative amount of solute in solvent for the cork powder is not described by any of the models; one possible explanation for this results could be the eventual formation of agglomerates, happening when the solvent wets the powder, agglomerates that vanish along time; this hypothesis is represented in Figure 5.13 by the red lines, solid and dash lines for the diffusional and shrinking core models respectively. In these simulations, $N_d$ is considered to vary along time, i.e., a $N_d$ value for particles of larger size was used in the beginning and it was varied linearly with time until a $N_d$ value corresponding to powder, at the end of the extraction.

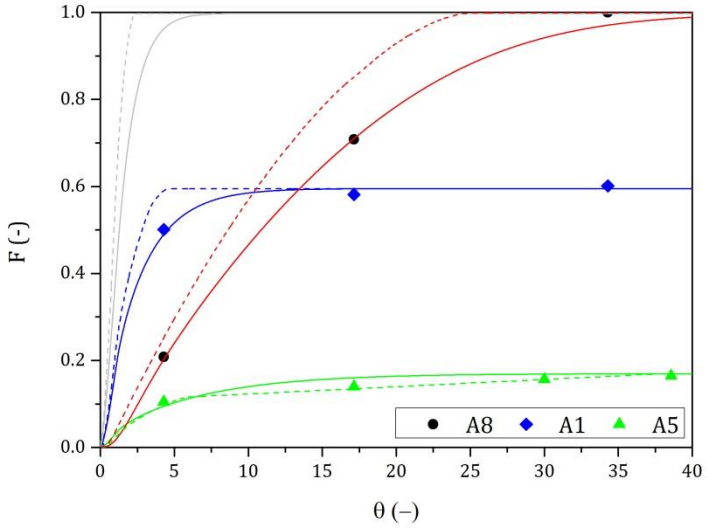


Figure 5.13 – Histories of amount of solute in fluid phase at the outlet of the packed-bed. For three particle size of granulated industrial cork: (triangle) 5 mm, (diamond) 0.75 mm and (circle) <0.20 mm – cork powder. Solvent: Ethanol. Solid lines represent the diffusional model and dash lines represent the shrinking core model while the red lines show the results for variable $N_d$.

Figure 5.14 shows the histories of $N_d$, for each particle size: cork powder (A8), 0.75 mm (A1) and 5 mm (A5), used for both models; the red dashed line represents the varying values of $N_d$ when it was considered that the solvent wets the powder forming agglomerates that vanish along time.

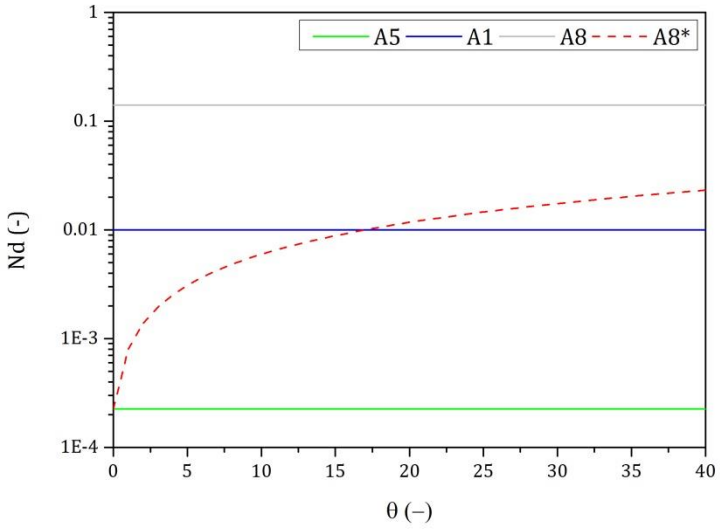


Figure 5.14 – Histories of $N_d$ value used in diffusional and shrinking core model for each particle size: (triangle) 5 mm, (diamond) 0.75 mm and (circle) <0.20 mm – cork powder; the dashed line represents the value of $N_d$ over the time when was assumed the possible formation of agglomerates (A8*).

It is to highlight that the $N_d$ parameter $\left(N_d = \tau \middle/ \left(R_p^2 \middle/ D_h\right)\right)$ considers the whole particle (Eq. 5.4 and Eq. 5.5); however, as previously described, only an outer layer is extracted for particle sizes higher than powder; a corrected value is expressed by,

$$N_d^* = \frac{1}{(1-\xi)^2} N_d \qquad \text{Eq. 5.23}$$

When the particle is fully extracted $N_d^* = N_d$, i.e., $\xi_c = 0$ (as in the case of the cork powder). Figure 5.15 shows the numbers of mass transfer units by diffusion considering the outer layer that it is extracted.

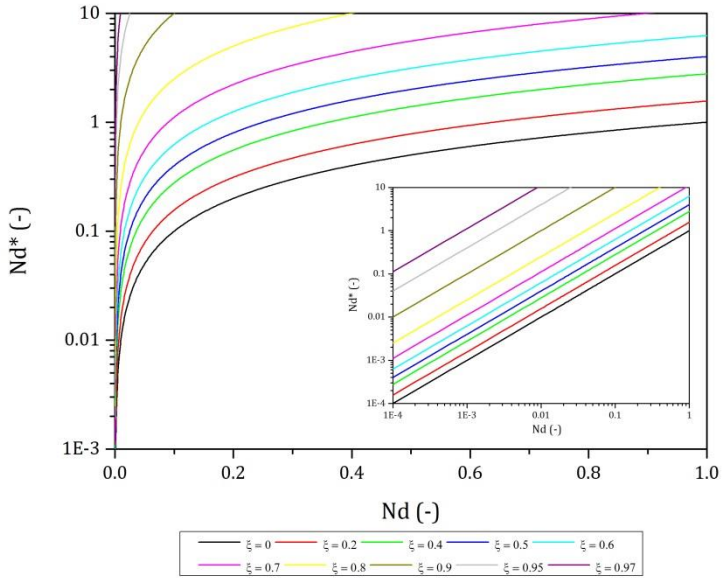


Figure 5.15 – $N_d$* (the outer layer extracted) *vs.* $N_d$ (whole particle).

For the supercritical fluid extraction, samples of sizes 0.75 mm (sample A1) and 5 mm (sample A5) were extracted, using carbon dioxide at supercritical conditions and its mixtures with ethanol (5 and 10%). As shown in the previous chapter (Chapter 4), for sample A1 (0.75 mm), using only $CO_2$, the higher yield (14.1 $\text{mg}_{\text{extract}} \cdot \text{m}^{-3}_{\text{DryCork}}$) was obtained at ~210 bar and 40°C; however, according to the results obtained for the soxhlet extraction, it was assumed that only an outer layer is accessible to be extracted for the particle sizes larger than powder; for powder, the maximum obtained at those operating conditions could be 23.4 $\text{mg}_{\text{extract}} \cdot \text{m}^{-3}_{\text{DryCork}}$. In the same way, considering a linear relation for the

extraction capacity of solvent (no interaction nor synergetic effect between the solvents), it is possible to estimate 27.7 and 32.3 $mg_{extract} \cdot m^{-3}_{DryCork}$, for 5 and 10% of ethanol in the mixture, respectively (at 210 bar and 40°C).

For sample A1 (0.75 mm), Figure 5.16 shows the histories of cumulative amount of solute in the fluid phase for a mixed solvent of $CO_2$ and (a) 5% or (b) 10% of ethanol; in this case, as the solvent is changed, the diffusion ($D_h$) was estimated as 1.40 x $10^{-8}$ $cm^2 \cdot s^{-1}$ and 0.93 x $10^{-8}$ $cm^2 \cdot s^{-1}$, respectively, while Péclet = 373 and $N_f$ = 10. The diffusional model simulates very reasonably the experimental results for 5% of ethanol in the solvent mixture; while for 10% ethanol, it is possible that something similar to the previous case (the cork powder in the soxhlet extraction) had occurred, i.e., the formation of agglomerates that vanish along time. In Figure 5.17, for both models it was assumed that $N_d$ changed its value over time ($R_p$ decreases) and this hypothesis, also, leads to a reasonable prediction of the experimental results.

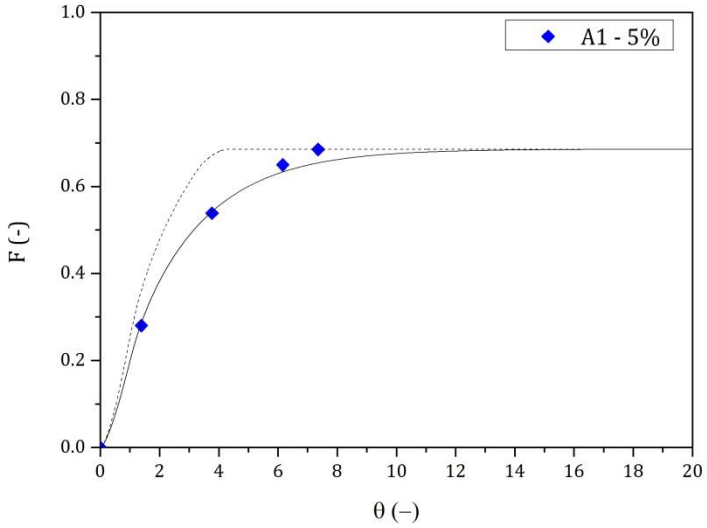


a)

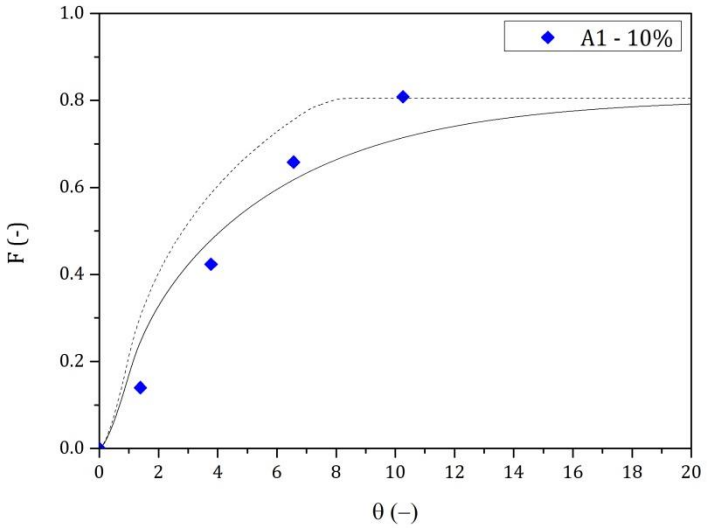


b)

Figure 5.16 – Histories of amount of solute in fluid phase at the outlet of the packed-bed; for sample A1 (0.75 mm). a) $CO_2$ and 5% ethanol and b) $CO_2$ and 10% ethanol. Pressure ~210 bar and 40°C. Continuous lines represent the diffusional model and dashed dot lines represent the shrinking core model.

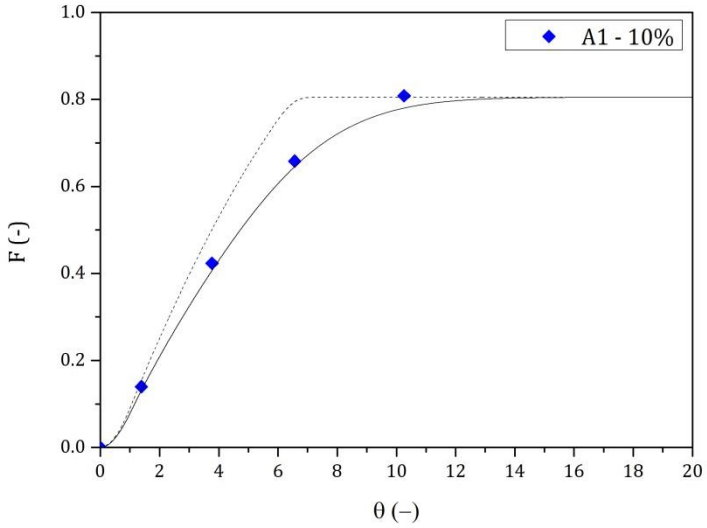


Figure 5.17 – Histories of amount of solute in fluid phase at the outlet of the packed-bed; for sample A1 (0.75 mm) and $CO_2$ and 10% ethanol at ~210 bar and 40°C. Continuous lines represent the diffusional model and dashed dot lines represent the shrinking core model considering a variable $N_d$

For sample A5 (5 mm), Figure 5.18 shows the experimental results when 10% ethanol is used in the solvent mixture; for the same conditions (~210 bar and 40˚C), the full line represents the simulation result with the diffusion model and the dash-dot line with the shrinking core model, considering $N_f = 10$ (negligible film resistance) and Péclet = 56; the effective diffusivity ($D_h$) was $1.87\ x\ 10^{-8}\ \ \text{cm}^2 \cdot \text{s}^{-1}$.

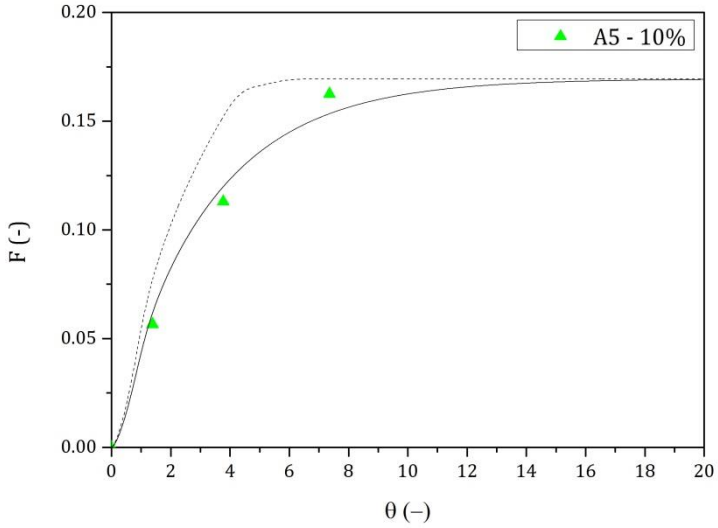


Figure 5.18 – Histories of amount of solute in fluid phase at the outlet of the packed-bed. For sample A5 (5 mm) using 10% ethanol and pressure ~210 bar and 40°C. Continuous line represents the diffusional model and dashed dot line represents the shrinking core model.

# Notation

| | | |
|---|---|---|
| $a_p$ | particle specific surface area (area/volume) | $\mathrm{m}^{-1}$ |
| $Bi_m$ | Biot number $Bi_m = \left(N_f / N_d\right)$ | - |
| $C_i$ | concentration of solute in the fluid phase | $\mathrm{g \cdot cm}^{-3}$ |
| $C_{s,i}$ | concentration of solute in the particle | $\mathrm{g \cdot cm}^{-3}$ |
| $D_{ax}$ | axial dispersion coefficient | $\mathrm{m}^2 \cdot \mathrm{s}^{-1}$ |
| $D_h$ | effective diffusivity | $\mathrm{m}^2 \cdot \mathrm{s}^{-1}$ |
| $F$ | cumulative dimensionless amount of solute transferred to the fluid phase | - |
| $k_f$ | mass transfer coefficient | $\mathrm{m \cdot s}^{-1}$ |
| $L$ | length of the bed | m |
| $N_f$ | number of mass transfer in the film surrounding particles, $N_f = \left(\tau / \tau_f\right)$ | - |
| $N_d$ | number of mass transfer units by diffusion inside the particles, $N_d = \left(\tau / \tau_d\right)$ | - |
| $Pe$ | Péclet number, $Pe = \left(u_i L / D_{\mathrm{ax}}\right)$ | - |
| $Pe_p$ | particle Péclet number $Pe_p = 2$ | - |
| $R_p$ | radius of particle | m |
| $t$ | time | s |
| $u_i$ | interstitial velocity | $\mathrm{m \cdot s}^{-1}$ |
| $x_i$ | dimensionless concentration of solute in the fluid phase | - |
| $x_{s,i}$ | dimensionless concentration of solute in the particle | - |
| $Z$ | dimensionless length of the bed, $Z = \left(z / L\right)$ | - |

# Greek letters

| | | |
|---|---|---|
| $\varepsilon$ | porosity or void fraction of the packed-bed | $m^3_{void\ space} \cdot m^{-3}_{bed}$ |
| $\xi$ | dimensionless radius, $\xi = \left(r / R_p\right)$ | - |
| $\theta$ | dimensionless time, $\theta = \left(t / \tau\right)$ | - |
| $\tau$ | $\tau = \left(L / u_i\right)$ | s |

# List of Acronyms

| | |
|---|---|
| SFE | Supercritical Fluid Extraction |
| $CO_2$ | Carbon Dioxide |

# References


Cocero, M. J., and Garcia, J. (**2001a**). "Mathematical model of supercritical extraction applied to oil seed extraction by CO2 plus saturated alcohol - I. Desorption model." *The Journal of Supercritical Fluids*, *20*(3), 229–243. doi:10.1016/S0896-8446(01)00068-7

Cocero, M. J., and Garcia, J. (**2001b**). "Mathematical model of supercritical extraction applied to oil seed extraction by CO2 plus saturated alcohol - II. Shortcut methods." *The Journal of Supercritical Fluids*, *20*(3), 245–255. doi:10.1016/S0896-8446(01)00069-9

de Melo, M. M. R., Silvestre, A. J. D., and Silva, C. M. (**2014**). "Supercritical fluid extraction of vegetable matrices: Applications, trends and future perspectives of a convincing green technology." *The Journal of Supercritical Fluids*. doi:10.1016/j.supflu.2014.04.007

Esquível, M. M., Bernardo-Gil, M. G., and King, M. B. (**1999**). "Mathematical models for supercritical extraction of olive husk oil." *Journal of Supercritical Fluids*, *16*, 43–58. doi:10.1016/S0896-8446(99)00014-5

Martinez, J., Monteiro, A. R., Rosa, P. T. V, Marques, M. O. M., and Meireles, M. A. A. (**2003**). "Multicomponent model to describe extraction of ginger oleoresin with supercritical carbon dioxide." *Industrial & Engineering Chemistry Research*, *42*(5), 1057–1063. doi:10.1021/Ie020694f

Naik, S. N., Lentz, H., and Maheshwari, R. C. (**1989**). "Extraction of perfumes and flavours from plant materials with liquid carbon dioxide under liquid-vapor equilibrium conditions." *Fluid Phase Equilibria*, *49*, 115–126. doi:10.1016/0378-3812(89)80009-3

Oliveira, E. L. G., Silvestre, A. J. D., and Silva, C. M. (**2011**). "Review of kinetic models for supercritical fluid extraction." *Chemical Engineering Research and Design*, *89*, 1104–1117. doi:10.1016/j.cherd.2010.10.025

Tan, C.-S., and Liou, D.-C. (**1989**). "Modeling of desorption at supercritical conditions." *AIChE Journal*, *35*(6), 1029–1031. doi:10.1002/aic.690350616

# 6 Fractionation of the cork extracts

Until now, it was determined that for the extraction of the granulated industrial cork, the yield increases when the solvent polarity increases (Figure 6.1); and, when the particle size increases, it is possible to note that the yield decreases since apparently only an external layer is extracted, for both soxhlet and SFE, Chapters 3 and 4, respectively.

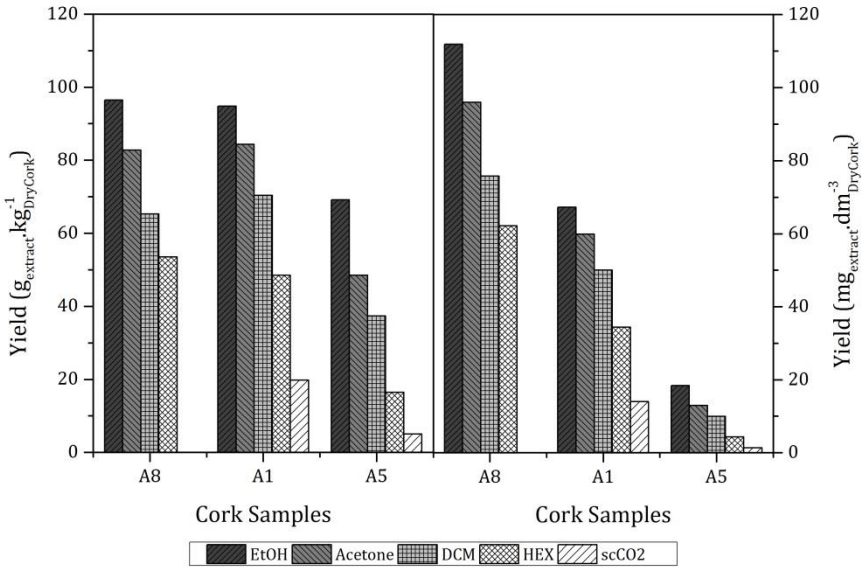


Figure 6.1 – Yields obtained for Soxhlet (ethanol, acetone, dichloromethane and hexane) and $scCO_2$ without co-solvent (at ~210bar and 41°C) for granulated industrial cork; samples A8 (powder), A1 (0.75 mm) and A5 (5 mm)

With respect to the target compounds in the cork extracts and cork, their cumulative composition at the end of each extraction is shown in Figure 6.2; despite the extract of hexane presenting the highest contents for the target compounds by mass of extract, by mass of dry cork it is the acetone that has the largest contents (Figure 6.2 b).

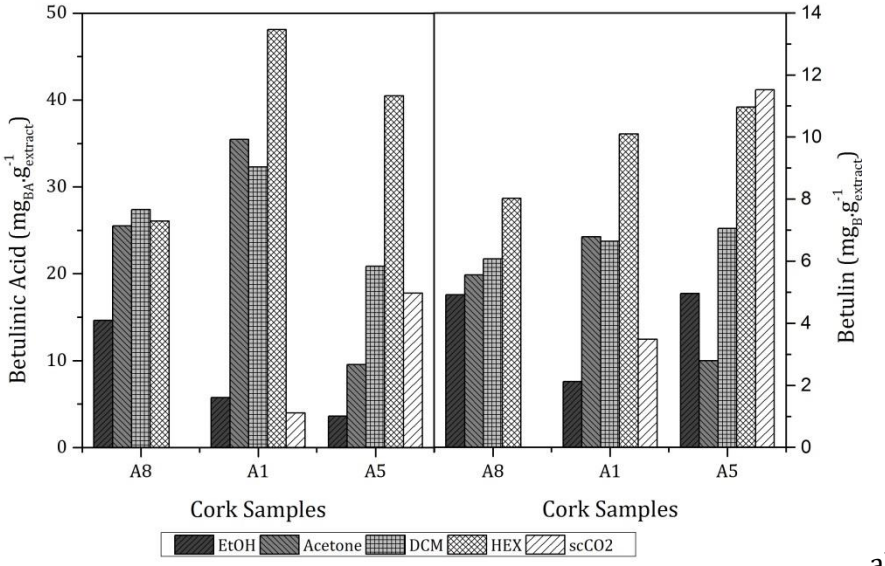


a)

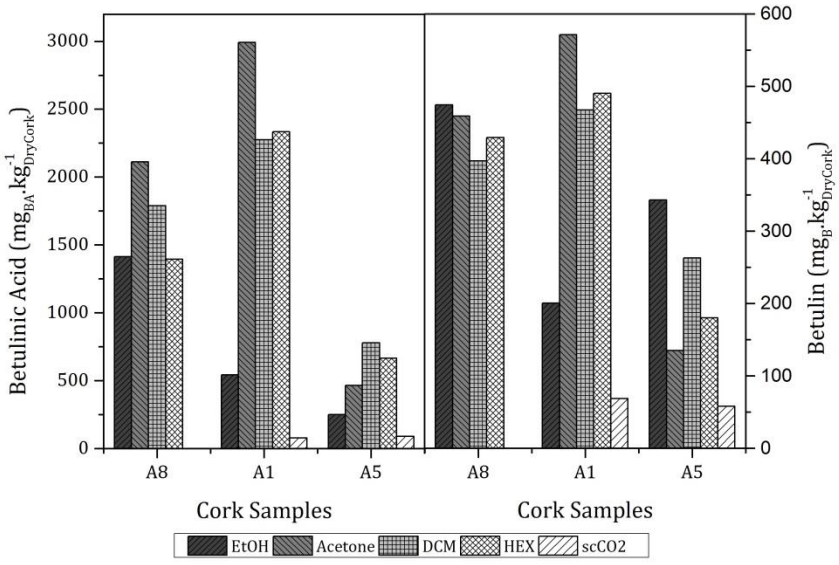


b)

Figure 6.2 – Betulinic acid and betulin content a) in the cork extract and b) in the cork; for Soxhlet (ethanol, acetone, dichloromethane and hexane) and $scCO_2$ without co-solvent (at ~210bar and 41°C) for granulated industrial cork, samples A8 (powder), A1 (0.75 mm) and A5 (5 mm).

In the following, the composition of the cork extracts along the extraction process, both in the soxhlet (ethanol) and in the SFE with co-solvent extractions,

will be reported; those data allow the estimation of the composition of the extracts along time and then enable the eventual programming of the fractions collection according to the target compounds. Moreover, the fractionation contributes to improve the design of a separation/purification process with the aim of achieving extracts with higher compositions of the target compounds

## 6.1 Soxhlet extraction

As it was referred in Chapter 3, the soxhlet extraction is a benchmark technology in which the solvent is continuously recirculated; Figure 6.3 shows the composition of the extract at different time intervals of the extraction, i.e., the solvent was removed after 1h, and new solvent was used in the extraction for more 3h, and then for 4h; at the end of the experiment the cork material was extracted by 8h, and three collections were made; it can be verified that, for the cork powder (Sample A8), the composition of the extract in the target compounds is practically constant over time; however, for the larger particles (A1 and A5) this does not occur; in the case of betulinic acid, this compound is at least 7 times higher in the first fraction collected for both samples (A1 and A5), while the betulin is at least 2 times higher in the same fraction. The last columns in Figure 6.3 represent the average contents of betulin or betulinic acid, i.e., considering that there were no intermediate collections

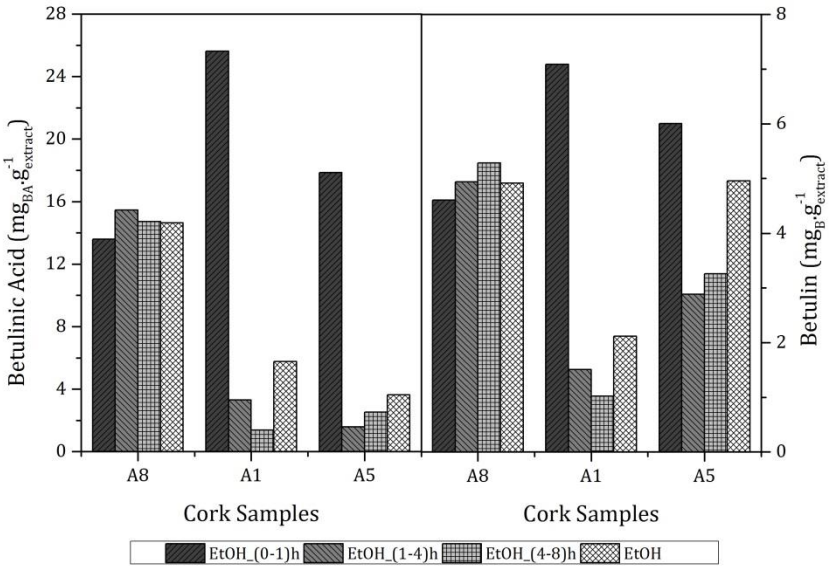


Figure 6.3 – Betulinic acid and betulin contents in the cork extracts for Soxhlet extraction at different times. Solvent: Ethanol. Samples: A8 (cork powder), A1 (0.75 mm) and A5 (5 mm).

## 6.2 Supercritical Fluid Extraction (SFE)

In this case, the samples were collected removing the co-solvent with the cork extract from the extraction setup at different times; the collections were made each hour; after evaporating the solvent, the composition of the extracts was analysed. Figure 6.4 shows, for samples A1 (0.75 mm) and A5 (5 mm), the composition of the target compounds in the extracts at different stages of the extraction process, for 210 bar and 41°C, when 10% of co-solvent (ethanol) was used. For the larger size sample (A5), the compositions of the target compounds were almost constant; however, for the sample A1, the last collected fraction was richer in betulinic acid and betulin, being 4.1 and 2 times higher than the first collected, respectively. If there were no collections the content of betulin or betulinic acid in the extract are represented in last columns of Figure 6.3 for each sample.

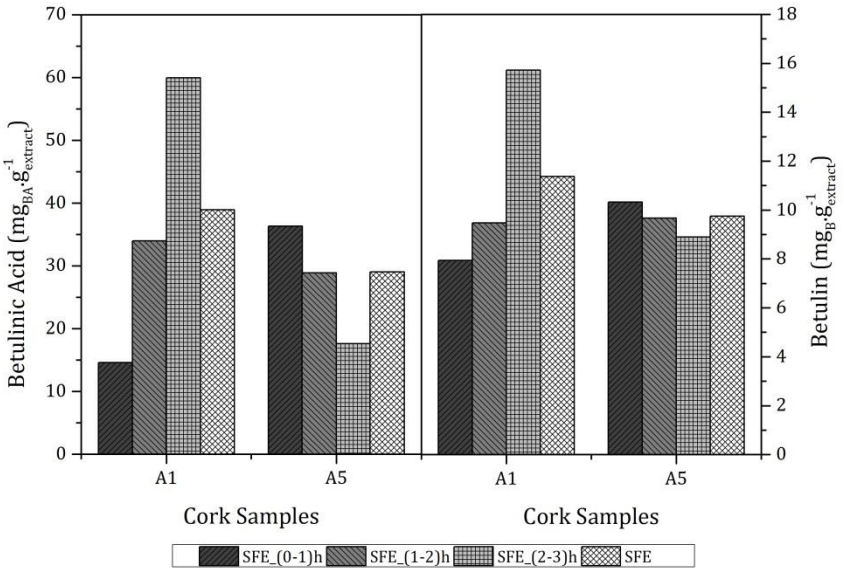


Figure 6.4 – Betulinic acid and betulin contents in the cork extracts for SFE with 10% ethanol at different times, (0-1h; 1-2h and 2-3h). Operating conditions: ~210 bar and 41°C.

The previous Figure compares the results for two samples (Samples A1 and A5) with different average particle size. Considering the sample with smallest particles (Sample A1), the effect of the addition of co-solvent in the composition of the cork extract was studied. Figure 6.5 shows the compositions of the cork extracts, for SFE using from 0, 5 and 10% of ethanol at the same operating conditions. In both cases where co-solvent was used, with 5% or 10% of ethanol as co-solvent in the SFE, the cork extracts were richer in the target compounds when compared with the SFE without co-solvent. Comparing the first and the last collected fractions, it is possible to note that, using fractional collections, the amount of the target compounds in the extracts can be doubled.

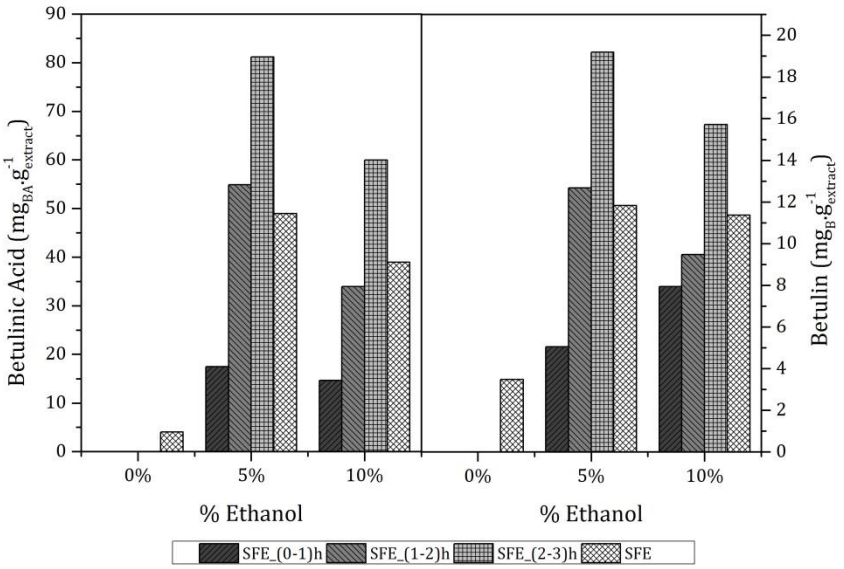


Figure 6.5 – Betulinic acid and betulin contents in the cork extracts for SFE at different times. Co-solvent: Ethanol. Operating conditions: ~210 bar and 41°C. For granulated industrial cork (0.75 mm – sample A1).

According to the results, the effect of adding ethanol in the SFE increases 1.4 and 1.9 times the yields ($g_{extract} \cdot kg^{-1}_{DryCork}$), for 5 and 10% of ethanol, respectively. In terms of the contents of betulin and betulinic acid in the extract ($mg_{B\ or\ BA} \cdot g^{-1}_{extract}$), even without fractional collections, the extracts are richer in the target compounds when compared with SFE without co-solvent or even with the soxhlet extraction.

*"That's one small step for man…"*
Neil Armstrong

# Conclusions

The main goal of this work was to show the feasibility to obtain new products/markets from granulated industrial cork, which means to "*Add a New Value to Cork*", that should constitute a push forward to the cork industry; the cork oak is considered a national heritage and more than fifty percent of the worldwide sales of cork products are assumed by the Portuguese cork industry. Being the production of cork stoppers the biggest sector of the cork industry, the raw material used in this work was constituted by the granulated industrial cork and cork powder generated in the facilities of natural cork stoppers production. Two different extraction processes, soxhlet and SFE, were studied; also, it was developed an analytical method to identify and quantify the target compounds, betulin and betulinic acid (B and BA), in cork.

With respect to the soxhlet extraction, the global extraction yields were influenced by all the parameters studied: solvent polarity, particle size, plank region, and particle bulk density. Yields increased with the polarity of the solvent, regardless of the average particle size (or bulk density) of the samples. The highest yield ($96.5\ g_{extract} \cdot kg_{DryCork}^{-1}$) was obtained for cork powder using ethanol as solvent. On the other hand, yields decreased, for all solvents, with increasing particle size. Particles from outer sections of the plank presented lower yields than samples from inner sections; for particles from inner sections, and with the same particle size, higher yields were obtained for samples with higher bulk density; the opposite behavior was verified for outer section samples.

The extracts for the soxhlet extraction have 2.5 to 4.6 times more betulinic acid than betulin. It was also shown that the contents of these target compounds extracted from cork decreased as the particle size increased, with the extracts from sample A1 being the richest (2991 $\mathrm{mg}_{\mathrm{Betulinic\ Acid}} \cdot \mathrm{kg}^{-1}_{\mathrm{DryCork}}$, and 571 $\mathrm{mg}_{\mathrm{Betulin}} \cdot \mathrm{kg}^{-1}_{\mathrm{DryCork}}$, with acetone as solvent). If we consider that around 20% of the total Portuguese exports of cork in mass could be extracted, then it would be possible to obtain by year ca. 3 ton of extract (assuming an 8% yield).

Taking the results of the soxhlet extraction as the benchmark, a bench scale setup for supercritical extraction was designed, assembled and tested; this setup can be operated both in batch or continuous modes as well as with or without co-solvent; also, it allows the recording of all operating conditions (pressures and temperatures), as well as the volume of $CO_2$ used in the extraction process. It is to remark that, although the setup was designed to extract granulated industrial cork, other materials can be used. The setup counts with a single separator. As the setup was built in-house, it is easily adaptable; e.g., it is possible to add another separator, to change the chamber of extraction, etc.

With respect to the supercritical extraction, the best result was obtained at 41°C and 210 bar with 19.7 $\mathrm{g}_{\mathrm{extract}} \cdot \mathrm{kg}^{-1}_{\mathrm{DryCork}}$; when 10% of ethanol was added, the yield increased almost 86% (to 36.4 $\mathrm{g}_{\mathrm{extract}} \cdot \mathrm{kg}^{-1}_{\mathrm{DryCork}}$).

In order to try to predict the experimental results, two phenomenological models were developed, one diffusional and one shrinking core models. In the development of both models, the film mass transfer resistance was neglected ($N_f$ = 10 was used throughout); and according with the experimental results and as cork is a liquid sealant, it was assumed that only an outer layer of the cork can be extracted; excluding the cork powder that was fully extracted, for particles bigger than 1 mm the dimensionless cork layer $(R_p - r_c)/R_p$ is nearly constant and only depends on the type of solvent; on average, it is ca. 0.22, 0.20 and 0.11 for acetone, dichloromethane and hexane, respectively.

For the same conditions, the mass transfer is faster in the shrinking core model than in the diffusional model. The diffusional model described reasonably well the experimental results; for soxhlet, the effective diffusivity was calculated as $1.7 \times 10^{-8}$ $cm^2 \cdot s^{-1}$, when the ethanol was used as solvent. While for the SFE the effective diffusivity was calculated as $1.4 \times 10^{-8}$ $cm^2 \cdot s^{-1}$ for 5% of ethanol, and $0.9 \times 10^{-8}$ $cm^2 \cdot s^{-1}$ for 10% of ethanol.

When fractional collections of the extracts were done, it was possible to double the contents of the target compounds in the cork fractions extracted.

*"Now this is not the end, it is not even the beginning of the end. But it is, perhaps, the end of the beginning"*
Winston Churchill

# Future Work

This thesis represented a first step to use the granulated industrial cork as a source of bioactive products; however, the author suggests new approaches to be done. First, analyse the performance for supercritical fluid extraction when another co-solvent is used, e.g., water; since the material used in this work is further used to produce cork stopper. Appendix 2 shows the methodology that will be used for those experiences. Needless to say, based in the results obtained in this work, granulated cork to be used in other technical applications can be a potential source of bioactive compounds with a high added-value, and for them other co-solvents can be used.

After obtaining the optimal operating conditions for extraction and fractionation with the new co-solvents (at the bench scale), the experimental setup should be adapted to a preparative scale, with the objective to evaluate the effects of scale-up and to prepare its eventual industrial application in the future.

Also, develop a model to predict the extraction and fractionation of the extractives from cork not only in terms of the total yields (as presented in this work), but also focused in each one of the target compounds.

Finally, it is essential to carry out an economic analysis for this process to determine the possibility to implement in the cork industry.

# Appendix 1 - Analytical Methods

Beyond the yields achieved to each cork extraction, it was essential to know their composition, i.e. the selectivity of the target compounds to each solvent. An analytical method was implemented to identify and quantify the compounds present in the cork extracts, by soxhlet extraction or even supercritical fluid extraction. A gas chromatograph (GC) was used to separate the cork extracts.

The quantitative GC analysis is based in the area of the chromatographic peak, and the qualitative analysis uses the retention time (McNair *et al.*, 1998). Nonetheless, the retention time cannot be the only parameter to confirm the compound identity; the spectrum from a mass spectrometer helps to identify the structure, elemental composition and molecular weight of the components in a mixture (Harris, 1999). In this work, two detectors coupled to the GC were used for the analysis of cork extracts: for the qualitative analysis, a MS detector was used, while for quantitative analysis a FID detector was coupled to the GC; the GC-FID was calibrated using pure reference compounds representative of the major classes of components present in cork extracts, relative to an internal standard (cholesterol).

## Gas Chromatography / Flame Ionization Detector (GC-FID)

FID responds to a wide range compounds, since it is a non-selective detector (McNair *et al.*, 1998). A GC (Chrompack CP-9003), that was equipped with a flame ionization detector and a DB-1 capillary column (30 m x 0.32 mm inner diameter and 0.25 μm film thickness), was used. To achieve a good separation of the compounds, a temperature program was defined, and helium was used as carrier gas (1 $mL \cdot min^{-1}$); the detector and injector temperatures were set at 300°C and a temperature program was defined as: 80°C during the first 5 min, an increase from 80 °C to 280°C with a heating rate of 4 $°C \cdot min^{-1}$, and 20 min at 280°C. Figure A1.1 shows a chromatographic separation between betulin and betulinic acid for the conditions described above.

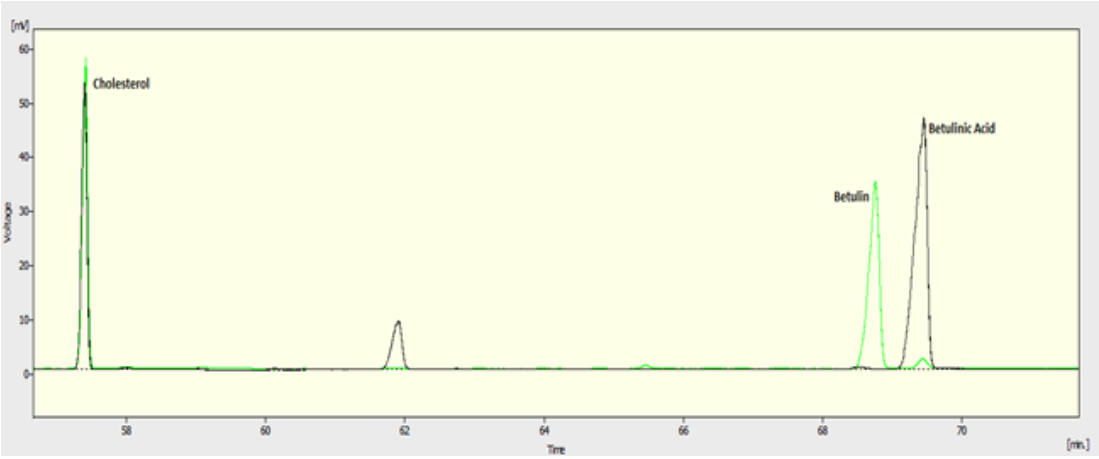


Figure A1.1 - Chromatogram for betulin (B) and betulinic acid (BA)separation using cholesterol as internal standard for the conditions described in the text.

To quantify the compounds in the samples, a calibration curve must be done; an internal standard should be used when high precision is required, since the internal standard and the samples are submitted to the same conditions during the analysis. Preferably, the internal standard must belong to a similar family of the compounds to be analyzed, and cannot be present in the sample, neither interfere with the other chromatographic peaks. As cholesterol is not present in cork extracts, it was used as the internal standard. The calibration curve is a method to determine the concentration of a substance in an unknown sample, comparing standard samples of known concentrations with the unknown samples. Figure A1.2 shows calibration curves for betulin and betulinic acid using cholesterol as internal standard.

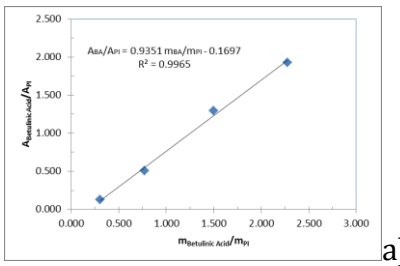


a)

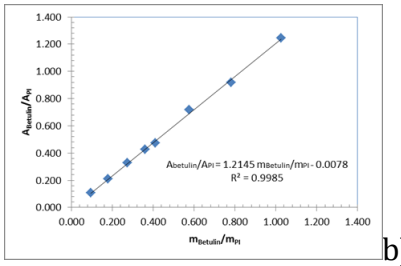


b)

Figure A1.2 – Calibration Cuve: a) betulinic acid b) betulin.

### Gas Chromatography / Mass Spectrometry (GC-MS)

The GC-MS combines the power of high-resolution separation with a very selective and sensitive mass detection (Harris, 1999). A mass spectrometer bombards molecules in the vapor phase (commonly, using electron-impact

mode) with a high-energy electron beam and records the result as a spectrum of positive ions separated on base of mass/charge (m/z) (Silverstein *et al.*, 1998).

Mass spectra are routinely obtained at an electron beam energy of 70 eV. With mass spectrometers, structural information to identify the analyte is obtained (Silverstein *et al.*, 1998). Figure 9 shows a mass spectrum for the cholesterol trimethylsilyl ether; this is a representation of the masses of the positively charged fragments versus their relative concentrations. The most intense peak in the spectrum (base peak), is assigned a value of 100 %, and the other peak intensities (including the molecular peak) are reported as percentages of the base peak (Silverstein *et al.*, 1998).

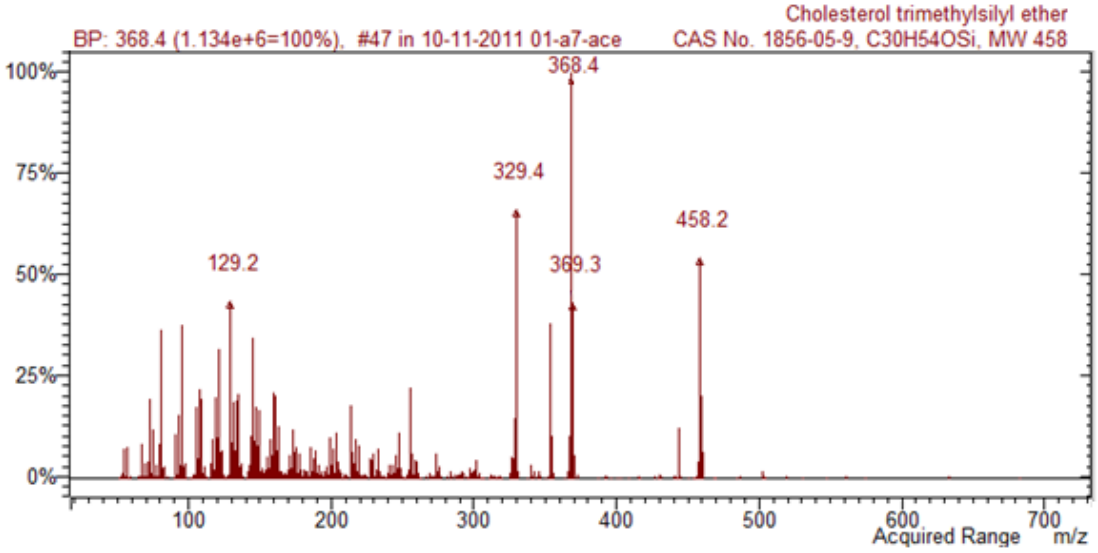


Figure A.3 - Mass spectrum for cholesterol trimethylsilyl ether.

For the identification of the components in the cork extracts, a gas chromatograph with a mass spectrometer was used (Varian 4000 GC-MS, USA). The compounds in the mixture were separated in a capillary VF-5MS (30 m x 0.25 mm ID x 0.25 µm film) column. The detector was set at 300°C and helium was used as carrier gas. The temperature program used is the one defined above (GC-FID). The MS is operated in the electron impact mode with an electron impact energy of 70 eV over a range of m/z 50 – 700. The ion source is maintained at 200°C.

## References

Harris, D. C. (**1999**). "Quantitative chemical analysis" (5th ed). Book, New York: W. H Freeman and Company.

McNair, H. M., and Miller, J. M. (**1998**). "Basic gas chromatography." *Techniques in analytical chemistry series*. Book, New York [etc.]: John Wiley & Sons.

Silverstein, R. M., and Webster, F. X. (**1998**). "Spectrometric identification of organic compounds" (6th ed). Book, New York: John Wiley & Sons.

# Appendix 2 - Response Surface Methodology (RSM)

## Design of experiments using response surface methodology

In order to evaluate the influence of each variable (pressure, temperature and amount of co-solvent) in the performance of the process, the response surface methodology (RSM) was used to design the experiments; Table A2.1 shows the range of values tested for each variable. It is to remark that despite the range proposed for pressure, the experimental set-up can be operated in a wider range (up to 300 bar).

Table A2.1 – Range of the process variable used in SFE with co-solvent.

| | **Low<br>-1** | **Medium<br>0** | **High<br>1** |
|---|---|---|---|
| **Pressure (bar)** | 170 | 205 | 240 |
| **Temperature (°C)** | 40 | 60 | 80 |
| **co-solvent (%)** | 0 | 5 | 10 |

To do a screening of the variables, the first experiments are obtained by a fractional factorial design as indicated in Table A2.2. With the results obtained, the response is fitted to a linear model through the first-order model represented in Eq. A2.1.

$$y = \beta_0 + \beta_1 x_1 + \beta_2 x_2 + \ldots + \beta_k x_k + \varepsilon \qquad \text{Eq. A2.1}$$

Where

- $x_i$ represents the variable "*i*",
- $k$ is the number of variables,
- $\beta_0$ is the constant term,
- $\beta_i$ represents the coefficients of the linear parameter "*i*",
- $\varepsilon$ is the residue associated to the experiments.

Table A2.2 – Experiments from fractional factorial design with 3 variables (6 runs)

| RUN | Pressure (bar) | Temperature (°C) | Co-solvent (%) |
|---|---|---|---|
| ***1*** | 170 | 40 | 10 |
| ***2*** | 240 | 40 | 0 |
| ***3*** | 170 | 80 | 0 |
| ***4*** | 240 | 80 | 10 |
| ***center-a*** | 205 | 60 | 5 |
| ***center-b*** | 205 | 60 | 5 |

In the case of a good fitting, the fractional factorial design is improved; so, a full factorial design is run, as described in Table A2.3. Figure A2.1 shows that the experiments from the fractional factorial design procedure are included in the full factorial design.

Table 4 – Experiments from the full factorial design with 3 variables (10 runs)

| RUN | Pressure (bar) | Temperature (°C) | Co-solvent (%) |
|---|---|---|---|
| ***1*** | 170 | 40 | 0 |
| ***2*** | 240 | 40 | 0 |
| ***3*** | 170 | 80 | 0 |
| ***4*** | 240 | 80 | 0 |
| ***5*** | 170 | 40 | 10 |
| ***6*** | 240 | 40 | 10 |
| ***7*** | 170 | 80 | 10 |
| ***8*** | 240 | 80 | 10 |
| ***center-a*** | 205 | 60 | 5 |
| ***center-b*** | 205 | 60 | 5 |

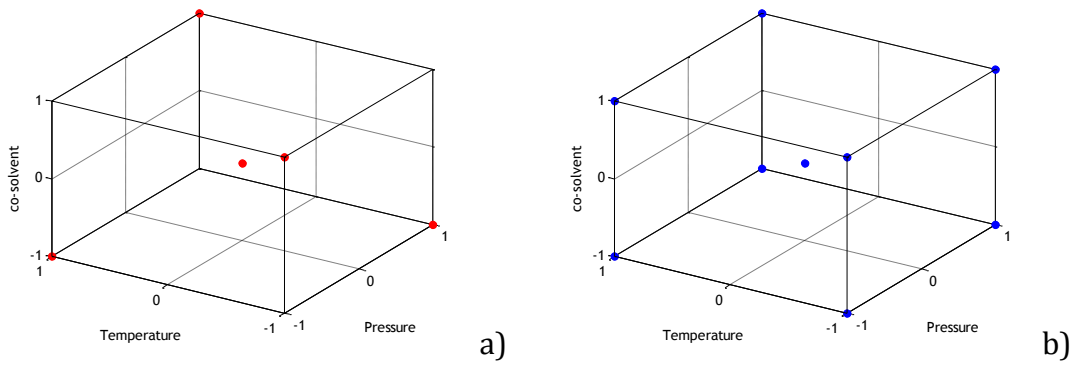


Figure A2.1 – Experimental design a) fractional factorial; b) full factorial.

The previous first-order model does not describe any curvature in the response; to evaluate a possible curvature, a second-order model is used (Eq. A2.2). In this

sense, a Box-Behnken design or a central composite design can be chosen; the experiments from these designs are presented in Table A2.4 and Table A2.5, respectively. The required number of runs from the Box-Behnken algorithm is given by $N = 2k(k-1) + c_{po\,\mathrm{int}}$, where $c_{po\,\mathrm{int}}$ is the number of replicates of the central run; in the case of the central composite, $N = k^2 + 2k + c_{po\,\mathrm{int}}$.

Table A2.4 – Experiments from the Box-Behnken design with 3 variables (15 runs)

| RUN | Pressure (bar) | Temperature (°C) | Co-solvent (%) |
|---|---|---|---|
| ***1*** | 170 | 40 | 5 |
| ***2*** | 240 | 40 | 5 |
| ***3*** | 170 | 80 | 5 |
| ***4*** | 240 | 80 | 5 |
| ***5*** | 170 | 60 | 0 |
| ***6*** | 240 | 60 | 0 |
| ***7*** | 170 | 60 | 10 |
| ***8*** | 240 | 60 | 10 |
| ***9*** | 205 | 40 | 0 |
| ***10*** | 205 | 80 | 0 |
| ***11*** | 205 | 40 | 10 |
| ***12*** | 205 | 80 | 10 |
| ***center-a*** | 205 | 60 | 5 |
| ***center-b*** | 205 | 60 | 5 |
| ***center-c*** | 205 | 60 | 5 |

Table A2.5 – Experiments from the central composite design with 3 variables (17 runs)

| RUN | Pressure (bar) | Temperature (°C) | Co-solvent (%) |
|---|---|---|---|
| ***L:A*** | 170 | 60 | 5 |
| ***H:A*** | 240 | 60 | 5 |
| ***L:B*** | 205 | 40 | 5 |
| ***H:B*** | 205 | 80 | 5 |
| ***L:C*** | 205 | 60 | 0 |
| ***H:C*** | 205 | 60 | 10 |
| ***1*** | 170 | 40 | 0 |
| ***2*** | 240 | 40 | 0 |
| ***3*** | 170 | 80 | 0 |
| ***4*** | 240 | 80 | 0 |
| ***5*** | 170 | 40 | 10 |
| ***6*** | 240 | 40 | 10 |
| ***7*** | 170 | 80 | 10 |
| ***8*** | 240 | 80 | 10 |
| ***cent-a*** | 205 | 60 | 5 |
| ***cent-b*** | 205 | 60 | 5 |
| ***cent-c*** | 205 | 60 | 5 |

Figure A2.2 shows the experiments with the Box-Behnken and central composite designs. The central composite design includes all runs of the full factorial. The second-order model is

$$y = \beta_0 + \sum_{j=1}^{k} \beta_j x_j + \sum_{j=1}^{k} \beta_{jj} x_j^2 + \sum \sum_{i<j=2}^{k} \beta_{ij} x_i x_j + \varepsilon \qquad \text{Eq. A2.2}$$

Where

$\beta_{jj}$ represents the coefficients of the quadratic parameter "j",

$\beta_{ij}$ represents the coefficients of the interaction parameter,

$k$ is the number of variables,

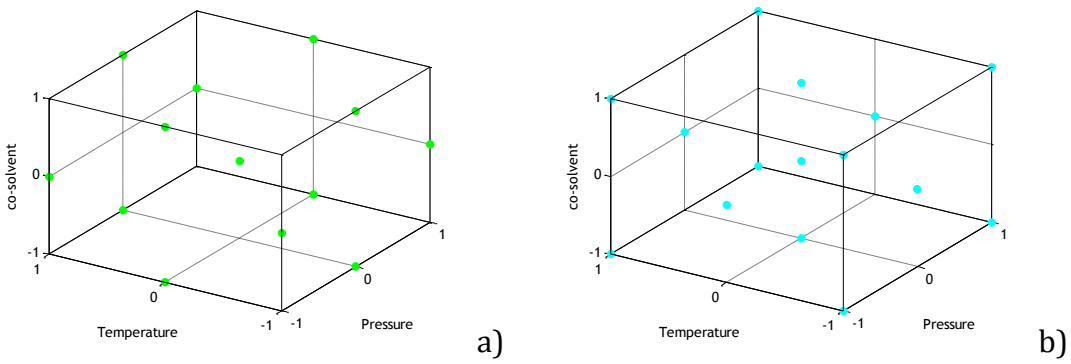


Figure A2.2 – Experimental design a) Box-Behnken and b) central composite.

## References

Bezerra, M. A., Santelli, R. E., Oliveira, E. P., Villar, L. S., and Escaleira, L. A. (2008). "Response surface methodology (RSM) as a tool for optimization in analytical chemistry." Talanta, 76(5), 965–977. doi:10.1016/j.talanta.2008.05.019

Myers, R. H., and Montgomery, D. C. (2002). "Response surface methodology process and product optimization using designed experiments." Wiley Series in Probability and Statistics (2nd ed). New York: John Wiley & Sons.